Summer 2021

Electricity Market Operations With Massive Renewable Integration: New Designs

Shengfei Yin
Southern Methodist University, gyin@smu.edu

ELECTRICITY MARKET OPERATIONS WITH
MASSIVE RENEWABLE INTEGRATION:
NEW DESIGNS

Approved by:

Dr. Jianhui Wang
Professor

Dr. Jungchih Chiao
Professor

Dr. Mohammad E. Khodayar
Associated Professor

Dr. Harsha Gangammanavar
Assistant Professor

Dr. Xin Fang
External Expert

ELECTRICITY MARKET OPERATIONS WITH MASSIVE RENEWABLE INTEGRATION: NEW DESIGNS

A Dissertation Presented to the Graduate Faculty of the

Bobby B. Lyle School of Engineering

Southern Methodist University

in

Partial Fulfillment of the Requirements

for the degree of

Doctor of Philosophy

with a

Major in Electrical Engineering

by

Shengfei Yin

Master of Science, Electrical Engineering, Illinois Institute of Technology
Bachelor of Engineering, Electrical Engineering, Hunan University

August 4, 2021

ACKNOWLEDGMENTS

I dedicate my sincerest gratitude to my academic advisor, Prof. Jianhui Wang, for his patience and guidance in my Ph.D. career. This study would not have been complete without his invaluable wisdom and constructive advice. I always feel privileged and honored to assist in his works and advance my research. Special thank passes to Prof. Harsha Gangammanavar and Dr. Xin Fang for their treasured input and help in developing solution algorithms and practical scenarios. Their fruitful knowledge and experiences helped me break many bottlenecks and enlightened the synergy between operations research and electrical engineering. Appreciation further extends to the respected graduation committee members, including Prof. Jungchih Chiao and Prof. Mohammad Khodayar, who have provided suggestions of value and set inspiring examples of scientific achievements.

I would like to thank Dr. Yonghong Chen, Dr. Jin Tan, Dr. Xiaohu Zhang, Dr. Feng Qiu, and Prof. Lei Wu for their consistent support on R&D projects and technical reviews, bolstering my research from various perspectives. I hope we could keep future collaborations in related fields and try to improve the industry practice further.

My academic life at SMU would not be so enjoyable without my peer researchers. I would like to acknowledge Prof. Saeed D. Manshadi for his genuine help and technical support when I started the journey of Ph.D. I also respect Ying Zhang's diligence and curiosity, which form a benign stimulation of my research. Furthermore, my fellow colleagues, Yihao Wang, Xinan Wang, Mahdi Khodayar, Mohammad Ramin Feizi, Yanling Lin, You Lin, Xinyun Lu, Tao Wu, Bin Huang, Tu Lan, Abdulraheem Hassan Z Alobaidi, Saeed Fazl Hashemi, take my heartfelt gratitude for the company and backup at all times.

Last but not least, I keep the deepest affection and thank-you for my family and my beloved Margaret, who have been my persistent champions as always.

Yin, Shengfei Master of Science, Electrical Engineering, Illinois Institute of Technology
Bachelor of Engineering, Electrical Engineering, Hunan University

Electricity Market Operations with
Massive Renewable Integration:
New Designs

Advisor: Dr. Jianhui Wang
Doctor of Philosophy degree conferred August 4, 2021
Dissertation completed date: July 19, 2021

Electricity market has been transitioning from a conventional and deterministic operation to a stochastic operation under the increasing penetration of renewable energy. Industry-level solutions toward the future electricity market operation ask for both accuracy and efficiency while maintaining model interpretability. Hence, reliable stochastic optimization techniques come to the first place for such a complex and dynamic problem.

This work starts at proposing a solution strategy for the uncertainty-based power system planning problem, which acts as a preliminary and instructs the electricity market operation. Formulated as a multi-year system planning problem from an independent system operator's perspective, it minimizes both expansion and operational costs under binary and continuous uncertainties, *i.e.*, system component contingency and load/generation variation. The original hybrid model is highly intractable, but we devise a combined decomposition strategy to relieve the computational burden. Considering 100% renewable penetration in the future, it analyzes the cost-effectiveness of renewable energy from a long-term point of view.

After the uncertainty-based system planning problem is well tackled, we turn our direction to the hierarchical market operation considering the transmission and distribution coordination. As distributed generators are increasingly penetrating the distribution networks, the central operator should be aware of their uncertainties. We develop a three-stage unit commitment model for the market operation of transmission and distribution coordination under the uncertainties of renewable generation and demand variations. As a multi-stage

stochastic programming problem, the proposed model is mixed-integer nonlinear, and we devise a generalized nested L-shaped algorithm to divide and conquer this problem efficiently.

With the study of new electricity market operations, current market protocols should be updated according to the growing variable resources in the power system, especially the ancillary service participation. To better let industry and research communities leverage our works, we develop an flexible software platform for the full-stack electricity market operations including both the day-ahead and real-time operations. In this platform, users could conveniently switch from conventional market models to the novel market framework that we designed. Various operation novelties, such as ancillary service provision from variable resources, multi-level energy storage participation, and model updates on the conventional non-spinning reserve, are integrated in the new model, considering the profitability of the variable renewable energy.

TABLE OF CONTENTS

LIST OF FIGURES

LIST OF TABLES

This dissertation is dedicated to my family and Margaret.

Chapter 1

INTRODUCTION

1.1. Motivations and Preliminaries

The electricity market serves as a system that enables electric power trading by long-term planning and short-term scheduling through bids to buy and offers to sell. The conventional deregulated electricity market has been well developed upon multi-timescale co-optimizations of energy and reserves to achieve the goal mentioned above. In general, a typical electricity market operation first solves a deterministic *ex-ante* market optimization that collects the bids and offers submitted by different stakeholders and clears the market with zonal or nodal pricing. Then, *ex-post* dispatch and settlement procedure in real-time are conducted to realize the cleared power schedules and finalize the payments/charges. This operation paradigm has been adopted or referred to by many electricity markets around the world, including the United States [1] and Europe [2].

However, this market framework is now challenged when renewable energy surges in the power system. Due to the increasing concern of environmental issues, renewable energy proliferates with generous governmental incentives and community supports. With the global installations of wind and solar energy depicted in Figure 1.1 (Data source: [3]), the overall penetration of renewables worldwide has reached 9% in early 2020 [4] and keeps accelerating phenomenally. From the electricity market's perspective, however, renewable energy not only imposes a nature of high capital cost and low operation cost, but also brings uncertainties that threaten the system reliability. Despite the governmental incentives such as feed-in-tariffs, renewable energy has been widely questioned for its capital payback and unreliable power supply [5].

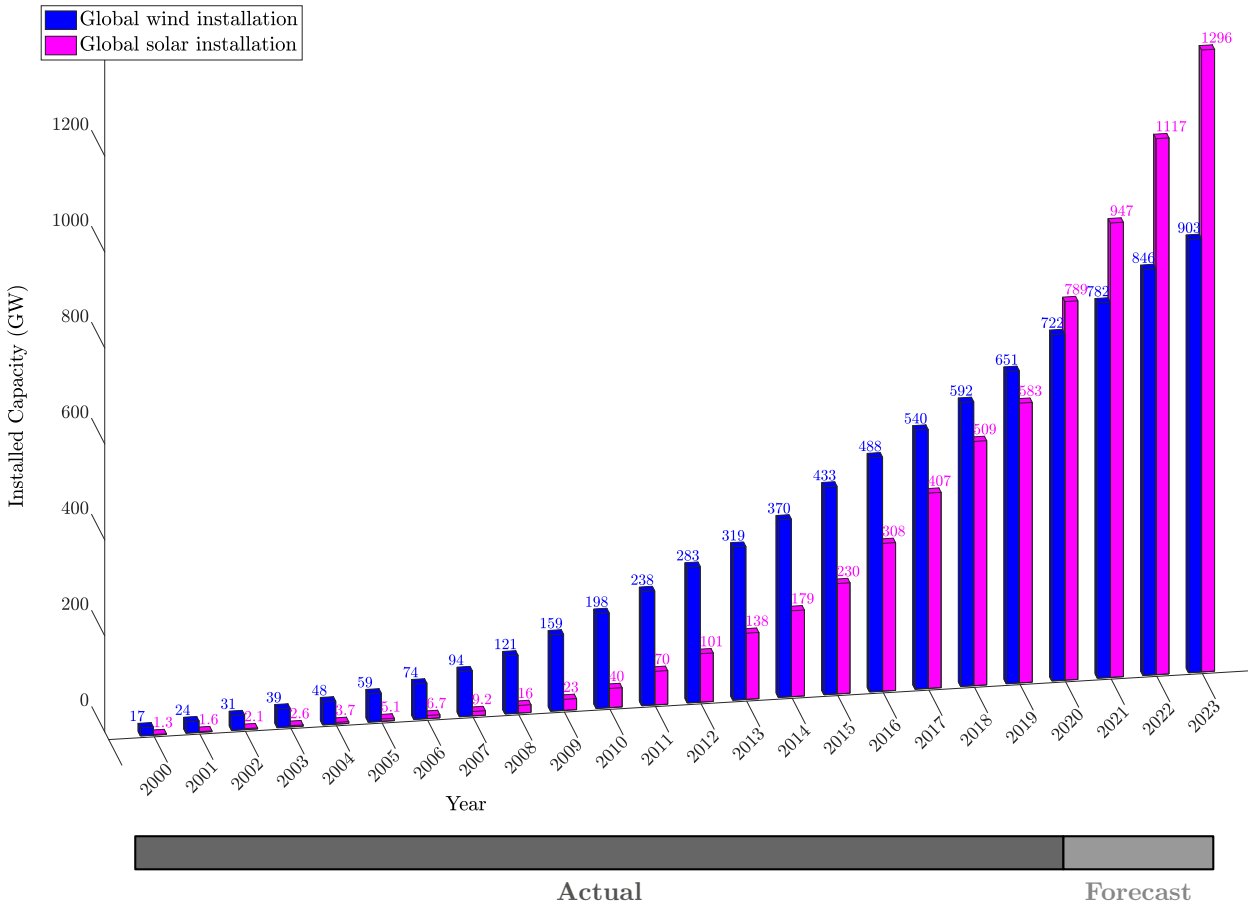

Figure 1.1. Global wind and solar installation.

On the one hand, from a long-term perspective, before stepping into the daily electricity market operation, the coordinated system planning should be investigated accounting for the massive renewable penetration. To what extent that renewable energy should be invested in the long-term power system planning becomes critical when determining the optimal investment portfolio of future electricity share. However, the uncertainty of renewable energy poses a difficult hurdle to the planner since the invested generators might have uncontrollable variable production. Studying the uncertainty-based system planning in a long-term horizon contributes to a more reliable and confident short-term or mid-term market operation [6].

On the other hand, the short-term market operation should also be treated very carefully since typical renewable energy such as wind and solar possesses short-term variability.

One of the most critical concerns is that the downstream markets, *i.e.*, the distribution-level markets, become increasingly active with the growing penetration of renewable distributed energy resources (DERs). The uncertainties brought by the DER introduce many unique challenges, such as the reverse power flow and local net load fluctuation. Hence, an enhanced market framework that considers the coordination between the transmission and distribution networks becomes an urgent task [7].

An envisioned overall market hierarchy, as shown in Figure 1.2, provides a road-map including the key components that should be coordinated in the future market operation. From the perspective of the central system operator, how to tackle the increasing renewable uncertainties in both the transmission and distribution networks in the manner of system operation calls for solutions. Towards the need for a better market operation design, this dissertation discusses potential solution strategies towards these future challenges while qualitatively and quantitatively analyzing the economic values.

1.2. Research Objectives and Achievements

As the proliferating renewable energy introduces more uncertainties to the power system, uncertainty-based market operations become a significant research milestone, to which this dissertation is devoting. As a holistic market operation study, both the long-term and short-term operation schemes are extensively investigated. From the long-term perspective, the coordinated system planning problem optimizes the multi-year investment portfolio of generation mix, including a massive portion of renewable generation, considering practical system contingencies and uncertainties. From the short-term perspective, transmission and distribution-coordinated day-ahead market operation considers uncertainties from both the upstream and downstream markets at different levels, and a new coordinated market paradigm paves the way for the distribution-aware system operation. We also develop a general simulation tool considering the renewable impacts in the future electricity market, which could help both the industry and research communities conduct more comprehensive studies on future market framework designs.

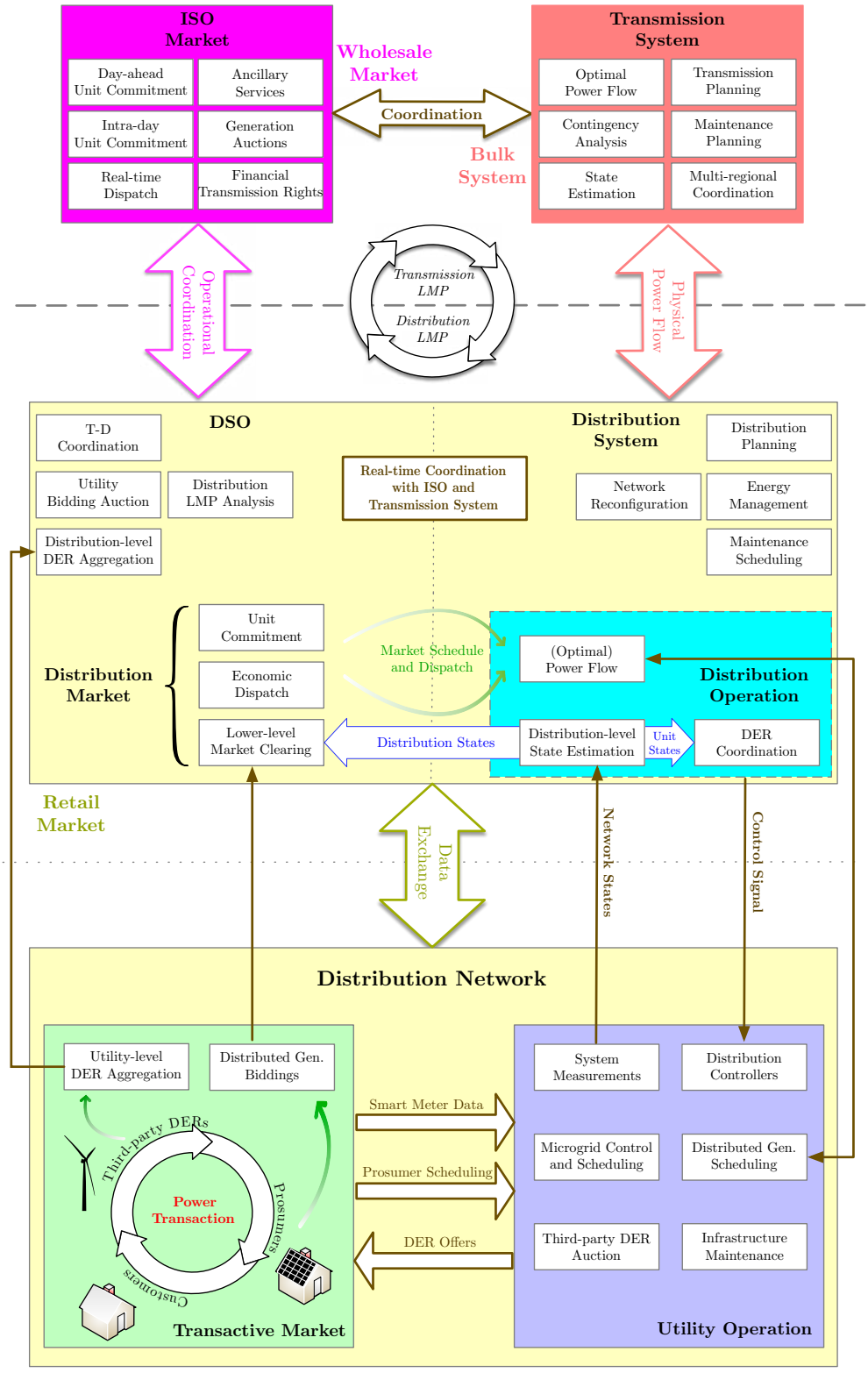

Figure 1.2. Future coordinated market hierarchy.

More specifically, we outline the detailed contributions and achievements of this work as below.

- **Long-term Operation: Coordinated System Planning:** We propose a novel modeling framework and decomposition-based solution strategy combining stochastic programming (SP) and robust optimization (RO) to deal with multiplex uncertainties in coordinated long-term power system planning. The problem is formulated as a multi-year generation and transmission planning problem from a system operator's perspective to minimize both expansion and operational costs under binary and continuous uncertainties, *i.e.*, system component contingency, and load/generation variation. N-k contingencies are captured in RO using the reformulated contingency criteria, while the load/generation uncertainty is considered in SP embedded with RO using operating scenarios generated from the historical data with spatiotemporal correlations. The original hybrid model is highly intractable, but the intractability can be relieved by the proposed decomposition strategy based on the column-and-constraint generation and L-shaped algorithms. We apply our model to perform long-term system planning under extremely high renewable penetration and investigate the case of 100% renewables in long-term planning.

- **Short-term Operation: Transmission and Distribution Coordinated Market:** We propose a three-stage unit commitment model for the market operation of transmission and distribution coordination under the uncertainties of renewable generation and demand variations. The first stage is for the independent system operator that determines the commitment decisions of the transmission-level generators and the distribution-level system reconfiguration; the second stage optimizes the transmission economic dispatch; then distribution system operators in the third stage perform their economic dispatch and exchange information with the transmission operator at the boundary nodes. Between the transmission and distribution networks, not only conventional thermal generators but renewables and variable demands are considered, which are tackled via a multi-stage stochastic programming approach. The model adopts a convexified alternating-current branch flow formulation in the distribution

system. We devise a generalized nested L-shaped algorithm to solve the proposed framework in an efficient manner.

- **Electricity Market Co-simulation: General Simulation Tool for User-friendly Flexibility:** With the growing penetration of renewable resources, market operators call for an evolving market framework with refined operational models considering the unique contributions from renewable resources and energy storage systems. In the same vein, real-time system-wide simulations also need to intercommunicate with power system dynamics. To meet the demand of a general testing environment for new market mechanisms and requirements, we develop a novel electricity market operation paradigm released as MIDAS-S, a flexible Python-based simulation platform. In this framework, MIDAS-S can efficiently build and solve multi-timescale market optimization models considering novel operation constraints while interfacing with system dynamic simulations performed in commercial software, *e.g.*, PSS®E. Numerical experiments corroborate the proposed platform's effectiveness by conducting economic assessments on real-sized systems with real-time dynamics.

We organize the remainder of this dissertation as follows.

Chapter 2 develops a long-term power system planning problem considering the unit contingencies and the renewable/load uncertainties. The hybrid stochastic and robust planning problem is solved by a combined algorithm of column-and-constraint generation and L-shaped method. Chapter 3 quantitatively analyzes the T-D coordinated market framework that takes the local DERs into account with utility-level renewable energy. We devise a generalized decomposition technique to facilitate the solution of such a complex problem. Chapter 4 first gives a comprehensive overview for state-of-the-art electricity market operations in the current industry practice and academia, then presents a general simulation platform devised for flexible market environment parameterization and use case designs. Chapter 5 concludes this dissertation with several remarks.

Chapter 2

GENERATION AND TRANSMISSION EXPANSION PLANNING TOWARDS A 100% RENEWABLE FUTURE

2.1. Nomenclature

We provide a detailed notation list for this chapter.

1) Sets:

$G \,/\, R \,/\, L$	Conventional generator / renewable generator / transmission line
$S \,/\, V$	Sending/receiving bus of transmission lines
C	Bus mapping of conventional generators, renewable generators, and demand
$X^G \,/\, X^R$	Candidate conventional / renewable generator
X^L	Candidate transmission line
T	Planning horizon (years)
H	Operation horizon (hours)
M	Planning / operation time index mapping
N	Control mapping between units and investable years

2) Indices:

$g \,/\, r \,/\, \ell$	Conventional generator / renewable generator / transmission line
d	Demand
n	Bus
ω	Scenario

k Iteration counter for C&CG algorithm

o Iteration counter for L-shaped algorithm

$t\,/\,h$ Planning / operating time index. $(t,h) \in M$

3) Parameters:

$IC^G_{g,t}/IC^R_{r,t}$ Investment cost for gth conventional / rth renewable generator in tth year [$]

$IC^L_{\ell,t}$ Investment cost for ℓth transmission line in tth year [$]

$OC_{g,h}$ Operating cost for gth generator in hth hour [$/MWh]

$PC_{d,h}$ Load-shedding cost for unserved load in dth demand in hth hour [$/MWh]

$B^G\,/\,B^L$ Investment budget for generators / transmission lines [$]

$K_t]$ Contingency criterion for system units in tth year

A_ℓ Line reactance of ℓth transmission line under base MVA [p.u.]

FL_ℓ Flow capacity of ℓth transmission line [MW]

$\overline{PL}^G_g$ Capacity limit of gth conventional generator [MW]

$\underline{\Delta}_n\,/\,\overline{\Delta}_n$ Angle limit of phase angle at nth bus [rad]

4) Uncertain Parameters:

$\overline{PL}^R_{r,h}(\omega)$ Available active power of rth renewable generator in hth hour [MW].

$P_{d,h}(\omega)$ Active demand of dth load in hth hour [MW].

5) Variables:

$x^G_{g,t}/x^R_{r,t}$ Binary expansion decision for gth conventional / rth renewable generator in tth year. $x = 1$ means built; $x = 0$ otherwise.

$x^L_{\ell,t}$ Binary expansion decision for ℓth transmission line. $x = 1$ means built; $x = 0$ otherwise.

$y^G_{g,t}/y^R_{r,t}$	Binary availability indicator for gth conventional / rth renewable generator in tth year. $y = 1$ means available; $y = 0$ otherwise.
$y^L_{\ell,t}$	Binary availability indicator for ℓth transmission line. $y = 1$ means available; $y = 0$ otherwise.
$a^G_{g,t}\,/\,a^R_{r,t}$	Binary outage indicator for gth / rth generator. $a = 1$ means outage; $a = 0$ otherwise.
$a^L_{\ell,t}$	Binary outage indicator for ℓth transmission line. $a = 1$ means outage; $a = 0$ otherwise.
$p^G_{g,h}(\omega)$	Scheduled active power of gth conventional generator in hth hour under scenario ω [MW].
$p^R_{r,h}(\omega)$	Scheduled active power of rth renewable generator in hth hour under scenario ω [MW].
$r_{d,h}(\omega)$	Scheduled load shedding in dth demand in hth hour under scenario ω [MW].
$f_{\ell,h}(\omega)$	Active power flow through ℓth transmission line in hth hour under scenario ω unit: [MW].
$\delta_{n,h}(\omega)$	Phase angle at nth bus in hth hour under scenario ω [rad].

2.2. Overview

The investigation on the operational patterns and economics of a power system with high renewable penetration attracts tremendous attention from both academia and industry. Despite the clean energy and zero operational cost that renewables have, the stochastic generation pattern of renewables challenges the reliability of power systems, especially when the grid requires a high level of reserves for contingencies. Thus, albeit the investment of renewables is greatly encouraged by the U.S. government and broader community [8], the system planning under high-level penetration of renewables needs to be further investigated.

Heretofore, researchers have done extensive work on the uncertainty-based system planning [6,9–11]. On the one hand, generators and lines are the biggest reliability concern from

an ISO's perspective, which has been omnipresent in many operation problems, *e.g.*, unit commitment problem [12] and transmission planning problem [9]. This type of uncertainty can be effectively tackled by robust optimization (RO), as described in [9] and [13]. The basic idea of RO is to find the worst-case scenario and then make preventative decisions, which in turn also makes the solution highly conservative. On the other hand, the uncertain nature of renewable energy and elastic demand is another challenge for the system planner. A significant amount of literature (*e.g.*, [14] and [15]) also adopts RO to deal with this type of uncertainty by setting conservative boundaries. However, comparatively, stochastic programming (SP) yields less conservative solutions than RO, and we can leverage the historical data to generate scenarios. Particularly, for a large system with high renewable penetration, the spatiotemporal correlations of renewables and demand can be accurately captured by scenario generation, *e.g.*, Monte-Carlo simulation together with a multi-stage scenario tree [16].

Since the uncertainties are multiplex in today's transmission networks, *e.g.*, the binary status of generator/line and continuous generation/load volatility, the combination of SP and RO is a promising formulation with higher reliability. Recently, many works (*e.g.*, [10, 11] and [17]) also consider the hybrid SP and RO formulation with only the continuous formulation, which provides a limited evaluation on uncertainties. There are few works considering the contingencies of power system components and stochastic generation together in a generation and transmission expansion problem (G&TEP), especially under high renewable penetration levels.

The co-optimization of G&TEP under multiplex uncertainties is a nontrivial problem due to its non-convexity and uncertainties involved. A. Moreira *et al.* [6] integrated binary contingencies with continuous uncertainties but did not explore the improvement of algorithms to facilitate the solution. L. Gallego *et al.* [18] used heuristic algorithms to avoid solving an intricate model but obtained local optima. It is not trivial, however, to evaluate how far this obtained optimum is away from the global optimum. We argue that for a large-scale economic assessment like the power system planning, which may involve multiple

planning years and hence does not need to be solved in real time, it would be better if we can have a guaranteed global optimum. This can be viewed as an advantage of our proposed method compared with those intelligent methods. Besides, most of the existing studies solve single-year planning problems [17,19,20], which do not capture certain aspects of power system planning such as the timing of the commissioning or retirement of a generator. In our study, however, the objective is to investigate whether an ultra-high renewable installation in the system is beneficial or not. Since the renewable units are widely considered as units without variable operation costs [21], the economic payback of renewable investment may outperform the conventional units over the long term. Hence, to ensure a fair comparison between different generation technologies, we also take the annuitized investment cost into the consideration and intend to uncover the cost-effectiveness of renewable investment, especially under an ultra-high renewable penetration case.

In order to investigate a 100% renewable system, the correlations between renewables, such as wind power in different regions, wind and solar, wind and demand, *etc.*, are also critical in system operation and planning. At any instant, the system should have enough generation from renewables to cover the demand. However, the system planner has to take a system-wide approach considering mutual support between regions and avoid generation shortage at a particular location. Besides, adequate transmission capacity, even in a degraded N-k line outage scenario, is paramount for inter-regional energy exchange to maintain the system energy balance. The final optimal G&TEP investment ought to consider an optimal generation mix and long-term renewable generation futures. Some researchers (*e.g.*, [20]) argue that 100% is less profitable than a generation mix with conventional units, but this is actually sensitive to the system settings.

In this work, we propose an effective modeling and solution approach for G&TEP towards 100% penetration of renewables. The column-and-constraint generation (C&CG) method developed by [22] can decompose our problem to a master problem and a subproblem. This method has been adopted in numerous studies like [10, 12, 17], and become a mainstream solution methodology for multi-stage RO problems. Besides, as reported in [17]

and [6], solving subproblems consumes the majority of the computational time. We propose to apply the L-shaped method [23] to further facilitate the solution of subproblems, which also enables parallel computing. In the meantime, we specifically consider the short-term and long-term spatiotemporal correlations between renewables and load by leveraging the Monte-Carlo sampling on regional renewables. Figure 2.1 provides a general framework of our proposed methodology.

Compared with the state-of-the-art research, The main contributions of this work are three-fold.

1. We analyze the coordinated system planning under an ultra-high level of renewable penetration and investigate the potential issues of a 100% renewable penetration on an IEEE test system and the WECC system with specific parameter settings.

2. To tackle multiplex uncertainties in the G&TEP, we propose a three-stage multi-year robust co-optimization model with a stochastic recourse. The robust counterpart captures the N-k contingency, whereas sampling-based scenarios considering spatiotemporal correlations between renewables and load realize the demand/renewable uncertainty.

3. The C&CG algorithm is leveraged to decompose the overall problem into a master-slave structure, and the stochastic subproblem is further reformulated based on the duality theory and decomposed by the L-shaped method. The computational efficiency is greatly improved, and multi-scale test cases verify the efficacy of the proposed methodology.

The rest of the work is organized as follows: Section 2.3 describes the mathematical formulation of the G&TEP model; Section 2.4 presents the proposed solution strategy and the detailed flowchart; case studies and a scalability test are analyzed in Section 2.5 and Section 2.6, respectively; Section 2.7 summarizes this work with several remarks.

2.3. Mathematical Formulation of the Generation and Transmission Planning

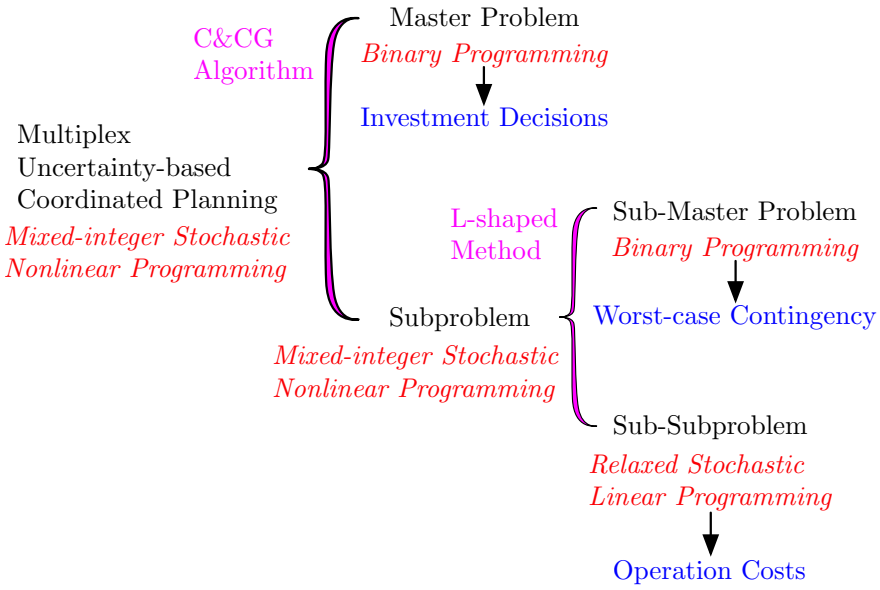

Figure 2.1. Framework of the proposed methodology.

We provide the detailed mathematical formulation of the multiplex uncertainty-based G&TEP in this section. First, we show the deterministic equivalent form (DEF) of the three-stage formulation of the hybrid SP and RO model in (2-1). The term "stage" we used here refers to the mathematical structure of the proposed optimization framework.

$$\min_{\substack{x^G_{g,t},x^R_{g,t},\\ x^L_{\ell,t}}} \sum_t^T \left(\sum_g^{X^G} IC^G_{g,t} x^G_{g,t} + \sum_g^{X^R} IC^R_{r,t} x^R_{r,t} + \sum_\ell^{X^L} IC^L_{\ell,t} x^L_{\ell,t} \right) + \max_{a^G_{g,t},a^L_{\ell,t}} \mathbb{E}_\omega \left\{ \min_{p^G_{g,h},r_{d,h}} \sum_h^H \left[\sum_g^G OC_{g,h} p^G_{g,h}(\omega) + \sum_d^D PC_{d,h} r_{d,h}(\omega) \right] \right\} \tag{2-1}$$

subject to

$$\sum_t^T \left\{ \sum_g^{X^G} IC^G_{g,t} x^G_{g,t} + \sum_g^{X^R} IC^R_{r,t} x^R_{r,t} \right\} \leq B^G, \tag{2-1a}$$

$$\sum_{t}^{T}\left\{\sum_{\ell}^{X^L} IC_{\ell,t}^{L} x_{\ell,t}^{L}\right\} \le B^{L}, \tag{2-1b}$$

$$\forall * \in \{g, r, \ell\},\ \forall (*, t) \in N(*, t):$$

$$\sum_{t' \ne t}^{T} x_{*,t'} = 0, \tag{2-1c}$$

$$\sum_{t' \ge t}^{T} y_{*,t'} = (T - t + 1) \cdot x_{*,t}, \tag{2-1d}$$

$$\sum_{t' < t} y_{*,t'} = 0, \tag{2-1e}$$

$$\sum_{g}^{G} a_{g,t}^{G} + \sum_{r}^{R} a_{r,t}^{R} + \sum_{\ell}^{L} a_{\ell,t}^{L} \le K_t, \quad \forall t, \tag{2-1f}$$

$$\forall \omega:$$

$$\sum_{g|C(g)=n}^{G} p_{g,h}^{G}(\omega) + \sum_{r|C(r)=n}^{R} p_{r,h}^{R}(\omega) - \sum_{\ell|S(\ell)=n}^{L} f_{\ell,h}(\omega) +$$
$$\sum_{\ell|V(\ell)=n}^{L} f_{\ell,h}(\omega) = \sum_{d|C(d)=n}^{D} \{\ P_{d,h}(\omega) - r_{d,h}(\omega)\ \}, \forall n, \forall h, \tag{2-1g}$$

$$f_{\ell,h}(\omega) = y_{\ell,t}^{L}(1 - a_{\ell,t}^{L}) A_{\ell}^{-1} \cdot [\delta_{n|S(\ell)=n,h}(\omega) - \delta_{n|V(\ell)=n,h}(\omega)],$$
$$\forall \ell \in L, \forall (t, h) \in M, \tag{2-1h}$$

$$-y_{\ell,t}^{L}(1 - a_{\ell,t}^{L}) FL_{\ell} \le f_{\ell,h}(\omega), \forall \ell \in X^{L}, \forall (t, h) \in M, \tag{2-1i}$$

$$f_{\ell,h}(\omega) \le y_{\ell,t}^{L}(1 - a_{\ell,t}^{L}) FL_{\ell}, \forall \ell \in X^{L}, \forall (t, h) \in M, \tag{2-1j}$$

$$-(1 - a_{\ell,t}^{L}) FL_{\ell} \le f_{\ell,h}(\omega), \forall \ell \in L \backslash X^{L}, \forall (t, h) \in M, \tag{2-1k}$$

$$f_{\ell,h}(\omega) \le (1 - a_{\ell,t}^{L}) FL_{\ell}, \forall \ell \in L \backslash X^{L}, \forall (t, h) \in M, \tag{2-1l}$$

$$p_{g,h}^{G}(\omega) \le y_{g,t}^{G}(1 - a_{g,t}^{G}) \overline{PL}_{g}^{G}, \forall g \in X^{G}, \forall (t, h) \in M, \tag{2-1m}$$

$$p_{g,h}^{G}(\omega) \le (1 - a_{g,t}^{G}) \overline{PL}_{g}^{G}, \forall g \in G \backslash X^{G}, \forall (t, h) \in M, \tag{2-1n}$$

$$p_{r,h}^{R}(\omega) \le y_{r,t}^{R}(1 - a_{r,t}^{R}) \overline{PL}_{r,h}^{R}(\omega), \forall r \in X^{R}, \forall (t, h) \in M, \tag{2-1o}$$

$$p_{r,h}^{R}(\omega) \le (1 - a_{r,t}^{R}) \overline{PL}_{r,h}^{R}(\omega), \forall r \in R \backslash X^{R}, \forall (t, h) \in M, \tag{2-1p}$$

$$\underline{\Delta}_{n} \le \delta_{n,h}(\omega) \le \overline{\Delta}_{n}, \forall n, \forall h, \tag{2-1q}$$

The objective function (2-1) formulates the investment cost of the proposed generator and transmission line expansions, plus the operating cost of scheduled conventional genera-

tors and possible load shedding.

Constraints (2-1a)-(2-1b) model the investment budget of both generators and transmission lines, which construct the first-stage feasible region. Constraints (2-1c)-(2-1e) represent that once an investment is made in year t, the component will be available for the rest of the planning horizon. Control sets $N(*,t)$ represent the mapping between the candidate units and planning time, in which we categorize the candidate units based on the investable years. These constraints formulate the constraint space for the first stage. Constraint (2-1f) shows the N-k criteria for both generators and transmission lines, where K_t can be adjusted to perform different contingency analyses. This constraint is in the second-stage (the second-stage objective function can be regarded as $\{\mathbf{0}^\top \boldsymbol{a}\}$, in which $\boldsymbol{a}$ is the vector of the outage indicators) formulating the uncertainty set [24]. This uncertainty set is discretely polyhedral.

For the third-stage, we first explain the relationship between t and h. Since we consider a long-term planning problem, traversing 8760 hours for a whole year renders heavy intractability in this model. Hence, we consider a 24-hour operation for the third stage as an analysis of hourly dispatch in one typical day. This operation is also adopted in [20]. Then the time index mapping set M can be described as

$$M = \big\{(t_1, h_1), ..., (t_1, h_{24}), (t_2, h_{25}), ...(t_2, h_{48}), ...\big\}.$$

We also note that this design further generalizes the application of selecting representative hours/days. When a system planner intends to select more representative hours to perform the G&TEP study, it is trivial to adjust the set M by increasing the number of hours. This also shows that our proposed framework is highly flexible and general to be expanded to the extent the system planner would like to use in G&TEP problems.

Notably, the outage indicator in our formulation is a day-based variable. As we indicated, the third-stage problem can be regarded as a 24-hour economic dispatch problem. For such operation problems, the contingency is often considered throughout the operation horizon, *i.e.*, 24 hours [25]. Practically, 94% of the planned and operational outage have a duration

of over 2 hours and 34.6% of them are over 48 hours [26]. In some works of system planning, the horizon-long contingency is also adopted [11]. For the sake of simplicity, since we choose one representative day for one year with multiple uncertain scenarios, we slightly abuse our notation and use a year-based index to represent a day-based variable, *e.g.*, $a^G_{g,t}$. Besides, for the third-stage operation problem, we choose using one representative day with multiple scenarios to investigate the short-term correlation between regional renewables and load, which can be better captured by hourly operations, as also adopted in [20].

Particularly, constraint (2-1g) is the nodal balance constraint, and constraint (2-1h) defines the DC line flow equations. Note that here, we slightly abuse the notation that the per unit reactance A_ℓ should be normalized under the system base MVA. Constraints (2-1i)-(2-1l) are line flow limitation constraints for both candidate and existing lines. Constraints (2-1m)-(2-1p) are the generation capacity constraints for both candidate and existing conventional and renewable generators. Note that the renewable generators can be dispatched, and thus we permit the renewable curtailment. Constraint (2-1q) shows the phase angle limitation. We can find that all of the third-stage variables are associated with the scenario index ω for different realizations of renewable generation and load. Note that the binary variables and the variable multiplications such as in (2-1h), (2-1i), (2-1j), (2-1m) and (2-1o) render this model mixed-integer nonlinear.

The proposed model (2-1) is a very general framework for the hybrid stochastic and robust optimization-based system planning and can be easily adjusted or expanded to include more constraints regarding various research directions or industrial applications. In our case studies, for example, we do not have any existing generator and we can hence disregard constraints (2-1n) and (2-1p) in the formulation. We also modify (2-1) to incorporate unique case settings such as the regional N-1 contingency and multiple investments in one candidate bus, which can be achieved by replacing constraint (2-1f) with (1-1r) and adding constraint

(1-1s) respectively as shown below.

$$\sum_{g}^{G^z} a_{g,t}^{G} + \sum_{r}^{R^z} a_{r,t}^{R} + \sum_{\ell}^{L^z} a_{\ell,t}^{L} \leq K_t, \qquad \forall t, \forall z \in Z, \tag{1-1r}$$

$$\sum_{g|C(g)=n^{cg}}^{G} x_{g,t}^{G} + \sum_{r|C(r)=n^{cr}}^{R} x_{r,t}^{R} \leq 2, \qquad \forall t, \forall n, \tag{1-1s}$$

where z denotes the region indicator, Z is the total region set, n^{cg} denotes the candidate bus for thermal generators, and n^{cr} denotes the candidate bus for renewable generators.

2.4. Problem Decomposition and Solution Strategy

The model described in Section 2.3 presents an intractable three-stage mixed-integer nonlinear problem with stochastic recourse. However, we can decompose the original problem into a structure of mixed-integer linear programming (MILP) master problem and mixed-integer bilinear subproblem, which can be solved iteratively based on the theory of the C&CG algorithm [22]. Linear relaxation techniques can tackle the nonlinearity of the subproblem. Besides, the subproblem can be further decomposed by the L-shaped method [23].

Figure 2.2 depicts the overall solution workflow. Generally, we adopt the C&CG algorithm to decompose the problem into a master-slave structure, and the L-shaped algorithm then further decomposes the subproblem by different scenarios. We will explain the procedure and notations of Figure 2.2 in the problem formulation. To be more concise, we use compact form below.

2.4.1. Master Problem

We formulate the master problem in the C&CG procedure as in (2-2). $\boldsymbol{x}$ denotes the first-stage variables, $\boldsymbol{z}$ denotes the third-stage variables with iteration index k', which encloses all the past iterations before the current iteration k. $\boldsymbol{IC}$ and $\boldsymbol{PC}$ represent the vectors of investment costs and penalty costs, whereas $\boldsymbol{p}^G$ and $\boldsymbol{r}$ denote the vectors of generator dispatch and load shedding. ϕ is an auxiliary variable that formulates a relaxed lower bound of the second-stage problem. The constraints for third-stage variables are (2-2d).

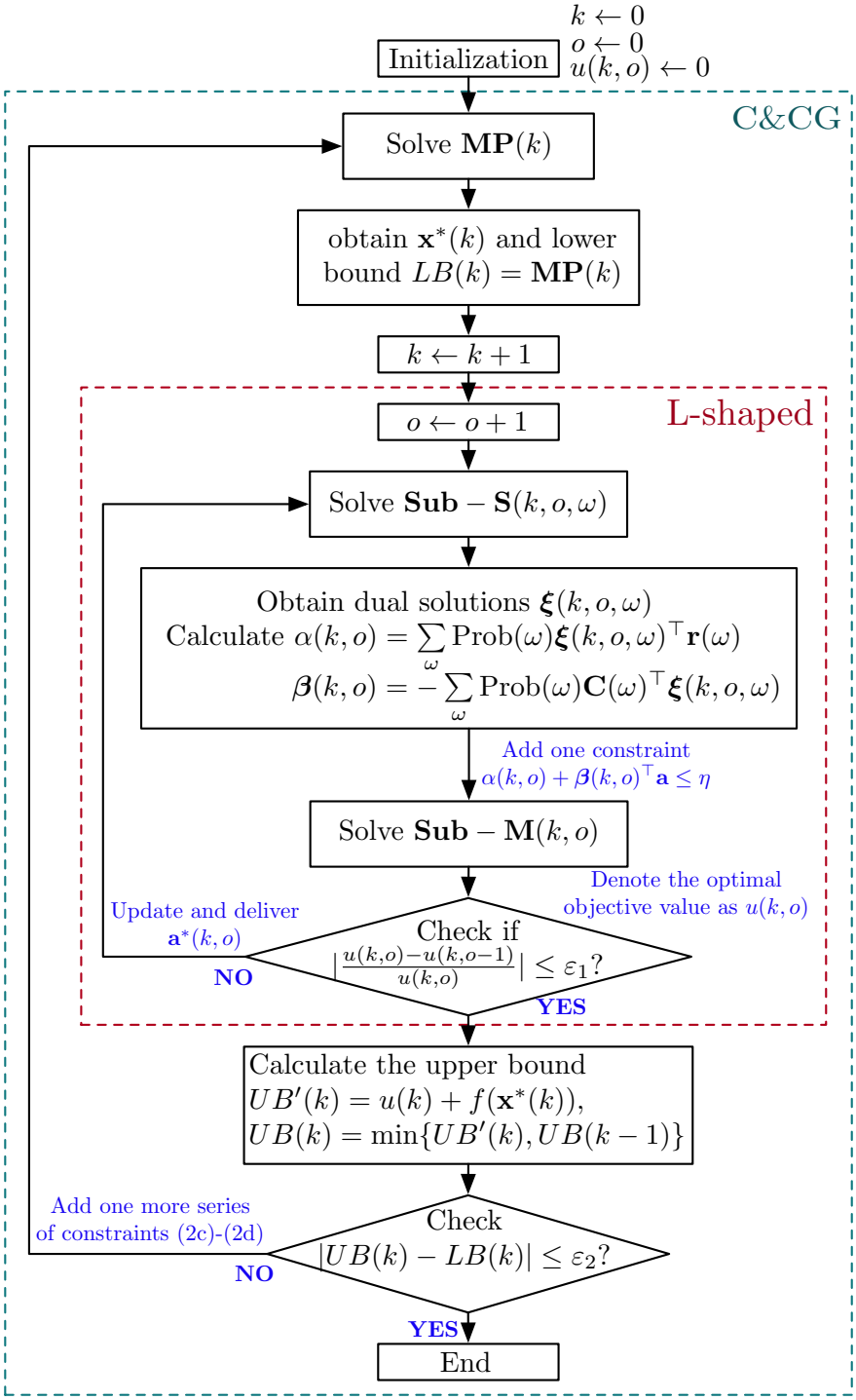

Figure 2.2. Workflow of the proposed algorithm.

Note that the second-stage variables $\boldsymbol{a}$ are fixed here, which are delivered from the subproblem. Hence, the master problem now becomes a deterministic MILP problem that can be efficiently tackled via off-the-shelf solvers. Here, $\boldsymbol{x}$ includes the first-stage variables, *i.e.*, $x^G_{g,t}, x^R_{r,t}, x^L_{\ell,t}, y^G_{g,t}, y^R_{r,t}, y^L_{\ell,t}$ and $\boldsymbol{z}$ includes the third-stage variables, *i.e.*, $p^G_{g,h}, p^R_{r,h}, r_{d,h}, f_{\ell,h}, \delta_{n,h}$.

$$\boldsymbol{MP} = \min_{\boldsymbol{x},\boldsymbol{z}} f(\boldsymbol{x}) + \phi \tag{2-2}$$

subject to

$$\text{Constraints (2-1a)-(2-1e)} \tag{2-2a}$$

$$f(\boldsymbol{x}) = \boldsymbol{IC}^\top \boldsymbol{x}, \tag{2-2b}$$

$$\phi \geq \mathbb{E}_\omega \Big\{ \boldsymbol{OC}^\top \boldsymbol{p}^G + \boldsymbol{PC}^\top \boldsymbol{r} \Big\}, \ \forall k' \leq k, \tag{2-2c}$$

$$\text{Constraints (2-1g)-(2-1q)}, \quad \forall k' \leq k \tag{2-2d}$$

2.4.2. Subproblem

The subproblem of the C&CG procedure is constructed from the second- and third-stage problems, *i.e.*, the problem determining the worst-case scenario of contingency. Here, $\boldsymbol{a}$ includes the second-stage variables, *i.e.*, $a^G_{g,t}, a^R_{r,t}, a^L_{\ell,t}$.

$$\max_{\boldsymbol{a}} \ \mathbb{E}_\omega \Big\{ \min_{\boldsymbol{p},\boldsymbol{r}} \ \boldsymbol{OC}^\top \boldsymbol{p}^G + \boldsymbol{PC}^\top \boldsymbol{r} \Big\} \tag{2-3}$$

subject to

$$\text{Constraints (2-1f)-(2-1q)}. \tag{3a}$$

Note that the first-stage variables in the constraints become fixed parameters obtained from the master problem in the previous iteration. Since the inner minimization problem of (2-3) has linear programming characteristics, according to the strong duality theory, it

is equivalent to rewrite (2-3) to its dual form (2-4), after giving an objective handle for the second-stage.

$$\boldsymbol{Sub} = \max_{\boldsymbol{a}} \quad \mathbf{0}^{\top}\boldsymbol{a} \; + \mathbb{E}_{\omega}\left\{ \max_{\boldsymbol{\pi}} \; Q(\boldsymbol{a},\boldsymbol{\pi}) \right\} \tag{2-4}$$

subject to

$$Q(\boldsymbol{a},\boldsymbol{\pi}) \in \Gamma_{\boldsymbol{a},\boldsymbol{\pi}}, \tag{2-4a}$$

where $Q(\boldsymbol{a},\boldsymbol{\pi})$ represents the dualized objective function, $\boldsymbol{\pi}$ is the vector of all dual variables in (2-3) and $\Gamma_{\boldsymbol{a},\boldsymbol{\pi}}$ consists of the constraint space. For better demonstration, problem (2-4) is further altered to a minimization problem (2-5) where we rewrite $\Gamma_{\boldsymbol{a},\boldsymbol{\pi}}$ in the form of (2-5a)-(2-5c). Specifically, (2-5a) constructs the uncertainty set, (2-5b) formulates the operational constraints, and (2-5c) ensures the dual feasibility of the Karush–Kuhn–Tucker condition.

$$\boldsymbol{Sub} = \min_{\boldsymbol{a}} \quad -\mathbf{0}^{\top}\boldsymbol{a} \; + \; \mathbb{E}_{\omega}\left\{ \min_{\boldsymbol{\pi}} \; -Q(\boldsymbol{a},\boldsymbol{\pi}) \right\} \tag{2-5}$$

subject to

$$\text{Constraint (1f)}, \tag{2-5a}$$

$$\boldsymbol{D}(\omega)\boldsymbol{\pi} \le \boldsymbol{r}(\omega) - \boldsymbol{C}(\omega)\boldsymbol{a}, \tag{2-5b}$$

$$\boldsymbol{\pi} \ge 0. \tag{2-5c}$$

Note that in the objective function, $Q(\boldsymbol{a},\boldsymbol{\pi})$ includes the first-stage decisions $\boldsymbol{x}^{*}$ determined from the master problem. This subproblem shows a typical two-stage stochastic mixed-integer bilinear minimization structure. Furthermore, linear relaxation techniques, *e.g.*, the Big M method (see Appendix A), can effectively relax the bilinear parts without sacrificing accuracy. As the binary nature of the integer variables tightens the convex relaxation, we can ensure the accuracy of the obtained solution. According to the stochastic

L-shaped method [23], the two-stage mixed-integer stochastic program with linear recourse and finite support is also decomposable, as shown in the following.

2.4.2.1. L-shaped Master Problem

$$\boldsymbol{Sub-M} = \min_{\boldsymbol{a}} \quad -\mathbf{0}^{\top}\boldsymbol{a} \ + \eta \tag{2-6}$$

subject to

$$\text{Constraint (1f)}, \tag{2-6a}$$

$$\alpha_{o'} + \boldsymbol{\beta}_{o'}^{\top}\boldsymbol{a} \leq \eta, \quad \forall o' \leq o \tag{2-6b}$$

In the L-shaped master problem, η is an auxiliary variable, $\alpha_{o'}$ and $\boldsymbol{\beta}_{o'}$ are subgradients computed from the dual of the L-shaped subproblem, which will be discussed in the next subsection. Note that this formulation is for the single-cut L-shaped algorithm.

2.4.2.2. L-shaped Subproblem

$$\boldsymbol{Sub-S}(\omega) = \min_{\boldsymbol{\pi}} \quad -Q(\boldsymbol{a}^{*}, \boldsymbol{\pi}) \tag{2-7}$$

subject to

$$\boldsymbol{D}(\omega)\boldsymbol{\pi} \leq \boldsymbol{r}(\omega) - \boldsymbol{C}(\omega)\boldsymbol{a}^{*} : \qquad \boldsymbol{\xi}(\omega), \tag{2-7a}$$

$$\boldsymbol{\pi} \geq 0. \tag{2-7b}$$

When the L-shaped master problem yields an optimal solution of $\boldsymbol{a}^{*}$, the subproblem receives this solution and solves the operation problem. Let $\boldsymbol{\xi}^{*}(\omega)$ denote the optimal dual

solution of the operation constraints (7a). After solving ω individual L-shaped subproblems, which can be done in parallel, the subgradients for each iteration can be computed as follows.

$$\alpha_o = \sum_{\omega} \text{Prob}(\omega) \boldsymbol{\xi}_o^*(\omega)^\top \boldsymbol{r}(\omega),$$
$$\boldsymbol{\beta}_o = -\sum_{\omega} \text{Prob}(\omega) \boldsymbol{C}(\omega)^\top \boldsymbol{\xi}_o^*(\omega).$$

Afterwards, the L-shaped master problem receives an optimality cut (2-6b). Finally, the inner iteration loop for the L-shaped procedure determines the final worst-case contingency $\boldsymbol{a}^*$ and sends it back to the C&CG master problem. As we enable load shedding, the feasibility of all problems is guaranteed, and the feasibility cut is therefore negligible.

The proposed algorithm guarantees its convergence by the finite extreme points of the uncertainty set and finite support in the second-stage stochastic recourse according to the convergence analysis [22] and [23]. For the convergence speed, according to Figure 2.2, the C&CG procedure does not influence the convergence of the embedded L-shaped method, which means we still retain the fast convergence of the C&CG method [22]. The convergence of the C&CG part relies on the convergence of the L-shaped algorithm, which is guaranteed by the finite support in the stochastic recourse. The motivation of leveraging the L-shaped method for the subproblem is that solving the original subproblem consumes the majority of the computational time, as reported in [6] and [17]. We enjoy the merit of parallel computing to facilitate solving subproblems when the L-shaped method is applied.

2.5. Case Studies

This section provides results and discussions for case studies on a modified IEEE 30-bus system based on [27]. We aim to investigate the benefit of ultra-high renewable penetration towards 100% in a long-term planning problem. We implement all of the experiments in GAMS 25.0.3 [28] with CPLEX 12.8 and run it on a 2.60GHz Windows PC with a 6-core Intel i7 CPU and 8GB RAM. We also leverage a GAMS-embedded parallel computing tool, *i.e.*, Gather-Update-Solve-Scatter (GUSS) [29], for the L-shaped subproblem to improve the

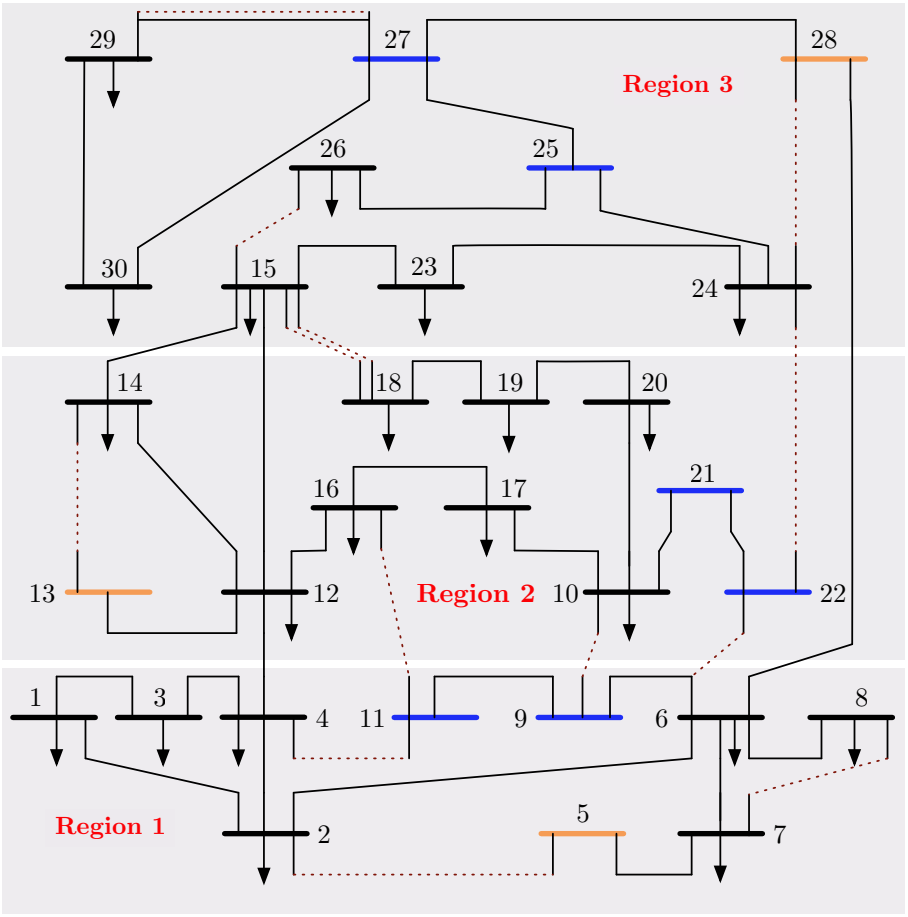

Figure 2.3. System topology of the modified IEEE 30-bus system.

computational efficiency.

To illustrate our proposed methodology, we modify the IEEE 30-bus system to have reduced transmission lines and no existing generators. Figure 2.3 provides the detailed topology, where the blue and orange buses indicate the candidate locations for building wind and solar generators, respectively. Thermal generators can be invested in any load bus. The dashed lines indicate the candidate transmission lines. Table 2.1 shows the investment information, whose reference can be found in [30–32]. The modified IEEE 30-bus system has a total daily peak power demand as 2,000 MW, distributed to the three regions. And we set the load shedding penalty cost as \$1,000/MWh.

Table 2.1. Data for Candidate Generation Units.

Generation Type	Operating cost [$/MWh]	Maximum capacity [MW]	Overnight capital cost [M$]
Wind	0	300	390
Solar	0	150	170
Thermal	41.2	300	67.8
Trans. Line	0	600	50

2.5.1. Scenario Generation & Reduction

There are three regions in the system, where different scenario sets of renewable and demand are applied. To verify the investment performance considering the spatiotemporal correlation between renewables and load, we create the scenario set for each region individually by using Monte-Carlo simulation on three different datasets of renewable output from [33]. Figure 2.4 depicts the regional 24-hour sequential wind, solar, and demand scenarios. The average capacity factors of wind and solar are 45.14% and 28.86%, respectively. We also assume that the two neighbored wind buses in Figure 2.3 share the same wind output time series, and one can easily simulate scenarios with respect to different time series for more detailed spatiotemporal studies.

For the spatiotemporal correlations between renewables and load, after sampling on three different datasets with respect to three different regions, we apply the Fast Backward/Forward method embedded in the GAMS SCENRED toolbox to reduce the scenario number according to the balance between the number of scenarios and the solution accuracy. This strategy is generally an approximation of the complete scenario tree benchmarked by different criteria such as the Fortet-Mourier metric [34] and L_r-distance [35], which have been widely adopted in many stochastic system planning works *e.g.* [36] and [37]. To capture the spatiotemporal correlations between renewables and demand, we use three temporal datasets for real renewable outputs and demand in three forecast zones in the ERCOT area as a basis

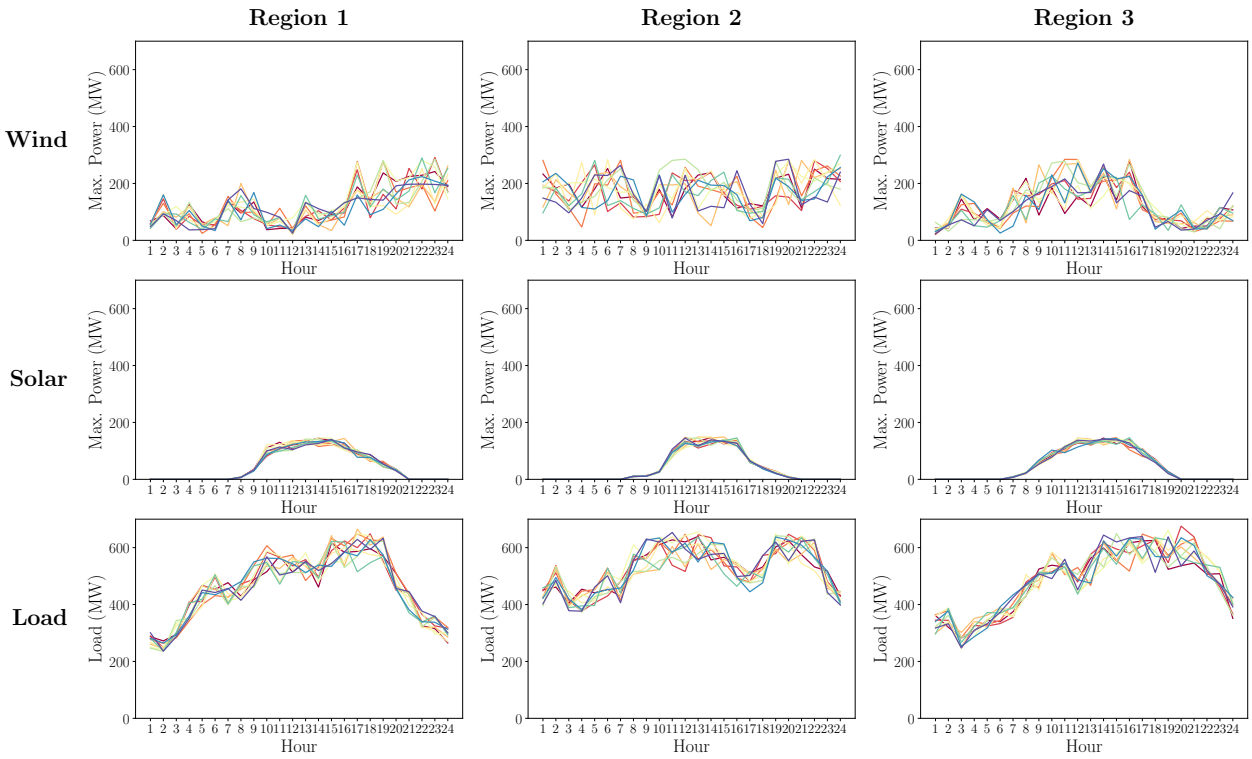

Figure 2.4. Regional scenario (10 for each).

for our Monte-Carlo sampling to create the scenario sets. With both the demand and renewable uncertainties being taken into consideration, the proposed G&TEP framework can yield planning results according to the correlations between multiplex uncertainties. It is also imperative to indicate that a more accurate and efficient scenario generation/reduction technique concerning the spatiotemporal correlation between uncertainties is of great future research interest, to which our proposed framework in this work can easily adapt.

To balance the tradeoff between the accuracy and tractability, we test different scenario sets by running a one-year planning problem where two respective investments on solar and wind generators are mandatory, as shown in Figure 2.5, and the highest computational time stands for the highest time of solving subproblems among all iterations. Since the difference in objective function values between 100 scenarios and 1000 scenarios is within 2%, we argue that the set of 100 scenarios is accurate enough to perform the following analyses. Besides, Figure 2.5 also validates the necessity of using decomposition techniques for solving

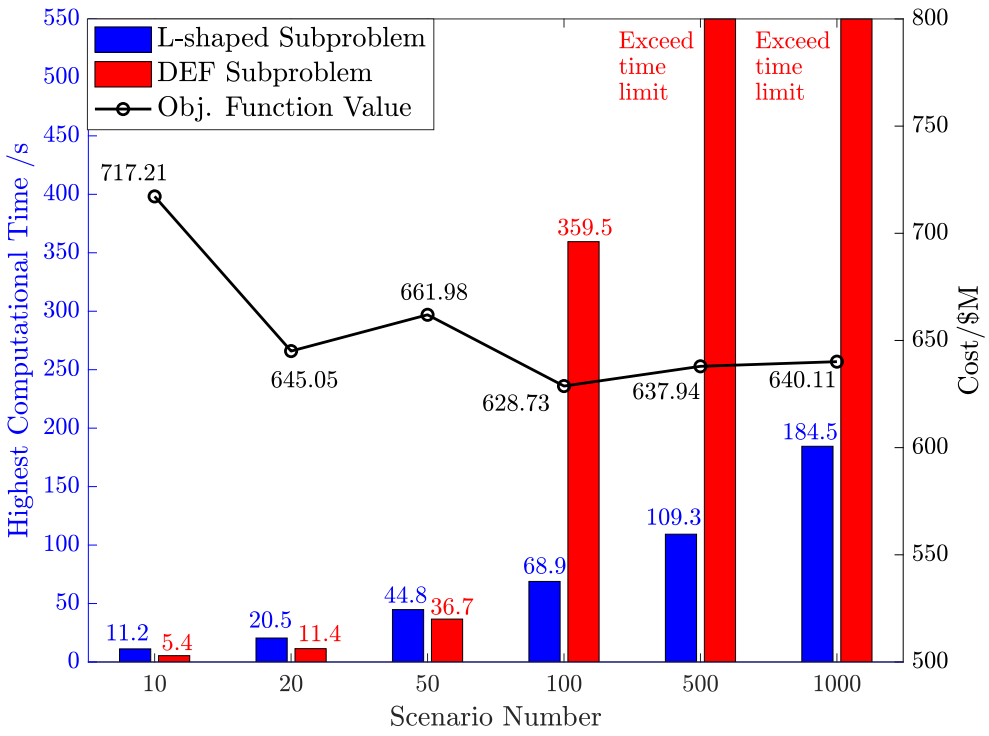

Figure 2.5. Comparison for different sizes of scenarios.

stochastic subproblems, as the computational burden grows exponentially with the increasing number of scenarios in the DEF problem as in [10] and [17], but grows linearly in the L-shaped problem in our work.

2.5.2. Case Studies: Towards 100% Renewable Penetration

We design three cases to show the pathways to achieve 100% renewable penetration. We apply the N-1 criterion to each region. Each candidate bus can build two generators in each year. The algorithmic convergence gap ε_2 is set to be 0.1%, and the solver's MIP gap is set as 0.01%.

- *Case 1.* $900M generation investment budget (6yrs);
- *Case 2.* $9,000M generation investment budget (6yrs);
- *Case 3.* $9,000M generation investment budget. Thermal units can only be installed

in the first year. All the thermal units will phase out by 20% capacity per year (6yrs) with a salvage income.

To be more practical, for thermal units, we consider a 5% annual inflation rate of the fuel price. For renewable energy, the investment cost has a discount factor of 5% per year as the technology develops. The salvage price of phased out thermal generators is 40% of the investment cost. The total system demand also increases by 5% per year. Table 2.2 shows the investment decisions, costs and system information obtained from the three cases.

For the salvage income, we directly add a salvage income term in the objective function of (2-1). The salvage of generators includes the sales of the salvageable parts of the unit, recycling worn-out equipment, and re-utilizing the designated real estate [37]. According to [38], the salvage value for generators is calculated based on a linear relationship with the proportion of the used life and the remaining life, resulting the following equation:

$$S = C_{replace} \cdot \frac{R_{remain}}{R_{component}}$$

in which $C_{replace}$ is the replacement cost that is about 80% of the initial investment cost, R_{remain} is the remaining life and $R_{component}$ is the component lifetime. We also refer to [39] for the lifetime of a pulverized coal power plant as 30 years. Thus, in year 6, the remaining lifetime of such unit is 24 years, and thus the salvage income should be $80\% \cdot (24/30) = 64\%$ of the investment cost. Considering the demolition cost and the personnel cost, we set the salvage value for a thermal unit in our study as 40% of the investment cost. We will revisit *Case 1* and *Case 2* in subsection E by considering the investment cost annuitization to further assess the economic aspects of renewable installations.

1). General investment plan and operation

For the generation investment, on the one hand, since we consider the N-1 criterion in each region, the system planner invests in a large amount of generation capacity, especially when the renewable is installed (*e.g.*, the total capacity in *Case 3* is 152.9% higher than

Table 2.2. Investment Portfolio Report for the 30-bus System.

Gen. Investment*	Case 1	Case 2	Case 3
Year 1	2, 4, 6, 8, 10, 12, 14, 15, 18, 24, 29, 30	2, 4, 5, 5, 10, 9, 14, 15, 18, 21, 22, 24, 27, 29	4, 5, 5, 9, 9, 11, 11, 16, 21, 21, 22, 22, 25, 25, 27, 27, 30
Year 2	None	21	9, 13, 21, 22, 25, 25
Year 3	None	None	None
Year 4	None	None	None
Year 5	None	None	None
Year 6	None	None	None
Line Investment	Case 1	Case 2	Case 3
Year 1	4-11, 7-8, 6-22, 9-10, 15-26, 22-24,	4-11, 7-8, 6-22, 9-10, 15-18, 15-26, 22-24	4-11, 7-8, 6-22, 9-10, 15-18, 15-24, 15-26, 22-24
Year 2-6	None	None	None
Gen. Invest. Cost	$813.6M	$2,812.9M	$7,237.4M
Gen. Opera. Cost	$5,976.81M	$3,542.70M	$168.93M
Line Invest. Cost	$300M	$350M	$400M
Load Shed Cost	0	0	$1,079.43M
Salvage Income	0	0	$81.36M
Total Cost	$7,090.41M	$6,705.60M	$8,754.40M
Avg. Load Shed Portion	0%	0%	0.96%
Avg. Renewable Curtailment	0%	7.75%	12.11%
Final Renewable Percentage	0%	42.86%	100%

* The numbers indicate the buses built with thermal, wind and solar.

the peak load). While the system planner has already known the demand increase rate for the later years, most of the new generation capacity is invested in the first year to meet the peak demand growth in the following years. However, since the renewable installation is limited compared with the thermal installation, and considering the yearly increasing system demand and the unit contingencies every year, there are still investments after the first year especially in *Case 2* and *Case 3* to ensure the system reliability. Another noteworthy issue is renewable curtailment. The peak curtailment in *Case 3* is 18.29% when the average curtailment across the scenarios also reaches 12.11%. They are comparatively small since the excess renewable power can be used to support other regions. Future works considering using the curtailed energy to provide ancillary services and storage charging can be envisioned.

On the other hand, for the transmission investment, new transmission lines tend to be built in the first year to prepare for the worst-case contingency in the subsequent years. The new transmission build-out is mostly to accommodate the injections from the new generators. Notably, lines 6-8, 12-15, and 6-28 are reported to be the ones with the most frequent outage under the worst-case contingency. Thus, in the investment portfolio, lines 7-8, 6-22, and 22-24 are always built in the three cases to aid power transmission. The system finally achieves the 100% renewable penetration level in the 6th year in *Case 3*. The 100% is based on the generation capacity percentage.

By comparing *Case 1* and *Case 2* in Table 2.2, we can find that if we have a sufficient investment budget at the beginning, it is more profitable to invest in a proper generation mix of thermal, wind and solar technologies from the system perspective. Since we consider a long-term investment plan, the operation cost for 6 years in *Case 1* far outnumbers the investment cost, whereas the renewable generators only have a one-time cost for installation.

By comparing *Case 2* and *Case 3* in Table 2.2, we find that the operation cost is further greatly decreased in *Case 3*, but the investment cost and the load shedding cost increase significantly, which results in a higher total cost. However, as the investment cost of renewable technology decreases yearly, in the long-term planning, the system will tend to have higher renewable penetration approaching 100%, which will be detailed in subsection 2.5.4.

Under the current setting, we do not consider the energy storage and the time-shifting demand response since we would like to investigate the cost-effectiveness of renewables only from their own economic aspects. However, it is imperative to state that considering 100% renewable energy without any energy storage or demand response is not beneficial for all circumstances. It can be envisioned that energy storage and demand response can greatly reduce the need for over-installation of renewable generation.

2). Interregional support with spatiotemporal correlations

The spatiotemporal correlations between renewables and regional differences of the uncertainty also influence the investment portfolio of renewables. When we do not consider any storage device or time-shifting demand response in our model, there could be a large amount of load shedding in a particular region when the renewable generation in that region is very low. However, such a situation can be largely mitigated with adequate transmission capacity with the other regions since the variation of renewable generation output from each region tends to cancel out over a large geographical area to provide a more stable output. Hence, by using the proposed scenario generation and the optimization framework, the new generators are built in the way that they can provide interregional energy support when needed, based on their spatiotemporal correlations.

On the one hand, from the long-term investment perspective, in Figure 2.4, the diurnal wind output in Region 1 is small, which incentivizes the investment of the solar unit at bus 5 and reduces the investment of wind units in the region. Besides, in *Case 3*, the lines connecting Region 2 and Region 3, *i.e.*, line 15-18 and line 22-24, are all constructed to help Region 3 cover its demand as the wind output in Region 3 in a long run is relatively lower compared with the other regions.

On the other hand, from the short-term operation perspective, in the 6th year of *Case 3*, we particularly analyze one operation scenario. Figure 2.6 depicts the active power flow in the tie-lines with Region 1, *i.e.*, lines 9-10, and 6-22. It can be seen that the power support from the other regions reaches the peak value at hour 10 due to the lack of local

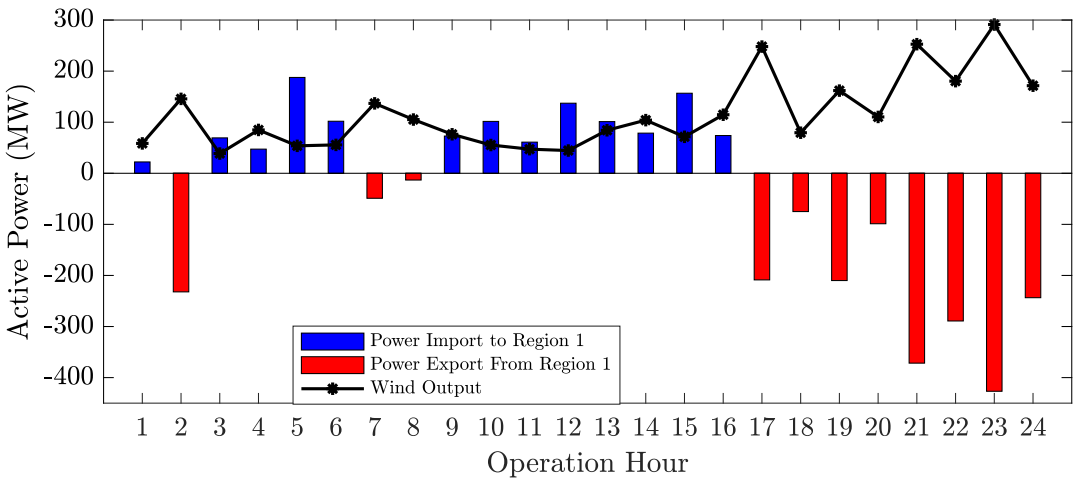

Figure 2.6. Power transfer from/to Region 1: one scenario.

wind power in Region 1, but Region 1 can export active power to the other regions at night when the wind output increases. This phenomenon validates the interregional support when the spatiotemporal correlations between renewables and load are present.

2.5.3. Case Studies: Contingency Criterion

Next, we elaborate on the contingency criterion and the impact of the worst-case contingency by comparing the following *Case 4* with the previous *Case 3*.

- *Case 4*. We apply no contingency criterion in all regions, *i.e.*, the robust counterpart in the model is omitted. The other settings are the same as *Case 3*.

Figure 2.7 demonstrates the generator's installation details of these two cases. It can be seen from the results that when the N-1 contingency criterion is applied for each region in *Case 3*, the system needs to have more renewable generators installed to secure the demand. Particularly for the worst-case contingency, the system is prone to increase the investment in generators to provide more contingency reserves, which is also one of the reasons of the huge installations in *Case 3*.

2.5.4. Case Studies: Long-term Cost-effectiveness

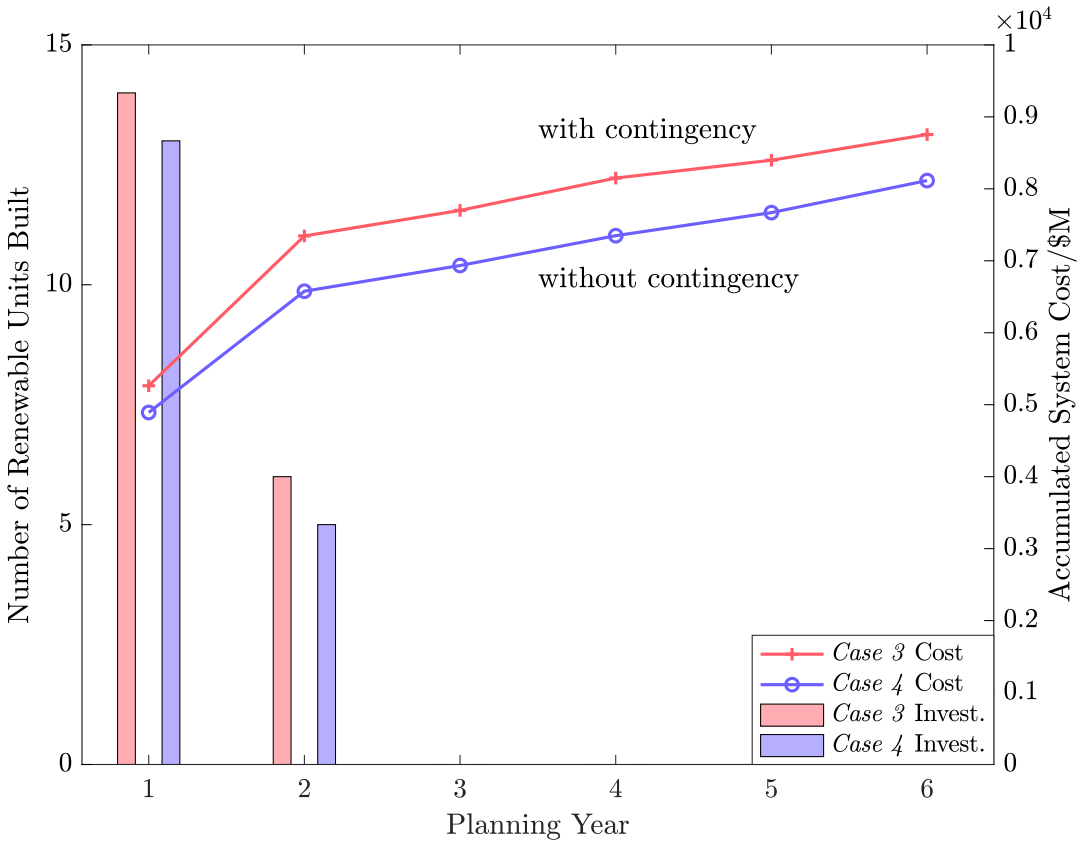

Figure 2.7. Comparison in the contingency criterion.

To further elaborate the cost-effectiveness of long-term investment in renewables, especially for the 100% renewable penetration, we carry out two case studies of a 12-year expansion in the following:

- *Case 5.* $12,000M generation investment budget (12yrs);
- *Case 6.* $12,000M generation investment budget. Thermal units can only be installed in the first year. All the thermal units phase 10% capacity out per year (12yrs).

It is straightforward that the 100% renewable penetration is accomplished in the 11th year in *Case 6*. We enable the transmission expansion between any two connected buses for the annually increasing demand, and the other system settings are the same as in the previous case studies. Figure 2.8 depicts the investment plans and system costs. Accordingly, the salvage value of conventional generators is set as 25% of the investment cost in this case.

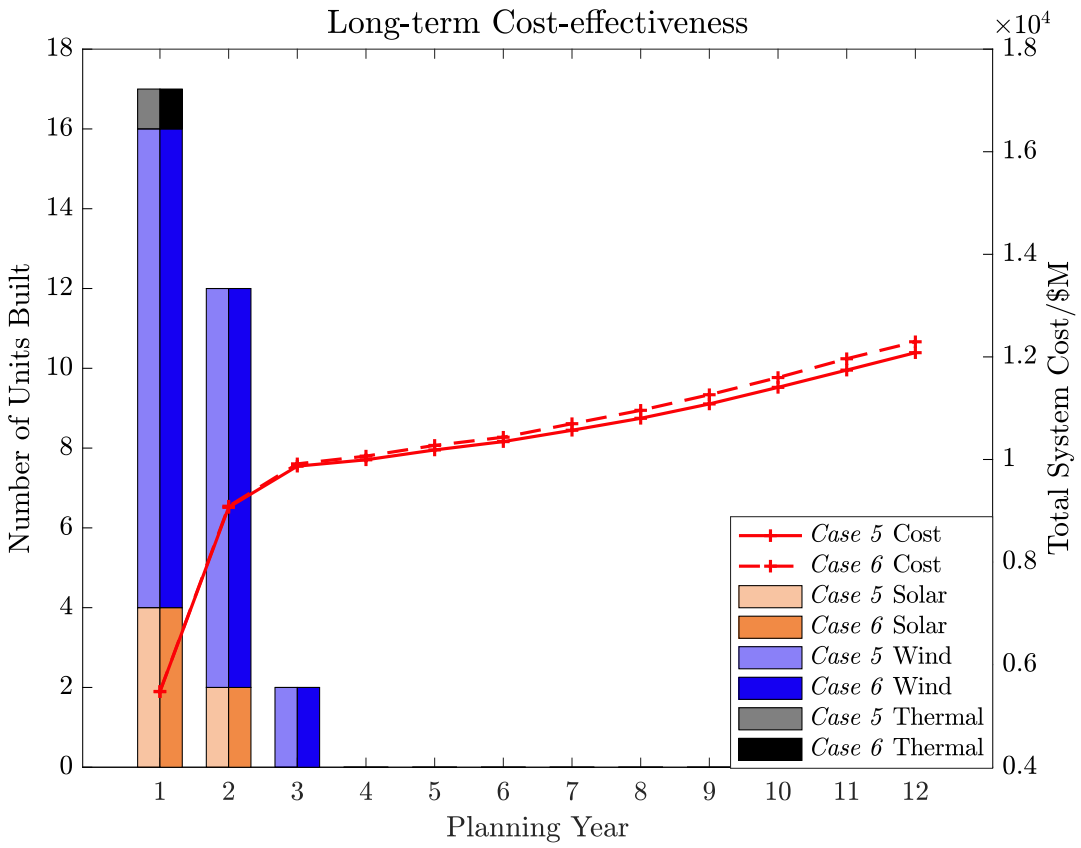

Figure 2.8. Investment plans and system cost of the long-term planning.

In *Case 5*, the installation of one thermal unit is mainly to balance the load shedding caused by stochastic generation, even when the interregional support from renewables has already largely mitigated this issue. And in *Case 6* when the condition changes that the thermal units are no longer able to fully provide energy, the system planner is still prone to invest one thermal unit due to the high load shedding cost. Though the 100% renewable case, *i.e.*, *Case 6*, still has a slightly higher cost than *Case 5*, we argue that the final cost difference highly depends on how we choose the system parameters. Nonetheless, from these two cases, we can see the potential of renewable generation's long-term cost-effectiveness. In *Case 5* when the phasing-out is not allowed, the system in the 12th year still reaches 96.43% renewable penetration, which implies the long-term economic payoff is higher than conventional units. It should also be noted that different settings of renewable-based G&TEP

studies could lead to different findings (*e.g.*, [20]) but the proposed general framework still applies.

2.5.5. Case Studies: Investment Annuitization

In many investment studies, investors often consider annuitization of the investment cost to distribute the investment over the planning horizon. Hence, in this section, we illustrate the effect of considering the annuitization of the investment cost with the same settings of *Case 1* and *Case 2*. We keep the same investment budget as in *Case 1* and *Case 2*, and consider a general annual interest rate i of the investment as 6.04% computed from the weighted average cost of capital (WACC) of 5.7% [40]. We adopt the investment annuitizing method from Appendix A in [40] as we first calculate the annual discount factor (DF_t) by

$$DF_t = \frac{1}{(1+i)^t},$$

then the annualized capital cost (ACC_g) and the discounted investment cost ($IC_{g,t}$) used in the objective function can be computed as

$$ACC_g = OCC_g \cdot \frac{i \cdot (1+i)^{LT_g}}{(1+i)^n - 1},$$
$$IC_{g,t} = ACC_g \cdot \sum_{t' \le \min\{LT_g, T^{\text{remain}}\}} DF_{t'},$$

where OCC_g denotes the overnight capital cost, LT_g denotes the generator lifetime, and T^{remain} denotes the remaining time of the planning horizon. The annual increase in thermal units' fuel cost and demand still applies.

Table 2.3 tabulates the results of the revisited *Case 1* and *Case 2* with considering the annuitized investment cost. In both cases, there is no load shedding. Thanks to the annuitization, the investment of generators can now be distributed to later planning years. Compared with the previous *Case 1* and *Case 2*, we find that both total costs do not differ much, and the results in *Case 1* remain nearly the same except for some investments

Table 2.3. Investment Portfolio with the Investment Annuitization.

Investment*	Revisited Case 1	Revisited Case 2
Year 1	10 0 0 6	5 6 1 6
Year 2	0 0 0 0	0 3 0 1
Year 3	1 0 0 0	0 0 1 0
Year 4	1 0 0 0	1 0 0 0
Year 5	0 0 0 0	0 1 0 0
Year 6	0 0 0 0	0 0 0 0
6-yr Invest. Payment	\$762.67M	\$4,153.67M
Line Invest. Cost	\$300M	\$350M
Gen. Opera. Cost	\$5,978.10M	\$2,163.77M
Total Cost	\$7,040.78M	\$6,667.44M

* The integrals denote the numbers of invested thermal, wind, solar generators, and line.

distributed to later years. But in *Case 2*, the renewable installation is more prioritized, as the investment annuitization makes the renewable investment more competitive with thermal investments. However, we can still draw similar conclusions that a proper generation mix of conventional and renewable technologies renders a more cost-effective planning portfolio if the budget allows for renewable installations. As the annuitization method has already taken the generators' lifetime into account [40], we do not apply the technique of considering salvage incomes [37] in the revisited cases. Leveraging the annuitization method can make the investment in multi-year planning more comparable, which should be included in a more realistic G&TEP study. Also, it is noteworthy that the performance is highly sensitive to the selected WACC determined by the tax rate and expected returns on equity and debt.

2.6. Scalability Test

To validate the scalability of the proposed framework, we modify the WECC 243-bus system based on [41] for G&TEP studies and carry out the scalability test. Four generation technologies are included, *i.e.*, coal, combined-cycle, wind, and solar. We carry out a

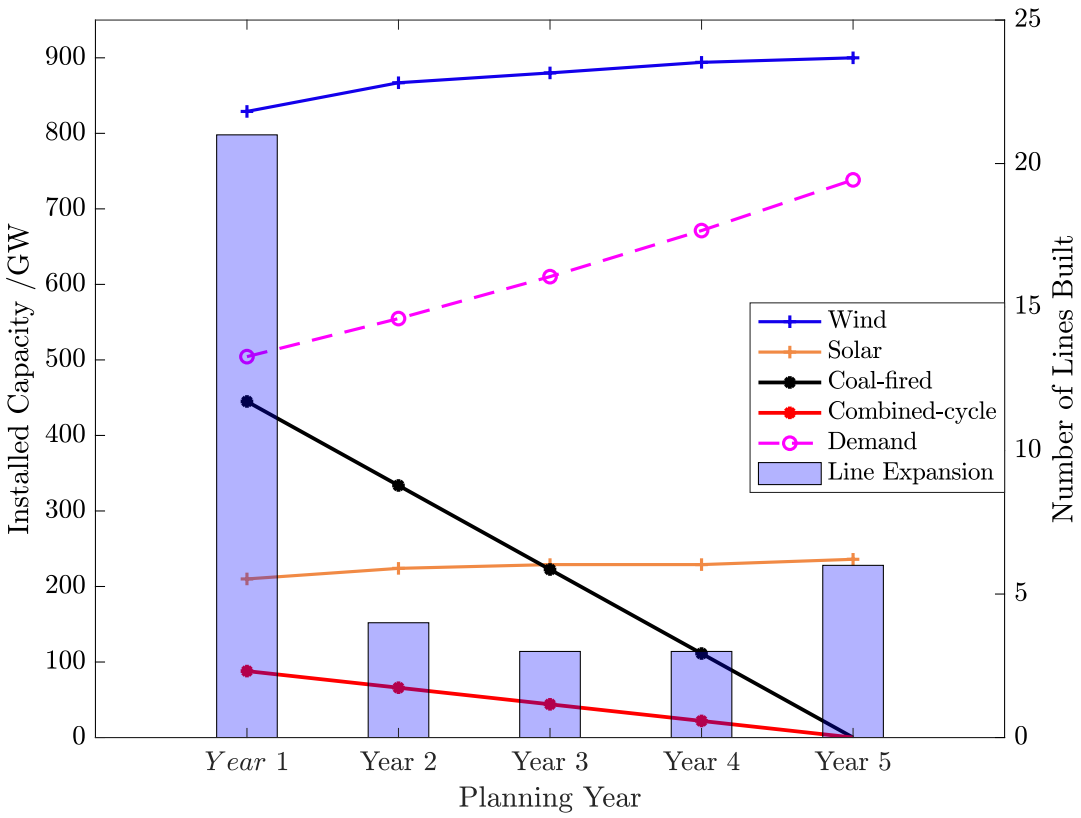

Figure 2.9. Installed capacity for the WECC system.

regionally N-1 contingency-constrained 5-year planning problem with the hourly operation. The number of combinatorial scenarios, in this case, is further reduced to 10 to reduce the computational burden. And we enable the phasing-out of conventional units as in *Case 3*.

Figure 2.9 depicts the scheduled installed capacity for each generation technology and transmission line, where we can observe that the investment in solar and wind generators grows sharply in the first year and keeps increasing, due to the 25% annual phasing-out rate of the conventional generators. The computational time of the WECC simulation is 27 hours, which is comparably reasonable concerning the scale of the multi-year stochastic and robust planning problem.

2.7. Discussions

To clarify the scope of our work and how it should be used as a reference for both

academia and industry, we provide several discussions on this work.

1. Though the day-based contingencies have already been adopted in this work and other works, *e.g.*, [11, 25], the contingencies of power system components can be evaluated in a practically smaller time resolution.

2. Using only a few representative days has been found to be not enough, and more representative days should be included in more realistic studies of power systems with large amounts of renewable [42].

3. In the case studies, multiple economic factors can affect the optimized planning portfolio, *e.g.*, the increasing fuel cost, decreasing renewable investment cost, annual interest rate, and the salvage income. Different economic settings may lead to a different result, but the conclusion of the renewable-involved G&TEP study should hold similarly as discussed in the work. Besides, when we consider a longer term of planning, renewables will begin to show the potential of higher cost-effectiveness in the G&TEP.

4. Other practical factors should be taken into account in future research to make more precise investment decisions for investors, including but not limited to the employment of energy storage devices, more types of renewables, demand response, and ancillary services.

This work aims at providing a general framework and a solution algorithm, which can be applied to different uncertainty-based G&TEP studies. The case studies in this work are carried out under simplified simulation settings and demonstrate different renewable investment scenarios under specific parameters. The observations of a more complete and comprehensive long-term G&TEP study for realistic large-scale power systems may vary from this work as the findings are dependent upon many sensitive parameters including cost, discount rate and other detailed operational constraints.

2.8. Summary

This work introduces a novel modeling and solution strategy for the generation and transmission expansion planning under ultra-high renewable penetration, which allows analyses

of discrete and continuous uncertainties. Based on the theoretical derivation and numerical experiments, several remarks are in order:

- We propose a general hybrid stochastic and robust model that can accurately capture the uncertainties in the modern power grid, whose discrete and continuous features are taken into consideration with high flexibility.
- We propose a combinatorial solution strategy leveraging the state-of-the-art C&CG and L-shaped algorithms that can efficiently tackle intractable and multiplex uncertainty-based planning problems.
- We investigate the long-term renewable cost-effectiveness in the test results. A proper portfolio of generation mix of the conventional and renewable generation is shown to be beneficial under our specific problem settings, and we also pave a way for future discussions on the 100% renewable penetration potentials by investigating the long-term cost-effectiveness of the renewable generation.

Chapter 3

STOCHASTIC MARKET OPERATION FOR COORDINATED TRANSMISSION AND DISTRIBUTION SYSTEMS

3.1. Nomenclature

We provide a detailed notation list for this chapter.

1) Sets:

$T \,/\, D$	Transmission (T) / distribution (D) system
$G^T \,/\, G^D$	Conventional thermal generator of T / D system
$E \,/\, I$	Renewable generator / connected bus
Q	Network reconfiguration set
$L^T \,/\, L^D$	Load of T / D system
$F^T \,/\, F^D$	Line of T / D system
$A^D \,/\, A^D_T$	Bus of D system / with substation
F^D_Q	Configurable line of D system
$S \,/\, N$	Sending / receiving bus of line
C	Generator or injection mapping with bus
H	Time horizon
O	Iteration

2) Indices:

$g^T \,/\, g^D$	Indices for conventional generators in T/D system

r^T / r^D	Indices for renewable generators in T/D system
ℓ^T / ℓ^D	Indices for loads in T/D system
f^T	Indices for transmission lines
mn	Indices for connected distribution branches
n^T / n^D	Indices for nodes in T/D system
i	Indices for boundary buses
ω^T / ω^D	Indices for operating scenarios in T/D system
o	Indices for iteration counter
h	Indices for time (hours)
c	Indices for multiple D systems
q	Indices for configurable swtich in D system

3) Parameters (in both T and D, otherwise specified):

PC	Penalty cost [$/MWh]
R / X / B	Resistance / reactance / susceptance [p.u.]
RD / RU	Ramp-down / up limits [MW/h]
SD / SU	Shut-down / start-up cost [$]
MO / MD	Minimum ON / OFF time limits [h]
$P_f^{T,\max}$	Active power flow limits [MW]
$Y_{mn}^{D,\max}$	Upper limit of the branch current [A]
$V^{\min}$ / $V^{\max}$	Lower/Upper limit of the nodal voltage [kV]
$P_g^{\min}$ / $P_g^{\max}$	Active power output limits of generators [MW]

4) Uncertainties (in both T and D):

$P_{r,h}^{\max}(\omega)$	Maximum available renewable power [MW]
$L_{\ell,h}(\omega)$	Nodal demand [MW]
$\Pr_{\omega}$	Probability for scenario ω

5) Binary Variables:

$u_{g,h}^{T} \,/\, d_{g,h}^{T}$	Start-up/shut-down indicator for generators
$i_{g,h}^{T}$	Unit commitment indicator for generators
$z_{q,h,c}$	Distribution configuration indicator

6) Continuous Variables:

$p_{(g,r)}^{(T,D)} \,/\, p_i$	Active generation output / power injection
$q_{(g,r)}^{D} \,/\, q_i$	Reactive generation output / power injection
$p_n^D \,/\, q_n^D$	Active / reactive node injection
p_f^T	Active line flow
$p_{mn}^D \,/\, q_{mn}^D$	Active / reactive feeder flow
x_{mn}^D	Line orientation variable
$v_n \,/\, \delta_n^T$	Squared nodal voltage magnitude / angle
y_{mn}^D	Squared branch current
s_ℓ	Active load shedding

3.2. Overview

Unit commitment (UC) and economic dispatch (ED) have been of capital importance in the market operations for system operators in the world. The coordination between transmission and distribution systems (T-D coordination) in the market operation has attacked

great attention. The primary motivation for T-D coordination is based on the fact that the distribution system has become active due to the increasing deployment of smart grid technologies including distributed energy resources (DERs), electric vehicles, microgrids, *etc.* The system dynamics within the distribution networks can propagate to the transmission side and *vice versa* [43]. A recent report from California Independent System Operator (CAISO) [44] supports this motivation. It indicates that, due to the growing penetration of the DERs, Independent System Operator (ISO), which regulates the upstream market in the transmission level, needs to attain more visibility on the downstream markets to reinforce its decision-making.

In the conventional market hierarchy, ISOs and utilities carry out UC and ED problems within their respective territories. The upstream operators make scheduling decisions according to the estimated information from the downstream aggregators [45]. Without the T-D coordination, the power mismatch at the boundary node between transmission and distribution systems proliferates as distribution systems become more and more active [46]. To cope with the issue of power mismatches, Z. Li *et al.* [47] proposed a distributed paradigm that ISO delivers its optimal locational marginal price (LMP) to distribution system operators (DSOs), whereas DSOs return their optimal energy demand to ISO. The mutually observable information in the T-D coordination should be limited to protect the confidentiality of stakeholders [47].

Recently, based on this decentralized framework, many papers have considered more elements and more efficient algorithms. P. Li *et al.* [48] built a distributionally robust optimization framework considering system uncertainties and adopted an analytical target cascading algorithm to decentralize the problem. R. Nejad *et al.* [49] and J. Zhao *et al.* [50] focused on the integrated system restoration using the alternating direction of multipliers method (ADMM) to decentralize the problem. M. Arpanahi *et al.* [51] proposed a decentralized framework for T-D coordination that considers robust optimization for the uncertainties, while using an enhanced ADMM algorithm to solve. A. Nawaz *et al.* [52] proposed a probabilistic coordination method to select one stochastic scenario to solve the T-D coordinated

problem. However, most of the works focus on ED or OPF, instead of the UC, which could not serve as a general reference for electricity market operations. It is also reasonable that the algorithms proposed above lie in the category of the augmented Lagrangian method, which would fail if integer variables are present in the problem.

For the modeling of T-D coordination, recently, research on this topic gains prevalence, and potential modeling frameworks from the perspective of DSOs can be categorized into three types, *i.e.*, centralized, decentralized, and transactive models, which are summarized in [7]. Among the models discussed therein, Model 3, *i.e.*, the distribution node utility model, acts as a transitional model from the centralized operation to the decentralized operation, where the ISO and DSOs take the responsibilities of market operations in the transmission and distribution level, respectively, and they exchange information in the boundary substation. The natural compatibility with the current market practice is the major advantage of this model [7]. Based on this framework, we propose a three-stage stochastic co-optimization for the T-D coordinated UC and ED. In this scheme, the ISO regulates the coordination between the transmission and distribution systems, where the transmission system operation is under control of the ISO and the distribution system operation is under control of the DSO. As in the current industry's practice [53], the ISO carries out the transmission-level market operations including UC and ED with the distribution-level inputs from DSOs. DSOs are utilities that own the distribution network with aggregated DERs. It is also noteworthy that the current research on decentralized or transactive models is fruitful and few are investigating centralized frameworks due to the computational hurdle. However, before the fully decentralized distribution operations, the industry needs a transitional model that allows the ISOs to take the local distribution information into account while regulating the coordination [54]. Hence, in the proposed market hierarchy, the ISO performs the day-ahead transmission-level UC and ED with the aggregated distribution information, and DSOs perform the distribution-level ED. The ISO does not need to attain detailed distribution system information, which protects the local utilities' confidentiality.

Apart from the scheduling, the distribution-level network reconfiguration drastically

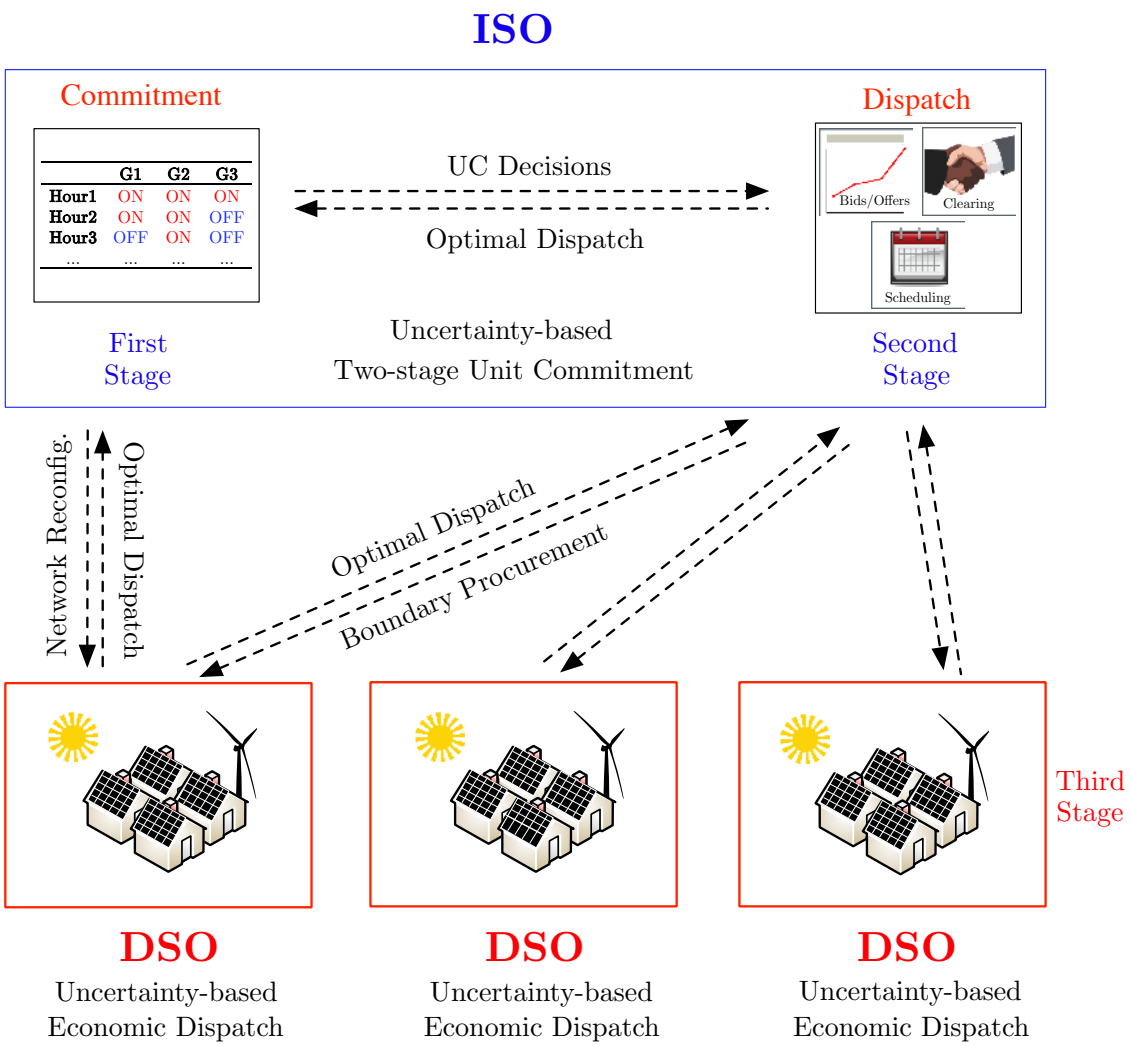

Figure 3.1. Proposed coordinated market paradigm.

influences the market operation in the distribution level, and the influence will propagate to the transmission level [55]. Since the ISO monitors the T-D coordination, the topology changes in the active distribution network (ADN) should be taken into consideration in the ISO's operation. Besides, utilities are using an hourly decision-making process to evaluate and perform the reconfiguration [56]. Considering that the reconfiguration cannot be changed frequently in one day and should be determined in a day-ahead manner [56], in this work, we add the network reconfiguration decisions in the first stage together with the UC decisions.

In summary, we propose a market paradigm for the T-D coordinated power system, which is depicted in Figure 3.1. Mathematically, the ISO needs to solve a mixed-integer linear programming (MILP) model for transmission-level UC with distribution network reconfigurations, when DSOs need to solve convex programming models for distribution-level ED. In the first stage, the ISO performs the transmission UC and determines the distribution network reconfiguration, then delivers the information to the subsequent stages. Then, the ED operation is carried out in the second stage and delivers the optimal boundary offer to the third stage. The structure of the first and second stages forms a two-stage transmission-level stochastic UC [57]. Finally, DSOs perform their ED operations in the third stage based on the determined configuration from the first stage and the energy offer from the second stage.

For the solution strategy, there has been a significant number of studies towards the efficient solution of large-scale SP problems. One of the most commonly used strategies is the Benders decomposition or the L-shaped method [58]. For multi-stage SP as in this work, scenario-wise decomposition like the progressive hedging [59] and stage-wise decomposition like the approximate dynamic programming [60] are discussed in the literature. Particularly for the dynamic programming category, stochastic dual dynamic integer programming (SDDiP) has been an effective method for multi-stage stochastic optimization [61], with various recent applications on power systems. J. Zhou *et al.* [62] proposed a SDDiP model for multi-stage stochastic UC and enhanced the algorithm by a regularized level approximation for Lagrangian cuts. M. Hjelmeland *et al.* [63] adopted SDDiP solving a hydropower scheduling problem with binary expansion on state variables and found that the strengthened Benders cut presented the highest performance score. T. Ding *et al.* [64] leveraged the SDDiP method in the distribution system planning with a multi-stage nested decomposition algorithm. Though it is well recognized that SDDiP attains fast convergence and accuracy, it could not solve the proposed T-D coordinated market operation. The reasons are twofold: 1) Each time stage in the SDDiP needs to assume the complete information of both transmission and distribution networks, which compromises the stakeholders' privacy; 2) There is

no evidence that the SDDiP retains global convergence if recourse problems are nonlinear.

Thus, since our work is both scenario-wise and stage-wise complex, we employ the nested L-shaped method [58] for the proposed T-D coordinated market operation. Furthermore, we enhance the conventional nested L-shaped method and algorithmically extend it to a multi-stage mixed-integer convex programming. To the best of the authors' knowledge, this is the first work implementing a practical T-D market operation considering accurate network modeling/reconfiguration and uncertainties.

Based on the state-of-the-art research, the main contribution of this work is summarized below.

- We formulate the T-D coordinated UC&ED problem considering the distribution network reconfiguration. System-independent scenario sets capture the uncertainty of renewable generation and elastic demand for each system.
- We propose a market paradigm for the T-D coordinated UC&ED. This paradigm considers the coordination between different market stakeholders while protecting their confidentiality, which ISOs can easily adopt.
- We extend the generalized Benders decomposition method to a nested and stochastic version, which can efficiently solve the proposed T-D coordinated market operation model. We also theoretically prove and analyze the algorithmic convergence.

3.3. Mathematical Formulation of T-D Coordinated Market Operations

We detail the three-stage stochastic formulation and the convexified AC branch flow for the distribution part in this section. The overall formulation of the stochastic T-D coordinated UC & ED is separated and distributed in the following subsections. Note that the DC power flow is adopted in the transmission level in order to mimic the industrial practice. In contrast, the second-order cone programming (SOCP)-based convexified AC branch flow formulation is adopted in the distribution network to retain accuracy.

3.3.1. The First Stage: ISO's UC Problem

The first stage solves a conventional transmission UC problem with the optimal distribution network reconfiguration, which is performed by the ISO.

$$\mathbf{K}_1 = \min_{\substack{u^T_{g,h}, d^T_{g,h}, \\ i^T_{g,h}, z_{q,h,c}}} \sum_{h}^{H} SU^T_g u^T_{g,h} + SD^T_g d^T_{g,h} + \mathbb{E}_{\omega^T}\left\{\mathbf{K}_2(\mathbf{x}^*_1, \omega^T)\right\}, \tag{3-1}$$

subject to

$$u^T_{g,h} + d^T_{g,h} \le 1, \qquad \forall g^T \in G^T, \forall h \in H, \tag{3-1a}$$

$$u^T_{g,h} - d^T_{g,h} = i^T_{g,h} - i^T_{g,h-1}, \qquad \forall g^T \in G^T, \forall h \in H, \tag{3-1b}$$

$$\sum\nolimits_{h-MO_g+1}^{h} u^T_{g,h} \le i^T_{g,h}, \qquad \forall g^T \in G^T, \forall h \in H, \tag{3-1c}$$

$$\sum\nolimits_{h-MD_g+1}^{h} d^T_{g,h} \le 1 - i^T_{g,h}, \qquad \forall g^T \in G^T, \forall h \in H, \tag{3-1d}$$

$$u^T_{g,h}, d^T_{g,h}, i^T_{g,h}, z_{q,h,c} \in \{0, 1\}, \tag{3-1e}$$

where $\mathbf{K}_2(\mathbf{x}^*_1, \omega^T)$ denotes the second-stage recourse and $\mathbf{x}^*_1 = [u^{T*}_{g,h}, d^{T*}_{g,h}, i^{T*}_{g,h}]$. "*" stands for obtained and fixed decisions. Constraints (3-1a) and (3-1b) enforce the binary exclusiveness of the start-up and shut-down indicators; constraints (3-1c) and (3-1d) model the minimum ON/OFF time; constraint (3-1e) indicates the binary nature of the variables. Note that there is no distribution configuration variable, *i.e.*, $z_{q,h,c}$, in the objective function and constraints, which is determined based on the information sent back from the DSO's stage.

3.3.2. The Second Stage: ISO's ED Problem

The second stage formulates a transmission-level ED problem based on the UC decisions

delivered from the first stage, which is detailed in (3-2). For each ω^T:

$$\mathbf{K_2}(\mathbf{x}_1^*, \omega^T) = \min_{p_{g,h}^T, s_{\ell,h}^T} \sum_h^H \left\{ \sum_{g^T}^{G^T} f^T(p_{g,h}^T) + \sum_{\ell^T}^{L^T} PC_\ell^T s_{\ell,h}^T \right\} + \sum_c w_c \cdot \mathbb{E}_{\omega_c^D} \left\{ \mathbf{K_3}(\mathbf{x}_2^*, \mathbf{y}^*, \omega_c^D) \right\} \tag{3-2}$$

subject to

$$\sum_{g^T|C(g^T)=n^T}^{G^T} p_{g,h}^T - \sum_{i_c|C(i_c)=n^T}^{I} p_{i_c,h} + \sum_{r^T|C(r)=n^T} p_{r,h}^T - \sum_{f^T|S(f^T)=n^T}^{F^T} p_{f,h}^T + \sum_{f^T|N(f^T)=n^T}^{F^T} p_{f,h}^T = \sum_{\ell^T|C(\ell^T)=n^T}^{L} \{ L_{\ell,h}^T(\omega^T) - s_{\ell,h}^T \}, \quad \forall n^T, \forall h, \tag{3-2a}$$

$$p_{f,h}^T = X_{f^T}^{-1} [\delta_{n|S(n^T)=f^T,h}^T - \delta_{n|N(n^T)=f^T,h}^T], \quad \forall f^T, \forall h, \tag{3-2b}$$

$$-P_{f,h}^{T,\max} \le p_{f,h}^T \le P_{f,h}^{T,\max}, \quad \forall f^T, \forall h, \tag{3-2c}$$

$$i_{g,h}^{T,*} P_{g,h}^{T,\min} \le p_{g,h}^T \le i_{g,h}^{T,*} P_{g,h}^{T,\max}, \quad \forall g^T, \forall h, \tag{3-2d}$$

$$0 \le p_{r,h}^T \le P_{r,h}^{T,\max}(\omega^T), \quad \forall r^T, \forall h, \tag{3-2e}$$

$$p_{g,h}^T - p_{g,h-1}^T \le RU_g^T (1 - u_{g,h}^{T,*}) + u_{g,h}^{T,*} P_{g,h}^{T,\min}, \quad \forall g^T, \forall h, \tag{3-2f}$$

$$p_{g,h-1}^T - p_{g,h}^T \le RD_g^T (1 - d_{g,h}^{T*}) + d_{g,h}^{T,*} P_{g,h}^{T,\min}, \quad \forall g^T, \forall h, \tag{3-2g}$$

where $\mathbf{K_3}(\mathbf{x}_2^*, \mathbf{y}^*, \omega_c^D)$ denotes the third-stage recourse, $\mathbf{x}_2^* = [z_{q,h,c}^*]$, and $\mathbf{y}^* = [p_{i_c,h}^*]$. w_c stands for the weight of different distribution systems pertaining to the importance of the corresponding system. For instance, hospitals and military regions require higher priority of electricity supply, which results in higher weight w_c in this model ($w_c \in (0, 1]$ and $\sum w_c = 1$). We also adopt the piecewise-linear thermal generation cost function as $f^T(\cdot)$ and enable load shedding to retain feasibility. Constraint (3-2a) enforces the active power balance, and constraint (3-2b) represents the DC power flow equation in the transmission lines. Line flow constraints and active power generation constraints for thermal generators are described in constraints (3-2c) and (3-2d), respectively. In constraint (3-2e), the renewable generation is

limited within the uncertain upper bound *w.r.t.* the scenario index ω^T. For brevity, we only give the scenario index to uncertain parameters, but the variables should be associated with the scenario index as well. Besides, constraints (3-2f) and (3-2g) represent the ramp-up/down limits, respectively.

3.3.3. The Third Stage: DSO's ED Problem

From DSOs' perspective, the third stage establishes a distribution-level ED, as shown in (3-3). Since DER generators are fast-responsive, their UC decisions are not considered. However, the distribution network is reconfigurable [56] and controlled by the ISO in the proposed T-D coordinated market operation. Note that ω_c^D for each c in the third stage is independent of each other and ω^T in the second stage. For each c and ω_c^D:

$$\mathbf{K_3}(\mathbf{x}_2^*, \mathbf{y}^*, \omega_c^D) = \min_{p^D_{g,h,c}, s^D_{\ell,h,c}} \sum_{h}^{H} \Bigg\{ \sum_{g^D}^{G^D} f^D(p^D_{g,h,c}) + \sum_{\ell^D}^{L^D} PC^D_{\ell,c} s^D_{\ell,h,c} \Bigg\} \tag{3-3}$$

subject to

$$P^{D,\min}_{g,h,c} \le p^D_{g,h,c} \le P^{D,\max}_{g,h,c}, \qquad \forall g^D, \forall h, \tag{3-3a}$$

$$-RD^D_{g,c} \le p^D_{g,h+1,c} - p^D_{g,h,c} \le RU^D_{g,c}, \qquad \forall g^D, \forall h, \tag{3-3b}$$

$$0 \le p^D_{r,h,c} \le P^{D,\max}_{r,h,c}(\omega_c^D), \qquad \forall r^D, \forall h, \forall \omega_c^D, \tag{3-3c}$$

$$0 \le y^D_{mn,h,c} \le x^D_{mn,h,c} Y^{D,\max}_{mn,h,c}, \qquad \forall (m,n) \in F^D_Q, \forall h, \tag{3-3d}$$

$$0 \le y^D_{mn,h,c} \le Y^{D,\max}_{mn,h,c}, \qquad \forall (m,n) \in F^D \backslash F^D_Q, \forall h, \tag{3-3e}$$

$$(p^D_{mn,h,c})^2 + (q^D_{mn,h,c})^2 \le y^D_{mn,h,c} v_{m,h,c}, \qquad \forall (m,n) \in F^D, \forall h, \tag{3-3f}$$

$$x^D_{mn,h,c} \ge 0, \qquad \forall (m,n) \in F^D, \forall h, \tag{3-3g}$$

$$x^D_{mn,h,c} = 0, \qquad \forall n \in A^D_T, \forall h, \tag{3-3h}$$

$$x^D_{mn,h,c} + x^D_{nm,h,c} = 1, \qquad \forall n \in F^D \backslash F^D_Q, \forall h, \tag{3-3i}$$

$$x^D_{mn,h,c} + x^D_{nm,h,c} = z^*_{q,h,c}, \qquad \forall n \in F^D_Q, \forall h, \tag{3-3j}$$

$$\sum_{n:(m,n)\in F^D} x_{mn,h,c} = 1, \qquad \forall m \in A^D \backslash A^D_T, \forall h, \tag{3-3k}$$

$\forall n^D, \forall h:$

$$p^D_{n,h,c} = \sum_{k:n\to k} p^D_{nk,h,c} - \sum_{j:j\to n} (p^D_{nj,h,c} - R_{nj} y^D_{nj,h,c}), \tag{3-3l}$$

$$q^D_{n,h,c} = \sum_{k:n\to k} q^D_{nk,h,c} - \sum_{j:j\to n} (q^D_{nj,h,c} - X_{nj} y^D_{nj,h,c}), \tag{3-3m}$$

$$v_{n,h,c} - v_{m,h,c} \le M(1 - x^D_{nm,h,c}) + (R^2_{mn} + X^2_{mn}) y^D_{mn,h,c} - 2(R_{mn} p^D_{mn,h,c} + X_{mn} q^D_{mn,h,c}), \tag{3-3n}$$

$$v_{n,h,c} - v_{m,h,c} \ge -M(1 - x^D_{nm,h,c}) + (R^2_{mn} + X^2_{mn}) y^D_{mn,h,c} - 2(R_{mn} p^D_{mn,h,c} + X_{mn} q^D_{mn,h,c}), \tag{3-3o}$$

$$p^D_{n,h,c} = \sum_{g^D|C(g^D)=n} p^D_{g,h,c} + \sum_{i_c|C(i_c)=n} p^*_{i_c,h} + \sum_{r^D|C(r^D)=n} p^D_{r,h,c} - \sum_{\ell^D|C(\ell^D)=n} \left\{ L^D_{\ell,h,c}(\omega^D_c) - s^D_{\ell,h,c} \right\}, \tag{3-3p}$$

$$q^D_{n,h,c} = \sum_{g^D|C(g^D)=n} q^D_{g,h,c} + \sum_{i_c|C(i_c)=n} q_{i_c,h} + \sum_{r^D D|C(r^D)=n} q^D_{r,h,c} - \sum_{\ell^D|C(\ell^D)=n} q^D_{\ell,h,c}(\omega^D_c), \tag{3-3q}$$

$$V^{\min}_{n,h,c} \le v_{n,h,c} \le V^{\max}_{n,h,c}, \tag{3-3r}$$

where $f^D(\cdot)$ represents the piecewise-linear cost function. The constraints for non-reconfigurable branches are identical to the transmission lines in the second-stage problem, while the constraints for reconfigurable branches are with the reconfiguration decisions, as shown in constraints (3-3d) and (3-3e).

We cast a SOCP relaxation for power flow modeling. Constraint (3-3f) is the convex SOC constraint. Note that we neglect shunt impedances for simplicity. k, j, m are notations for connected buses. We also assume that the distribution networks can well control the voltage and reactive power performance. Hence, we only consider the reactive power in the distribution systems and no reactive power exchange will happen [65]. Future works include that the

distribution systems can provide reactive power support to the transmission system, where our proposed model can also be adopted. Also, note that we employ the widely-adopted branch flow model for the SOCP relaxation [66] of the AC power flow. However, other SOCP relaxation techniques, including the bus injection model and its variants [67], could also be adopted in the proposed framework, given that the feasibility region is convex.

To ensure the distribution network's radiality, we also enforce constraints (3-3g) - (3-3k). Note that x_{mn} are continuous variables and will be either zero or one to keep arborescence [68], which retains model (3-3)'s convexity. Upon using this, we restrict the distribution network information in the third stage, which protects the confidentiality of distribution utilities. Other constraints are with the typical branch flow model under SOCP relaxation [69].

3.4. Decomposition-based Solution Strategy for the Three-Stage Market Operation

In this section, we provide an efficient solution strategy towards the multi-scale and multi-stage SP problem for T-D coordinated market operation. As the original formulation follows a stage-decomposable structure, it can be readily tackled by the L-shaped method, as adopted in multiple works [58, 70]. However, since the proposed T-D coordinated hierarchy is a three-stage problem, the L-shaped method needs to be nested. In this work, we tailor a generalized nested decomposition based on the nested L-shaped method to facilitate the solution upon different and individual scenario sets. To be more concise, we use the compact form for equations in this section, and similarly, we only put the scenario indices (ω^T) and (ω_c^D) with the uncertain parameters.

3.4.1. ISO's Master Problem

The ISO's UC problem (3-1), *i.e.*, the first-stage problem, serves as the master problem. The complicating variables in the master problem include the unit commitment decisions, *i.e.* $u_{g,h}, d_{g,h}, i_{g,h}$ (denoted by vector $\mathbf{x}_1$), and the reconfiguration decisions, *i.e.* $z_{q,h,c}$ (denoted

by vector $\mathbf{x}_2$). A compact form for the master problem (3-1) is represented in (3-4).

$$M = \min_{\mathbf{x}_1, \mathbf{x}_2} \quad \mathbf{c}_1^\top \mathbf{x}_1 + \mathbf{0}^\top \mathbf{x}_2 + S_t^*, \tag{3-4}$$

subject to

$$\mathbf{A}_1 \mathbf{x}_1 + \mathbf{B}_1 \mathbf{x}_2 \leq \mathbf{b}_1, \tag{3-4a}$$

$$\mathbf{A}_2 \mathbf{x}_1 + \mathbf{B}_2 \mathbf{x}_2 = \mathbf{b}_2, \tag{3-4b}$$

$$S_t^* = \max_{o \in O} \left\{ \alpha_t^o + (\boldsymbol{\beta}_{t1}^o)^\top \mathbf{x}_1 + (\boldsymbol{\beta}_{t2}^o)^\top \mathbf{x}_2 \right\}, \tag{3-4c}$$

where S_t^* denotes the maximum of cuts returned from the second-stage subproblem, and constraint (3-4c) includes the optimality cuts returned from the second-stage problem with the information of the second and third stages for all iterations.

3.4.2. ISO's Subproblem

The second-stage problem (2), *i.e.*, the ISO's subproblem (S_t), models the transmission-level ED, as shown in (3-5).

$$\forall \omega^T : \quad S_t(\omega^T) = \min_{\mathbf{y}} \quad \mathbf{c}_2^\top \mathbf{y} + S_d^*, \tag{3-5}$$

subject to

$$\mathbf{K}_1 \mathbf{y} = \mathbf{r}_1(\omega^T) : \qquad \boldsymbol{\gamma}, \tag{3-5a}$$

$$\mathbf{H}_1 \mathbf{x}_1^* + \mathbf{A}_3 \mathbf{y} \leq \mathbf{b}_3 : \qquad \boldsymbol{\phi}, \tag{3-5b}$$

$$S_d^* = \max_{o \in O, c} \left\{ w_c \cdot \left[\alpha_d^o + (\boldsymbol{\beta}_{d1}^o)^\top \mathbf{y} + (\boldsymbol{\beta}_{d2}^o)^\top \mathbf{x}_2^* \right] \right\} : \qquad \boldsymbol{\mu}, \tag{3-5c}$$

where $\mathbf{x}_1^*$ and $\mathbf{x}_2^*$ are delivered from the master problem, $\mathbf{y}$ is the second-stage variable vector, including the generation dispatch, load curtailment and line flows, *etc.* $\boldsymbol{\gamma}$, $\boldsymbol{\phi}$ and $\boldsymbol{\mu}$ are the dual vectors, whereas auxiliary variable S_d^* and constraint (3-5c) formulate the

relaxed counterpart of the third-stage problem. To update the optimality cut (3-4c) in the master problem, we calculate the subgradients as follows.

$$\alpha_t^o = \sum_{\omega^T} \Pr_{\omega^T} \left\{ \boldsymbol{\gamma}^\top \mathbf{r}_1(\omega^T) + \boldsymbol{\phi}^\top \mathbf{b}_3 - \boldsymbol{\mu}^\top [\alpha_d^o + (\boldsymbol{\beta}_{d2}^o)^\top \mathbf{x}_2^* - S_d^*/w_c] \right\}$$

$$\boldsymbol{\beta}_{t1}^o = -\sum_{\omega^T} \Pr_{\omega^T} \mathbf{H}_1^\top \boldsymbol{\phi}; \qquad \boldsymbol{\beta}_{t2}^o = -\sum_{\omega^T} \Pr_{\omega^T} \boldsymbol{\beta}_{d2}^\top \boldsymbol{\mu}.$$

3.4.3. DSO's Subproblem

The third-stage problem (3-3), *i.e.*, the DSO's subproblem (S_d), which is a convex SOCP model, formulates the distribution-level ED, as shown in the compact form (3-6). Without loss of generality, we group the affine constraints with the SOC one in constraint (3-6a), as affine functions are a special case of SOC when $\mathbf{K}_2$ is a zero matrix.

$$\forall c, \forall \omega_c^D: \quad S_d(w_c, \omega_c^D) = \min_{\mathbf{z}} \quad \mathbf{c}_3^\top \mathbf{z}, \tag{3-6}$$

subject to

$$\|\mathbf{H}_2 \mathbf{y}^* + \mathbf{K}_2 \mathbf{z} + \mathbf{e}\|_2 \le \mathbf{q}^\top \mathbf{y}^* + \mathbf{p}^\top \mathbf{z} + \mathbf{H}_3 \mathbf{x}_2^* + \mathbf{r_2}(\omega_c^D), \tag{3-6a}$$

where $\mathbf{x}_2^*$ and $\mathbf{y}^*$ are decisions delivered from the first-stage problem and the second-stage problem, respectively. Then we write the dual form of (3-6) in (3-7).

$$S_d^{\text{dual}}(w_c, \omega_c^D) = \max_{\mathbf{u},\mathbf{v}} \quad \Big[\mathbf{u}^\top (\mathbf{H}_2 \mathbf{y}^* + \mathbf{e}) - \mathbf{v}(\mathbf{q}^\top \mathbf{y}^* + \mathbf{H}_3^\top \mathbf{x}_2^* + \mathbf{r}_2(\omega_c^D)) \Big], \tag{3-7}$$

subject to

$$\mathbf{K}_2^\top \mathbf{u} + \mathbf{v}^\top \mathbf{p} = \mathbf{c}_3, \tag{3-7a}$$

$$\|\mathbf{u}\|_2 \leq \mathbf{v}, \tag{3-7b}$$

where $\mathbf{u}$ and $\mathbf{v}$ are the dual vectors of the Euclidean norm and the SOC, respectively. Note that this dual problem is also a convex SOC and only satisfies the weak duality. However, given the assumption that the nodal voltage constraint is not binding, which is a mild assumption in the realistic power system, there exists an interior in the primal and dual feasibility regions and hence Slater's condition holds, which means the strong duality can be retained [71]. Then the subgradients can be calculated for the optimality cut in the ISO's subproblem.

$$\alpha_d^o = \sum_{\omega_c^D} \Pr_{\omega_c^D} [\mathbf{u}^\top \mathbf{e} - \mathbf{v} \cdot \mathbf{r}_2(\omega_c^D)];$$

$$\boldsymbol{\beta}_{d1}^o = \sum_{\omega_c^D} \Pr_{\omega_c^D} [\mathbf{u}^\top \mathbf{H}_2 - \mathbf{v} \cdot \mathbf{q}]; \ \boldsymbol{\beta}_{d2}^o = -\sum_{\omega_c^D} \Pr_{\omega_c^D} \mathbf{v} \cdot \mathbf{H}_3^\top;$$

3.4.4. Generalized Nested Decomposition Algorithm

To cope with the proposed T-D coordinated hierarchy, we devise a generalized nested decomposition (GND) algorithm. The general procedure is demonstrated in Figure 3.2. In particular, with an initial feasible point of the complicating variables determined from the initial master problem, the problem in each stage can deliver the optimal complicating variables back to the previous stage problem via creating the lower bounding affine cuts by subgradients. If any recourse is infeasible, a feasibility cut will be returned to the upper stages and repeat the loop in Figure 3.2 [72]. For more details about the feasibility check, please see Appendix B. These cuts formulate the relaxed counterparts of the respective subproblems and hence decompose the overall problem. Each subsystem in the second-stage and

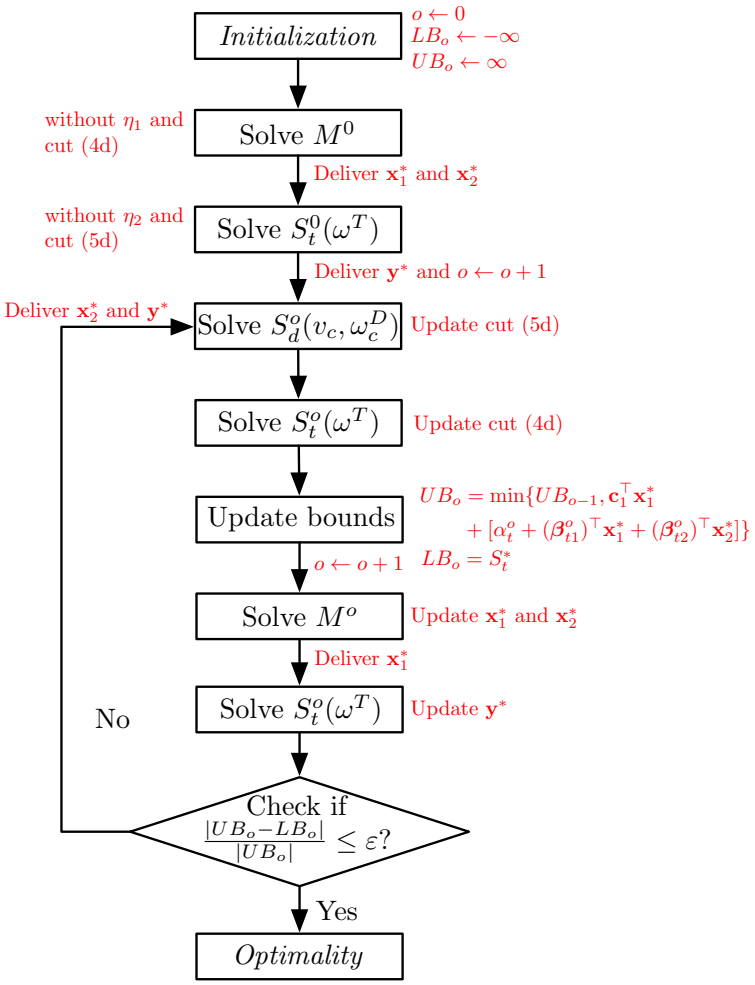

Figure 3.2. The GND algorithm workflow

third-stage can keep its own scenario set and return its own single cut. For multiple distribution systems in the third stage, they return multiple cuts to the second-stage problem based on the single cut from respective scenario sets. From the third stage to the second stage, it is promising to adopt the cut sharing [73] between each second-stage scenario to facilitate the solution, which does not compromise exactness. Besides, The non-anticipativity in any current stage is implicit since we only have one copy of wait-and-see variables in the previous stage. For the convergence proof, we first give the following assumption.

Assumption 1. *1) The second-stage and third-stage problems are convex and have complete recourse; 2) all recourse stages have finite support; 3) all the scenario sets are stage-wise in-*

dependent.

These are all mild assumptions in the current electricity market in terms of system operations. For the first two items, current industrial ED problems are mostly convex and feasible (with load shedding allowed), and if we consider stochastic scenarios, they should be finite in practice. For the third item, the transmission system should have an independent and different scenario set with DSOs, as well as scenario sets between DSOs. Then based on [61], consider the following proposition.

Proposition 1. *Provided with Assumption 1, constraints* (3-4c) *and* (3-5c) *provide accurate approximations for the second stage and the third stage, respectively.*

Proof. From problem S_d to S_t, subproblem (3-7) is solved for each ω_c^D, yielding corresponding optimal dual solutions. As problem S_d is convex and has complete recourse, the Slater's condition holds. Consider $Q(\mathbf{x}_2, \mathbf{y}, \omega_c^D)$ as the third-stage problem's dual:

$$\begin{aligned} Q(\mathbf{x}_2, \mathbf{y}, \omega_c^D) = \mathbf{u}^\top(\mathbf{H}_2\mathbf{y} + \mathbf{e}) - \\ \mathbf{v}(\mathbf{q}^\top\mathbf{y} + \mathbf{H}_3^\top\mathbf{x}_2^* + \mathbf{r}_2(\omega_c^D)). \end{aligned}$$

Based on the convexity of S_d, the subgradients provide:

$$\begin{aligned} Q(\mathbf{x}_2, \mathbf{y}, \omega_c^D) \geq \mathbf{u}^\top(\mathbf{H}_2\mathbf{y} + \mathbf{e}) - \\ \mathbf{v}(\mathbf{q}^\top\mathbf{y} + \mathbf{H}_3^\top\mathbf{x}_2^* + \mathbf{r}_2(\omega_c^D)). \end{aligned}$$

Taking the expectation according to the distribution of uncertainty ω_d, and using the subgradient notations, we have:

$$Q(\mathbf{x}_2, \mathbf{y}) \geq \alpha_d + \boldsymbol{\beta}_{d1}^\top\mathbf{y} + \boldsymbol{\beta}_{d2}^\top\mathbf{x}_2^*.$$

Thus, the affine function below for iteration o gives an exact outer linearization for problem

S_d and is returned to S_t:

$$F(\mathbf{y} : \mathbf{y}^o) = \alpha_d^o + (\boldsymbol{\beta}_{d1}^o)^\top \mathbf{y} + (\boldsymbol{\beta}_{d2}^o)^\top \mathbf{x}_2^*$$

When there are multiple S_d in the third stage, each of them returns the corresponding affine cut to S_t. Thus, the optimality of the problem follows from the complete recourse of all subsystems, and the approximation is exact if and only if $Q^o = \max_o\{F(\mathbf{y} : \mathbf{y}^o))\}$, *i.e.*, constraint (3-5c). Proof is similar for the approximation of S_t in M, *i.e.*, constraint (3-4c).

And here concludes the proof. ■

Remark 1. As the approximation of constraints (3-4c) and (3-5c) is accurate for recourses, based on Remark 4 and Remark 5 in [61], the cuts from subsequent stages formulate accurate approximations only containing the subgradient information. Hence, provided with Assumption 1, when the cuts provide exact approximations of later-stage problems, after a sufficiently large number of forward and backward iterations, the algorithm will converge to a solution within a sufficiently small gap from the global optimality with probability 1.

Remark 2. The assumption that the nodal voltage constraint is not binding is mild [71] because the voltage deviations in distribution networks should be well controlled by voltage regulators. It is unnecessary to consider the local voltage stability issue in a market clearing problem from the ISO's perspective since there is no such a market product. A Volt/VAR optimization problem could be solved by local utilities to tackle this issue once the hierarchical market is cleared [74].

Remark 3. Note that in our case, M is a MIP. Hence, the final optimal solution satisfies the potential MIP gap without loss of generality as the affine cuts are created from convex subproblems. Practically, we admit that the GND's algorithmic gap is hard to achieve zero, and together with the MIP gap, the final solution might not be optimal. However, the theoretical global optimality remains if convexity holds for recourses.

Remark 4. The first three blocks in Figure 3.2 are for the initialization. However, if we can find an excellent warm-start initial point, the algorithm will converge faster. Besides,

since the cut herein gives an affine approximation, cut sharing and cut selection can further contribute to the acceleration.

Remark 5. The ISO's master problem receives only the cut information consisting of subgradients from the lower-level problems. With only the subgradients, one cannot recover the full network information, which prevents the ISO from having the network information and thus protects the confidentiality.

3.5. Numerical Experiments

To test the efficacy of the proposed T-D coordinated market operation and the solution strategy, we carry out case studies on a modified *Tran6+Dist7+Dist9* test system from [75] and a *Tran118+Dist30×5* from [46] for day-ahead UC & ED problems. We solve all of the experiments by Gurobi on a Windows PC with quad-core Intel i7-6700 CPU and 8GB of RAM.

3.5.1. Tran6+Dist7+Dist9 Test Case

We depict the system topology in Figure 3.3, which consists of one transmission system (TS) and two radial ADNs. The original test system [75] did not consider the resistance and reactive demand/generation limits. In this study, they are obtained via a fixed R/X ratio (assume all distribution branches are with the same configuration and R/X ratio is 1:2) and power factor (assumed to be V-I 0.95 lagging) using the existing data. We also have four switches K_1-K_4 installed to enable the network reconfiguration of each ADN while the switch can be reconfigured every 8 hours.

For uncertainties, one wind generator G_3 and two PV units RG_1 in ADN_1 and RG_2 in ADN_2 are added in the system, whose power outputs are uncertain and sampled from three different historical datasets obtained from [76]. Note that for the renewables, we scale the historical data to a distribution level, with the maximum output as 25MW. We also slightly reduce the capacity of DG_1 and DG_2 in the original data. The hourly load profile is also assumed to be stochastic that respects the sampled demand scenarios and is distributed

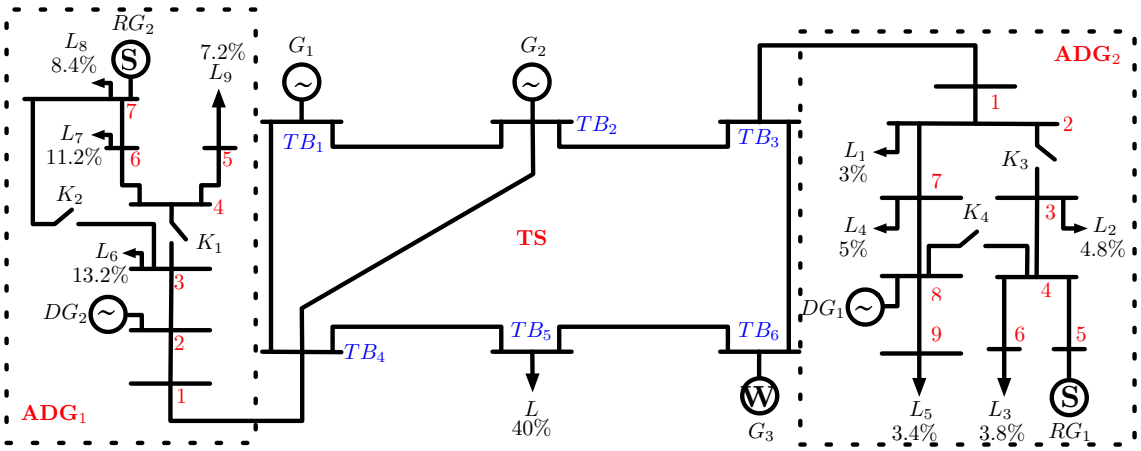

Figure 3.3. *Tran6+Dist7+Dist9* system topology.

according to the factor shown in Figure 3.3. The penalty cost for the load shedding is \$1,000/MW, in order to make the ADN decisions comparable with the TS.

First, 150, 200, and 200 scenarios for the renewable generators G_3, RG_1, and RG_2 are sampled, and 180 scenarios for the demand are sampled using Monte-Carlo sampling from the historical data, respectively. The number of joint renewable and demand scenarios is very high and could jeopardize the computational efficiency. Then, we employ the Fast Forward/Backward approach [34] in the GAMS SCENRED toolbox to reduce the numbers of the joint renewable and load scenarios in the three grids. Figure 3.4 shows the sensitivity analysis of scenario number reduction. We have a base scenario reduction Δ that has 5, 10, and 12 scenarios for the TS, ADN_1, and ADN_2, respectively, and we linearly increase the number of the desired scenarios as shown in the x-axis of Figure 3.4. It can be seen that using $10 \times \Delta$ scenarios has a solution gap of 2.12% compared with using $50 \times \Delta$ scenarios. Hence, we argue that using $10 \times \Delta$ scenarios achieves the tradeoff between the accuracy and complexity. Note that the scenarios are *i.i.d.* w_c for the two distribution systems are set equal in this study, and the convergence criterion ε is 0.01%.

Figure 3.5 shows the algorithmic performance in this case. The GND algorithm converges in the 31th iteration. The total load shedding upon convergence is zero. The costs of the two ADNs start at extremely high levels in that the TS draws a large amount of

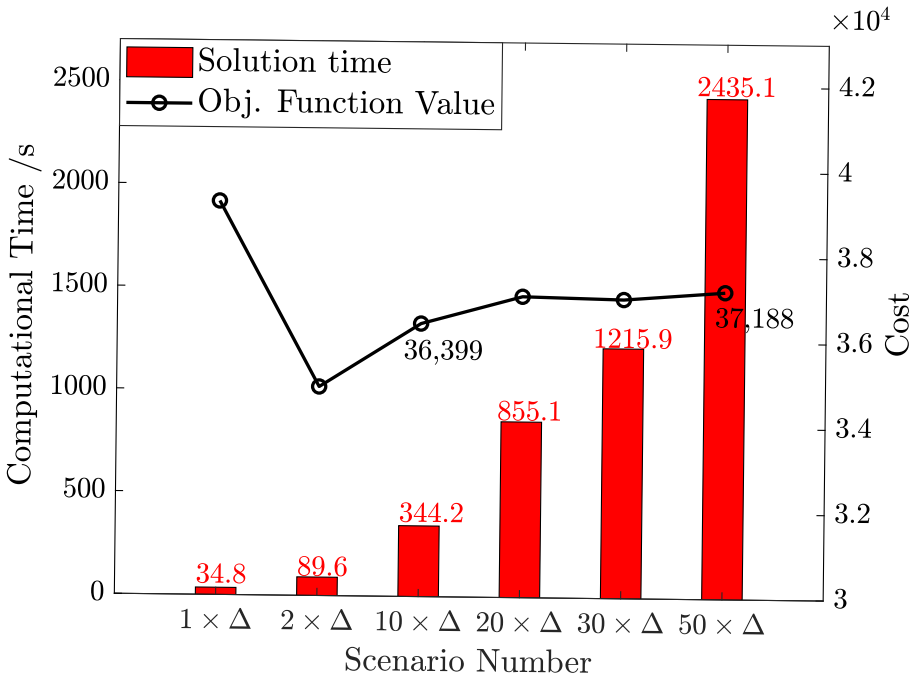

Figure 3.4. Sensitivity analysis on the scenario number

energy from the distribution sides to reduce its power outputs in the first iteration. This phenomenon is because there is no restriction on the power exchange when the two ADNs have to feed the TS even with high load shedding in the local area. However, the injections from the TS to ADNs finally become incentivized as the operation cost of the conventional units in the TS is much lower than the load shedding price in ADNs, and the DER units in ADNs cannot fully support the local demands. Note that the solution reaches \$36,449 in iteration 17, and it is within a gap of 0.14%, as shown in Figure 3.5. Thus, if we have a slightly higher tolerance on the optimality, we can greatly reduce the computation time.

Figure 3.6 provides the unit commitment decisions as well as the network reconfiguration solutions of the master problem upon convergence. G_1 is committed ON throughout the time due to its low generation cost and large capacity. G_2 is mainly used during the twilight time since the PV generation is low at that time, but the energy consumption is high. ADN_1 changes its topology once in this operation based on the optimized switch decisions, whereas ADN_2 remains the original topology. The topology change in ADN_1 is mainly due to the

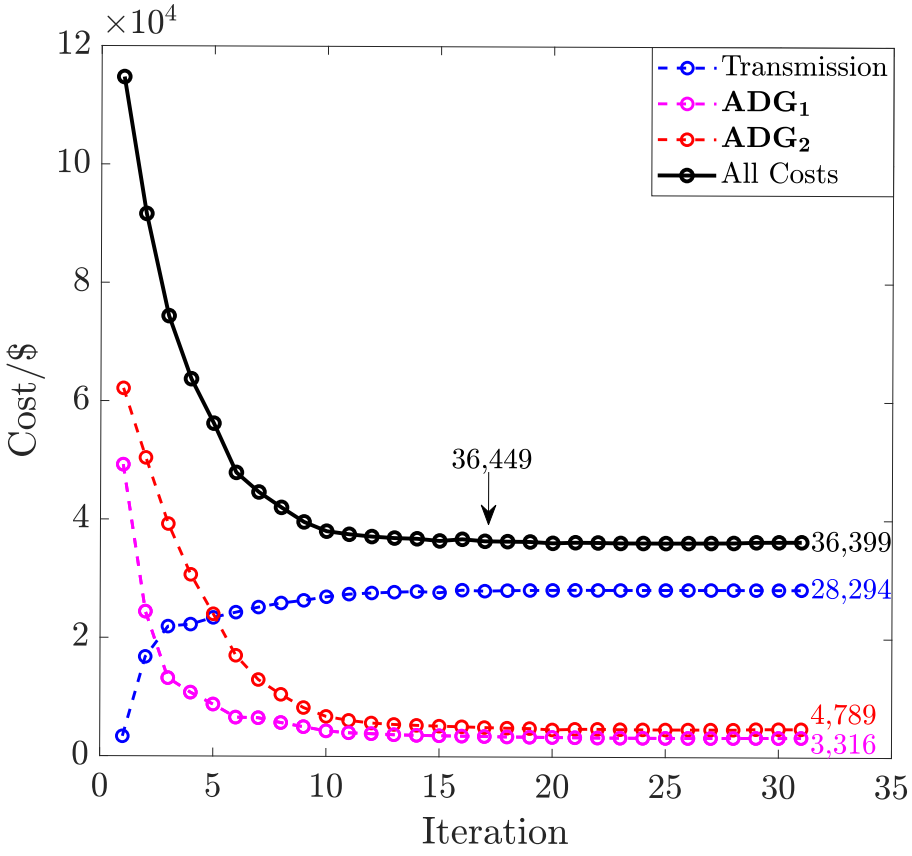

Figure 3.5. Algorithmic performance in the *Tran6+Dist7+Dist9* case

capacity of lateral 3-7 at hour 16 cannot support the increasing demand of load L_8 and L_9, and lateral 3-4 can relieve the congestion pressure by bifurcating the flow to two laterals, *i.e.*, 4-5 and 4-6, towards the demand nodes.

Besides, to illustrate the necessity of the T-D coordination, we carry out the other two comparative experiments on isolated UC&ED and report the results in Table 3.1 in comparison with the results of the T-D coordinated case. $IUCED_1$ mode means that TS forecasts the boundary power demand as all demands in the ADN, and $IUCED_2$ mode forecasts it as the maximum forecast demand minus the maximum generation outputs in the ADNs. $TDC-UCED$ stands for the proposed T-D coordinated UC&ED setting. It can be observed from the table that in both isolated modes, there exists a notable power mismatch, even if the $IUCED_2$ mode can fairly approximate the coordination used by some current industry

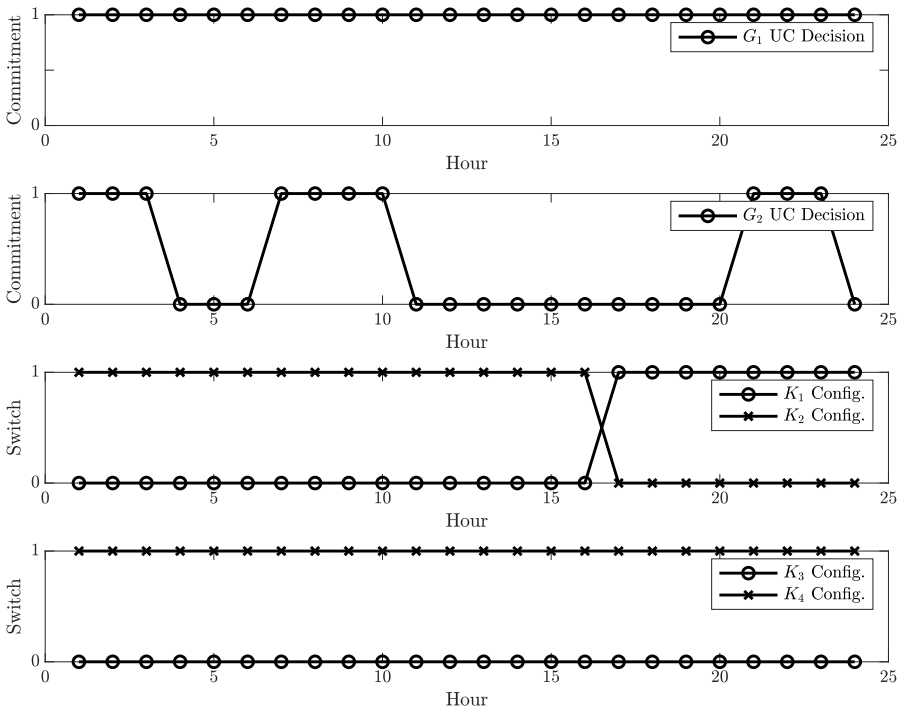

Figure 3.6. *Tran6+Dist7+Dist9* commitment and reconfiguration solutions

practice [46]. A small power mismatch, however, can still raise severe conditions for system operators as it influences the system stability. We also notice that the received LMP in both ADNs is decreasing, which is due to the relieved line congestion by the distribution network reconfiguration considered in the T-D coordinated framework. This observation defends the necessity of adopting the network reconfiguration-embedded T-D coordination in the future market. We further conduct two additional analyses to illustrate the algorithmic performance.

1). Exactness of the SOCP relaxation

While the branch flow model adopted in this work has been widely recognized as a nearly exact relaxation of the actual AC power flow [66], we further demonstrate its exactness by the SOCP gap, which is also a well-known index for evaluating the SOCP performance [77]. Table 3.2 tabulates the maximum SOCP gap values throughout scenarios in the two ADNs.

Generally, the smaller the gap is, the higher exactness the formulation achieves [77]. It

Table 3.1. Comparative Analysis on Isolation and Coordination.

$IUCED_1$	**TS**	Total Costs:	$38,943.87
		ADN$_1$	**ADN**$_2$
	Power Mismatch	31.1%	37.8%
	Total Costs	$4,324.82	$5,609.71
	Received LMP	$16.83/MWh	$16.83/MWh
$IUCED_2$	**TS**	Total Costs:	$27,835.94
		ADN$_1$	**ADN**$_2$
	Power Mismatch	5.8%	8.4%
	Total Costs	$3,658.62	$5,119.84
	Received LMP	$15.47/MWh	$15.47/MWh
$TDC-UCED$	**TS**	Total Costs:	$28,294.12
		ADN$_1$	**ADN**$_2$
	Power Mismatch	0%	0%
	Total Costs	$3,316.20	$4,789.09
	Received LMP	$14.73/MWh	$14.73/MWh

Table 3.2. Maximum SOCP Gaps of the two ADNs (p.u.)

Network	**ADN**$_1$	**ADN**$_2$
SOCP gap	0.0064	0.0037

can be shown from Table 3.2 that our proposed model is accurate enough. Though this approximation still cannot fully replace a complete AC power flow model, it gives an excellent starting point for such analyses run by ISOs with superior computational efficiency. Figure 3.7 also shows that under normal system conditions, the nodal voltage constraints are non-binding, which supports the strong duality of the SOCP-based subproblem.

2). Sensitivity analysis for initial values

To technically support Remark 4, we conduct a sensitivity analysis for initial values in the algorithm. Note that we are particularly interested in the distribution reconfiguration variables' initial values since the unit commitment variables will render no infeasibility in subsequent stages. We use five cases of initial values for the sensitivity analysis.

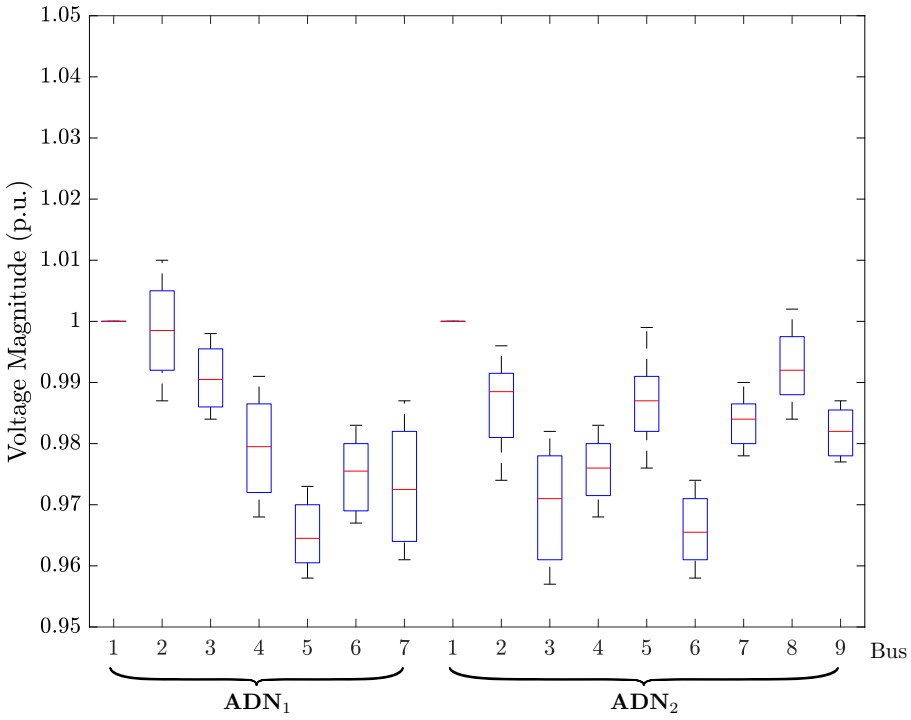

Figure 3.7. Boxplot for voltage magnitudes of the two networks

- *Case 1.* Throughout the horizon, $K_1 = 1$ and $K_2 = 0$, $K_3 = 1$ and $K_4 = 0$.
- *Case 2.* Throughout the horizon, $K_1 = 0$ and $K_2 = 1$, $K_3 = 0$ and $K_4 = 1$.
- *Case 3.* Throughout the horizon, $K_1 = 1$ and $K_2 = 1$, $K_3 = 0$ and $K_4 = 0$.
- *Case 4.* Throughout the horizon, $K_1 = 0$ and $K_2 = 0$, $K_3 = 1$ and $K_4 = 1$.
- *Case 5.* The optimal configuration settings obtained by the simulation.

It is straightforward that *Case 1* and *Case 2* give a feasible set of initial values, while *Case 3* and *Case 4* give an infeasible one. *Case 5* serves as a comparison with a perfect initial value. Figure 3.8 depicts their performance. It is shown that all five cases converge to the optimal solution, whereas *Case 1* and *Case 2* spend fewer iterations than *Case 3* and *Case 4*, but *Case 5* achieves the fastest performance. The additional iterations spent in *Case 3* and *Case 4* are mostly feasibility-check iterations, where distribution systems return feasibility cuts.

This experiment shows that a feasible initial value leads to a better performance, whereas a perfect initialization would further save the computational time.

3.5.2. Tran118+Dist34×5 Test Case

To test the scalability of the proposed method, we carry out experiments on a *Tran118+Dist34×5* test case modified from [46], which consists of one IEEE 118-bus transmission system and 5 IEEE 34-bus distribution systems. A similar data modification such as R/X ratio and power factor is conducted to make the original system suitable for our study. Moreover, we also perform similar scenario generation and reduction for the additional ADNs (only 20 scenarios are considered in each ADN, and 10 scenarios are considered in the TS). The load shedding cost is set as \$1,000/kW in ADNs to keep comparability.

Three cases with different stopping criteria ε for the GND algorithm, namely 3%, 1%, and 0.1%, are set up to test the algorithmic performance in a large system. Figure 3.9 shows the comparative results. The boundary purchase here is defined by the sum of multiplications between boundary LMPs, which are the dual values of the boundary nodal balance constraints in the second stage, and the power injections from the TS. We multiply the total ADN cost and the purchase cost by 10 to make costs comparable. It can be observed that the convergence speed greatly depends on the choice of the stopping criterion. And the algorithm spends a great number of iterations to close the gap between 1% and 0.1%, which is also a feature of optimality conditioned algorithms.

The CPU time for the case when ε = 1% is around 4.5 hours, which is acceptable considering such a stochastic, complex, and accurate modeling for both transmission and distribution systems. However, directly running the corresponding deterministic equivalent SP problem drains up the RAM and returns no solution. This observation defends the necessity of using the proposed decomposition technique for acceleration. Note that with a more powerful simulation platform, such as high-performance CPU clusters, solving all the second-stage and third-stage subproblems with each scenario realization could be implemented in parallel, which can significantly reduce the computational time.

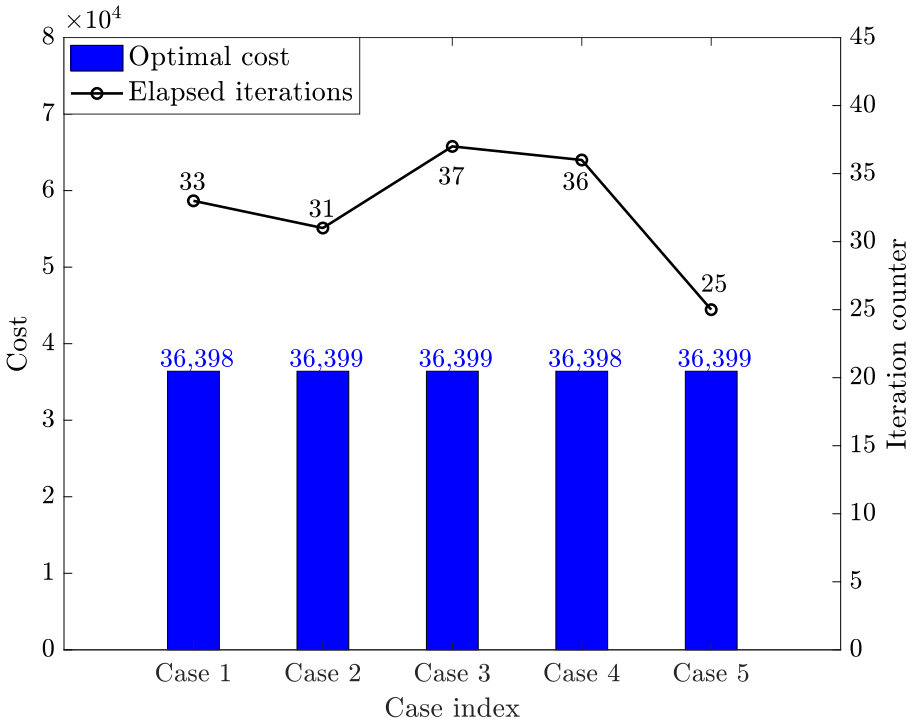

Figure 3.8. Sensitivity analysis on the initial values

3.6. Summary

To help the ISO with tackling the increasing system intermittency from the active distribution system and reduce the boundary power mismatch, we propose a T-D coordinated market paradigm including UC and ED. This work is mainly from the ISO's perspective to optimize its daily operation considering the DSO's performance. A generalized nested decomposition method is tailored and efficiently decomposes the problem, which greatly facilitates the solution. The theoretical convergence proof of this algorithm is also articulated. Numerical experiments corroborate the effectiveness of the proposed strategy and show the necessity of the T-D coordination.

Future studies include exploring more effective cut selection from the convex relaxation of subproblems, *e.g.*, the Lagrangian dual cut, to reduce the computational time. Besides, with the increasing DER installation in distribution systems, similar coordinations between DSOs and microgrids await in-depth investigation.

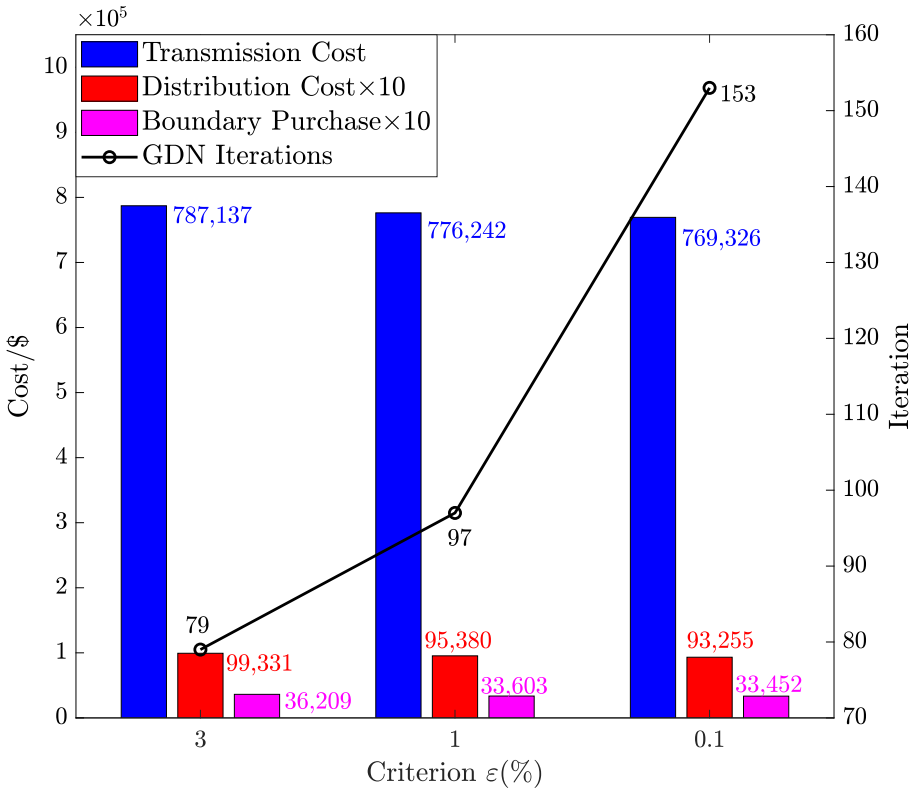

Figure 3.9. Comparative analysis with different stopping criteria

Chapter 4

FUTURE ELECTRICITY MARKET DESIGNS AND GENERIC SIMULATION PLATFORM

In this chapter, we comprehensively discuss the state-of-the-art progress of the electricity market operations considering renewable resources, which is summarized in an overview. We throw a draft design of the future market structure based on the renewable impacts and the increasingly distributed framework. Then, we also present a general simulation platform for researchers and industry partners to conduct state-of-the-art electricity market operations. We implement this platform as a potential open-source simulation package for future users' flexibility. The main contents of this chapter, thus, can be divided as follows.

- State-of-the-art market operations considering variable renewable energy are reviewed. Several questions are raised against the development of the future electricity market.
- A draft design on the future market structure considering renewables and the distributed framework is discussed.
- Attempting to solve the revealed questions, a general electricity market operation simulation platform considering heterogeneous participants with novel market models is presented.

4.1. Overview for State-of-the-art Market Operations with Renewables

Renewable energy has become one of the dominant renewable resources in current power systems. To meet the growing requirement of the deregulated market structure, most market operators in the world, *e.g.*, the independent system operators (ISOs) in the U.S. and the transmission system operators (TSOs) in Europe, have been conducting research in renewable integrations. With the accelerating penetration of renewable energy on both sides, how

to coordinate renewable generation with conventional generation technologies in short-term market operations with reliability and robustness attracts research attention.

Short-term electricity market operations include energy markets, reserve markets, and other ancillary service markets [78]. Unit commitment (UC) and economic dispatch (ED) are two essential operation routines in the electricity market, which is also the main focus of the research in this field [79]. UC and ED determine the process of daily generation feeding system demands in multiple timescales. The reserve market ensures system reliability, where the renewable participation can significantly alleviate the pressure of conventional reserve providers [80]. Researchers are also interested in the PV's capability providing other ancillary services such as voltage regulation and frequency regulation, which are also still open questions in the renewable-integrated market operation. With renewable uncertainty considered in these operations, challenges for grid reliability and system dynamics arise.

While the ISOs keep using deterministic market operations to ensure tractability, numerous research studies aiming at improving these market operations propose various approaches to tackle renewable uncertainties, such as stochastic programming (SP) and robust optimization (RO). Additionally, before solving these problems, it is requisite to address the renewable uncertainty modeling with effectiveness and accuracy, which is also under extensive discussion with the development of data analytics and statistical learning algorithms. It can be envisioned that in the future market operations, these uncertainty-based modeling and optimization approaches can substantially contribute to the social welfare upon addressing the challenge of renewable intermittencies. However, before the real-world application of these methods, their robustness and scalability need to be further verified by realistic simulation and field demonstration. Recently, the Federal Energy Regulatory Commission (FERC) releases an order that allows distributed energy resources (DERs) to participate in the electricity wholesale market [81], the idea of the transactive energy and peer-to-peer (P2P) market will gain more significant interest in utilities and ISOs, which is directly related to the household PV generation and retail market design.

In addition, long-term contractual arrangements for renewable integration can also influ-

ence their short-term operation cost. For example, mid-term or long-term power purchase agreements (PPAs) have been widely used for solar power integration [82]. According to [83], many European countries and the U.S. are actively promoting the feed-in-tariff mechanism for solar energy to incentivize a long-term carbon-free electricity investment. In general, a simplified and unified market structure that considers both short-term and long-term market operations has proven to be an effective strategy to maximize the benefits of renewables [84]. Though these long-term measures have various impacts on renewable integration cost, this review article will limit the range of discussion in the short-term electricity market.

4.1.1. Renewable Integration in the Electricity Market

As the installation of renewable resources grows sharply, market operators have developed different rules for renewable integration in their daily operations. In this work, the discussion on various forecasting methods, which have enjoyed thorough investigation in academia, is not the main focus. Instead, the focus is on how these renewable generation forecasts can be leveraged in realistic market operations. More specifically, renewable participation in different types of electricity markets is delineated. These forecasting methods are briefly discussed later.

4.1.1.1. Renewable Participation in the Energy Market

Solar units in most ISOs rarely bid into the markets. Instead, solar units are more generally considered as negative demands and integrated to the demand forecast in daily operations, especially for distributed PVs, which is reasonable in the transmission-level market because of its emphasis on the bulk generation scheduling. For utility-scale solar units, however, there have already been some active PPA contracts in some ISOs with high renewable penetration such as CAISO, and their bidding price keeps decreasing as the renewable penetration grows. As the current installed capacity of solar energy is relatively incomparable with the coal-fired and nuclear power plants, most of the generation portfolio still comes from the conventional generation companies (GENCOs). However, the changes in market

design vary greatly. Some market rules and protocols are under substantial development in places such as CAISO where the local solar penetration has already reached around 25.1% to feed the daily demands in California and keeps increasing.

Industry operations for the uncertainty-based renewable integration remain deterministic. Currently, different ISOs have their own methods to take intermittent solar resources into the consideration. Electric Reliability Council of Texas (ERCOT) uses the exact solar forecast and performs adjustment if necessary, and during real-time operation, renewables should follow the energy offer curves or be considered fixed as the telemetered output; Midcontinent Independent System Operator (MISO) performs its planning and operation with dispatchable solar units considering multiple levels of the forecast, *i.e.*, peak, mean and minimum values; CAISO clears the market using the bid submitted by solar assets. Specifically, for CAISO, a unique reserve called online PV solar reserve is procured based on 15% of the hourly sum of all solar at-risk forecasts as a regular contingency reserve, for potential loss of solar. On the contrary, the European electricity market has a different strategy from the U.S. cases. The European Network of Transmission System Operators for Electricity (ENTSO-E) has four submarkets in the market operation, *i.e.*, the day-ahead spot market, intraday market, balancing market, and imbalance settlement. The solar units, together with other types of renewables, can bid in these submarkets with integration costs, but the current solar integration in the E.U. is not incentivized because the designed cost scheme is not competitive compared with the low carbon prices. To this end, researchers are actively developing novel market structures and designs, especially the cost mechanism, to help accommodate more renewables with reliable and robust operations.

For details about the operation, day-ahead schedulers not only use the forecasts provided by the forecast vendors but use asset optimization software including the operating characteristics of the installed renewable generators to make reliability-driven UC and ED decisions. Then, real-time schedulers use the obligations from day-ahead schedulers and assessment of the conditions throughout the operating day to adjust the decisions. It is convenient to implement and monitor this process, which satisfies the requirement of interpretability and

high reliability in ISO's operations.

Notably, based on the famous duck curve report from CAISO, it has also been indicated that the operators use pre-dispatch and re-dispatch with high reserves to bolster the system reliability with the renewable intermittency. For the daily market, ISOs perform a day-ahead operation with a resolution of one hour for UC decisions, then a real-time dispatch is performed with a resolution ranging from 5 minutes to 15 minutes, under the real-time forecast and system requirements, together with contingency screening and corresponding rescheduling if contingencies occur.

In addition, it is noteworthy that the market settlement for solar in the current U.S. wholesale market remains identical with other generation types, which means that there is no difference in terms of the final power deployment between renewables and conventional generation. Taking ERCOT as an example, for the day-ahead operation, the settlement price is exactly the day-ahead locational marginal price (LMP), whereas the real-time settlement point price is the real-time LMP plus a UC reliability deployment price adder, *i.e.*, the energy imbalance charge with a reserve price adder. Both the day-ahead price and the real-time price apply to all resource types.

However, particularly for distribution systems, New York Independent System Operator (NYISO) is now exploring a different settlement scheme of distributed PV in the market. It is proposed that the under-generation and over-generation of DERs need to be taken into consideration the settlement point price. From the research community, though, there have been some papers regarding the renewable settlement such as the Gaussian residual bidding proposed in and the stochastic bilevel programming-based settlement proposed in, solar settlement in the market operation still requires further investigation.

As the intermittency issue of renewables is tackled deterministically by re-dispatch and reserve procurements in the industry practice, the information of renewable generation profiles provided to ISOs should be as complete and accurate as possible. Especially for the solar generation, as the distributed PV installations grow more and more popular, the coordination between ISO and potential distribution-level markets is needed. While there have been some

works regarding the transmission and distribution coordination, it is well acknowledged that it is important to enable the information exchange between transmission and distribution markets with variable solar generation. Besides, with the transactive energy framework on the demand side, small-scale local markets such as microgrids, are currently under research and real-world experiment. These localized and decentralized markets possess considerable potential to emerge in the future's market hierarchy, requiring ISOs to find a better solution for coordination between the wholesale market and retail markets.

On the methodology side, numerous studies aim at addressing the solar uncertainty directly in stochastic models, such as SP and RO, rather than the deterministic formulation. While the technical details of these models are introduced in the subsequent section, the advantage of leveraging stochastic models is based on the reliable and robust solutions. With the forecast or historical data of renewable resources at hand, one can model the solar uncertainty in various ways and make risk-averse decisions by these models. In the summer of 2019, CAISO provides its assessment on the summer load and resource for a short-term UC using a scenario-based SP approach. ISO-New England (ISO-NE) and MISO also pay attention to the application of RO in the UC and conduct several research projects. Though these studies show the potential of leveraging stochastic models in the real-world market operations, however, large-scale application of stochastic models in the electricity market is not ready until issues such as the computational efficiency are fully addressed.

The main reason lies on the capacity difference between them. For instance, the entire installation of wind capacity in the Pennsylvania-New Jersey-Maryland (PJM) area is nearly 14 times the solar installation. However, due to the rapidly increasing solar penetration, it is much needed to model and capture solar variability and uncertainty in market operations. Also, in the market optimization models, the uncertainty modeling for wind and solar is dealt with similarly. For instance, the uncertainty set-based robust optimization is applied to model both the solar uncertainty and wind uncertainty. We will detail the discussion on the solar uncertainty modeling later. Meanwhile, some ISOs also follow the same forecast-optimization-settlement procedure for wind and solar, like MISO and CAISO. It should be

noted that although the modeling techniques used for wind and solar are similar, the underlying drivers for their output are inherently different: solar radiation vs. wind speed. Besides, solar energy obeys the pattern of daily volatility, which differs from the seasonally volatile feature of wind energy, posing a unique technical barrier for the development of solar integration.

4.1.1.2. Renewable Participation in the Reserve Market

For the reserve provision from renewables, which has drawn extra attention for its intermittency issue, several research teams also gain some experiences from conducting pilot projects. National Renewable Energy Laboratory (NREL) and Argonne National Laboratory (ANL) have already published reports and revealed the impact of renewables on the power system reserve provision [43]. For a high renewable penetration scenario, balancing reserves should be increased and respond faster to maintain the system reliability and stability, which increases the integration cost of renewable energy. To tackle this issue, North American Electric Reliability Corporation (NERC) recommends that PV plants must provide their share of grid supports, and relevant research is performed for a grid-friendly PV plant, which is reportedly capable of providing various ancillary services including the primary reserve in the test. On the other hand, a significant economic opportunity for renewable systems is revealed if renewables participate in secondary and tertiary controls of the reserve markets as discussed in. Inspired by these findings, enabling renewables to provide such active power reserves and other grid supports takes shape.

If we take solar energy as an example, in general, the research from this perspective can be classified into two groups: the first is combining PV systems with auxiliary storage systems to provide reserves; the second is making PV systems operate under the maximum available capacity to provide reserves using the curtailed power. Particularly in, partial shading conditions are considered, which is closely related to the realistic PV operating conditions. In parallel with this research advancement, First Solar, NREL and CAISO started a project in 2016 to test a 300 MW utility-scale PV power plant in California. The field tests

demonstrate that advanced controllers can be installed in PV systems to provide services that range from spinning reserves, load following, ramping, frequency response, frequency regulation, and voltage support, which paves a potential path that power electronics and control strategies can help PV compete in the ancillary service market. Another demonstration project led by NREL, First Solar and ERCOT also comes to a similar conclusion. In summary, the advancement of control strategies enables the provision of different levels of reserves from PV systems for power system operations, when the value of this practice has been substantiated so far.

In addition to the aforementioned technical research and demonstration projects, another widely discussed issue is how the reserves provided by renewable units participate in the markets. From this perspective, He *et al.* developed a general framework on the optimal offering strategy for CSPs in a joint day-ahead energy, reserve and regulation market, which adopts RO to address solar energy uncertainty and SP to address market price uncertainty. Xu *et al.* extended this work by considering that an electric heater (EH) is additionally integrated with CSPs, which further enhances the flexibility of CSPs in terms of the reserve provision and bidding strategy in the market. The reserve provision from renewables is often associated with the energy storage system (ESS), as proposed an annual bidding strategy for industry-level PV plants with ESS participating in the secondary reserve market.

4.1.1.3. Potential Market Designs for the Solar Integration

Recent research on the renewable-integrated electricity market design focuses on how to increase competitivity among market participants while maintaining system reliability. Some featured development of new renewable integration mechanisms and market rules are summarized as follows.

- **Renewable bidding strategy**. Renewable units are widely recognized as units with a nearly zero marginal cost. As reported in [85], bidding zero for renewables in the current LMP-based market environment may not help the investors recover the long-

term payback as the renewables are of high capital cost. L. Marshall *et al.* [86] proved that, under the current market environment, zero-marginal-cost generators gain more advantage when competing with other generators using collusive shadow prices, which illustrates the inefficiency of the existing market mechanisms towards high renewable penetration. Some other works focus on distribution market designs, including the capacity-price game for renewable investors [87] and the average pricing market with abundant renewables [88].

- **Systems reliability**. As distributed renewable units contribute largely to the total solar installations, ISOs/RTOs concern that the uncertainties and fluctuations in the downstream network may propagate back to the upstream market. Z. Li *et al.* [89] provided a new distributed algorithm to cope with the transmission-distribution coordination in economic dispatch without compromising each stakeholder's confidentiality. Then, P. Li *et al.* [48] tailored this method and applied it to a centralized distributionally robust optimization-based dispatch model, where the renewable uncertainty is considered. The key factors to be considered in this type of market design include the confidentiality of information exchanged between transmission and distribution operators, and the uncertainty modeling of renewables on the distribution side.

- **Transactive energy**. Distributed market frameworks are under development to accommodate the growing distributed energy resources, and it closely relates to the transactive market framework. Supported by the breakthrough of power electronic control strategies (*e.g.*, [90]), discussions over localized trading of solar power in an islanded microgrid are presented [91]. A. Jafari *et al.* [92] proposed a new profit allocation strategy for multi-energy microgrid management with energy storage-embedded distributed renewables. T. Khalili *et al.* [93] provided a novel multi-objective scheduling framework for microgrid management with abundant renewables.

It is noteworthy that different market designs lead to different operation strategies, and later sections in this chapter will delineate the market operation strategies focusing on how to integrate the solar power reliably.

4.1.1.4. Impact of Future Market Designs

As discussed above, various market designs suggest transitioning the electricity market structure from a conventional top-down hierarchy to a distributed bottom-up one due to the proliferating renewable penetration on the distribution side. Particularly, the ancillary service requirement and settlement will also be updated in the new market designs to cope with new challenges introduced by the increasing renewables. However, such a transition may impact future solar investment and the associated risk management.

Extensive works have been devoted to novel ancillary service procurement based upon the new challenges raised by renewables. Apropos of the industrial practice, recently, P. Du *et al.* [94] proposed a novel ancillary service market framework considering the increasing renewables for ERCOT. Apart from the conventional regulation and primary frequency reserves, fast frequency response and contingency reserve can be added into the new market framework with practical implementation protocols. They are to equalize the decreasing system inertia and more severe frequency events from renewables. G. Zotti *et al.* [95] proposed a framework called Ancillary Service 4.0, a top-down market structure, to appropriately allocate the ancillary service in multi-scale system operations. Different scales of ancillary service trading occur locally in the distribution systems or microgrids, monitored by a new ancillary service operator in a distributed manner, whereas the central system operator collects the cleared bids and offers. D. Jay *et al.* [96] proposed a Stackelberg game in the system operation for the reactive power ancillary services, in which the ISO acts as a leader to co-optimize and GENCOs act as followers to bid ancillary services. This asynchronous process can serve as a reference to the centralized operation to system operators. To date, both the centralized and decentralized approaches have been well investigated in terms of new designs for ancillary services, which lays a solid foundation for the future market transformation.

As a result of the market structure transformation, renewable investment is also reconsidered. Most of the studies, taking solar as an example, concerning the investment evaluation are conducted for distributed energy resources, using performance metrics such as the Energy Payback Time [97] and Baker-Finch parameterization [98]. The results show that a

single state-of-the-art PV panel is able to finish the investment payback in 7 to 12 months. For utility-scale PV farm investment, though the payback time increases to years due to higher investment cost, analyses show that solar is the most competitive renewable type together with wind, considering various environmental factors [99]. It is also reported that mergers and acquisitions could help with large-scale investments, which can also support risk management. Concerning system operations, renewable energy has been practically proved to be a cost-effective resource with long-term financial payoff, even in a full energy market case [54]. However, many investors still hold a conservative attitude to the liquidity and market power of solar energy, especially the utility-scale PV plants [100]. In fact, under the current industry operation protocols, most of the bulk solar investments fail to pay back without an appropriate feed-in-tariff, which is beyond the free market competition. Nonetheless, thanks to the future market structure transformation and advanced control strategies, when renewables are free to provide all types of market services, it can be envisioned that solar energy will gain significantly increased competitivity against other resources. Besides, enabling multi-type ancillary service provisions could also reduce energy curtailment and hence de-risk solar investment.

4.1.2. Renewable Uncertainty Modeling in Electricity Markets

As discussed in the previous section, the biggest challenge in the renewable-integrated market is how to tackle the growing system supply intermittency. For industry practice, the forecast values of renewable generation are directly put into the deterministic model, and the supply intermittency is tackled via corrective control. The mainstream research, however, suggests leveraging stochastic models and dynamic analytical methods on the uncertainties. As the priority is modeling the uncertainty accurately and concisely, this section serves as an introduction of the uncertainty modeling. In this chapter, the discussion on various forecasting methods, which have enjoyed thorough investigation in academia, is not the main focus. Instead, the focus is on how these renewable generation forecasts can be leveraged in realistic market operations. More specifically, renewable participation in different types

of electricity markets is delineated. Note that these approaches are for the future solution methodologies, which hold potentials to be applied in the renewable-integrated electricity market studies. The interpretability of uncertainty modeling is also one of the industry's concerns. Typically, there are three ways of renewable uncertainty modeling, which are detailed in the following subsections, respectively.

4.1.2.1. Sampling-based Modeling

The most widely used method in the renewable modeling, as well as other types of renewable models, is the sampling-based technique. As a basic idea of data analytics, the sampling method draws a representative sample for the raw data profile by generating subsets chosen from the overall population, each of which represents one realization of the variable uncertainty with a probability. This method is welcomed by researchers for the excellent interpretability and implemental convenience.

The approaches for the sampling technique vary according to the problem formulation and data characteristics. For the sampling of a single-dimensional uncertain parameter in the SP formulation, Monte-Carlo simulation [61] is the most popular method, which generates scenarios from the historical data profile concerning a specified probability distribution function (PDF). When the uncertainty becomes multi-dimensional, a multi-stage scenario tree [101] is the most common approach. The scenario tree constructs scenarios based on the uncertainty dynamics in multiple stages, usually coinciding with the temporal correlations of the underlying uncertainty, while the decisions are also made in each stage correspondingly.

The drawbacks of sampling-based techniques are apparent, as the accuracy of data realizations highly relies on the number of scenarios used in the model and the confidence of the specified PDF. Many works adopt scenario reduction methods to balance the tradeoff between the computational complexity and model tractability. Typical works include the fast forward/backward method [34], the Kolmogorov metric [102], and K-means clustering [103]. Interested readers can refer to [104] for more details about the taxonomy of scenario reduction. However, when there is a reduction of scenarios, there is always a reduction of

the solution quality. The tradeoff between accuracy and tractability for the sampling-based method is the major obstacle before the real-world application. Besides, the choice of PDF also affects this tradeoff, as the PDF's fitting accuracy of the raw data controls the confidence of the results. Particularly, Beta distribution [105] and kernel density estimated non-Gaussian distribution [106] are the most popular metrics to draw daily scenarios for the renewable uncertainty.

4.1.2.2. Boundary-based Modeling

To avoid the curse of dimensionality in the sampling-based approaches, the uncertainty can be modeled within a confidence interval, which is often leveraged by RO techniques. To formulate this boundary-based uncertainty set, extreme value identification and probabilistic identification are the most popular approaches, of which the latter finds a specified probability level of the look-ahead forecast output and hence combines multiple PDF values to formulate the boundaries [79].

It is requisite that the boundary-based uncertainty set encloses finite extreme points or extreme supports to guarantee the finite convergence of robust algorithms [22]. Thus, the utilization of polyhedral sets [107] and ellipsoidal sets [108] for constructing the convex boundary of the uncertainties leads the mainstream in the RO's uncertainty modeling. Particularly, the ellipsoidal set is mainly considered for discrete or spatiotemporal correlated scenarios [109]. Equations (4-1) and (4-1) introduce the general formulations of these sets,

$$W_{\text{polyhedral}} = \{\omega : \hat{\omega}_{\text{lower}} \leq \omega \leq \hat{\omega}_{\text{upper}}\}, \tag{4-1}$$

$$W_{\text{ellipsoidal}} = \{\omega : \| - \sqrt{\Sigma} \cdot \omega\|_2 \leq \Omega\}, \tag{4-1}$$

where the polyhedral set is created by the value bounds of the uncertainties and the spatiotemporal correlations are captured by the covariance matrix Σ within a 2-norm limit Ω in the ellipsoidal set.

Apart from them, there are also other types of uncertainty sets which address the extreme

scenarios, such as the umbrella set [110] and chance-constrained (CC) reformulation [111]. However, for the renewable energy, using a polyhedral set to construct the robust uncertainty enjoys the highest popularity, since the daily performance of renewable outputs can be easily interpreted via box constraints with the maximum at noon and minimum at night.

Another kind of boundary-based uncertainty modeling tries to model the uncertainty by constructing the ambiguity set instead of explicit box constraints. It uses a portion of the observed data or temporal data to extract statistical properties from the moment information or distribution divergence. And the ambiguity set does not require the exact and complete data profile like SP or the overconfident boundary settings. The most typical formulation of this moment-based boundary uncertainty set is shown in (4-3), which is created by moment boundaries.

$$W = \left\{ F_\omega : \begin{array}{l} P(\omega \in \Xi) = 1, \\ (\mathbb{E}\{\omega\} - \mu)^\top \Sigma^{-1} (\mathbb{E}\{\omega\} - \mu) \leq \gamma_1, \\ (\mathbb{E}\{(\omega - \mu)(\omega - \mu)^\top\} \leq \gamma_2 \Sigma \end{array} \right\}, \tag{4-3}$$

where F_ω denotes the moment distribution, μ and Σ denote the mean and variance of the empirical data, and hyperparameters γ_1 and γ_2 adjust the level of robustness. To be more specific, the three constraints in (4-3) define the probability support, first and second order moment boundaries, respectively.

Generally, this approach constructs the boundary with probability confidence from an empirical dataset, which is naturally adaptive to the CC formulation [112]. When (4-3) could conveniently evaluate the Kullback-Leibler divergence applied in [113], the ambiguity set can also be constructed via the Wasserstein metric [114]. Both of them aim at evaluating the distance between PDFs and only differ from the computational dimension. This uncertainty modeling lays the foundation of the distributionally robust optimization, which will be discussed in the next subsection.

Table 4.1. Comparison of different learning-based approaches and their applications.

Applications	Examples	Features research	Learning-based method
Economic applications	Transmission markets	[115]	Ensemble learning
		[116]	Recurrent neural net
		[117]	Autoregressive
		[118]	Generative adversarial net
	Distribution markets	[119]	Ensemble learning
		[120]	Artificial neural net
		[121]	Radial basis function neural net
Engineering applications	Angle stability	[122]	Decision tree
		[123]	Extreme learning machine
		[124]	Convolutional neural net
	Voltage stability	[125]	Extreme learning machine
		[126]	Ensemble learning
		[127]	Convolutional neural net

4.1.2.3. Learning-based Modeling

Recent advance of data analytics, statistical pattern recognition, and machine learning has enabled the learning-based modeling of renewable uncertainty. Besides the sampling-based and boundary-based methods discussed above, the learning-based methods try to extract or "learn" the statistical information of the existing data and then use the learned model to represent the data patterns for forecasting and uncertainty modeling. Novel renewable forecasting methods have been used extensively to enhance the renewable-integrated market, *e.g.*, [115]. Generally, the improvement of the renewable forecast can dramatically enhance the decision-making of the market operation. Scenario generation techniques have also been proposed to capture renewable uncertainties in a stochastic optimization setting, *e.g.*, [118]. Table 4.1 gives a detailed comparison of relevant research articles focusing on different applications.

It can be observed that for each category of applications, various learning-based methods

are adopted. For a more comprehensive review of recent advances in renewable forecast techniques, readers can refer to [128]. It is shown that learning-based techniques can better capture the dynamic nonlinearity and the spatiotemporal correlation of renewable generation data. This advantage gives the learning-based methods a promising future. Besides, more accurate renewable uncertainty modeling and forecast will also help reduce the investment risk when performing portfolio analyses.

4.1.3. Future Solution Methodologies in the Renewable-Integrated Electricity Market

Associated with the modeling of solar uncertainty, the discussion on the solution methodologies, which highly depend on the type of market formulation and scenario generation for the solar-integrated market, is also prevalent. Concerning the uncertainty-based market operations, on the one hand, the solutions towards the transmission-level market, are mostly related to model-based stochastic market formulations, such as SP and RO. These methods have broad applications in UC, ED and market bidding/pricing problems, taking the current research focus. For distribution- and customer-level market, on the other hand, which raises recent research attention, the market formulation sometimes links with the model-free dynamic game, while conventional stochastic models are found to be less applicable to precisely describe the operation. From the application perspective, the upstream markets are promising to solve the intermittency issues via these stochastic and robust models, as the newly added stochastic analytical functionalities do not alter greatly the current market rules. Besides, though the local solar-based market operations are mainly of the utility's interest, ISOs are also supporting the research conducted in this area to fortify the upstream operations from the origin of the intermittencies. Table II tabulates the research literature using these approaches (abbreviations are defined in the following) and the subsequent subsections address the details of each. Note that in this section we extend the survey from solar-integrated models to renewable-integrated models, as many approaches are claimed to be general and scalable to all types of renewables.

4.1.3.1. Stochastic Programming

SP theory has been under thorough investigation throughout the last decades and gained considerable research interest in the market operation with uncertainties. Associated with the sampling-based modeling techniques described in the previous section, SP leverages the generated scenarios to implement reliability-assured stochastic models in a preventive manner. Amongst the research in the market operation with uncertainties, the stage-wise formulation receives widely adoption due to its natural fit to the market hierarchy. Taking a solar uncertainty-based day-ahead UC (SUDAUC) problem as an example, a two-stage formulation can be constructed as (4-4).

$$\begin{aligned} \min_{\mathbf{I}_t, \mathbf{P}_t} \quad & \sum_t \mathbf{c}^\top \mathbf{I}_t + \mathbb{E}_\omega\{\mathbf{g}^\top \mathbf{P}_t\} && \text{(4-4)} \\ \text{s.t.} \quad & \mathbf{A} \cdot \mathbf{I}_t \le \mathbf{J}, && \forall t, \\ & \mathbf{B} \cdot \mathbf{I}_t + \mathbf{C} \cdot \mathbf{P}_t \le \mathbf{K}(\omega), && \forall t, \end{aligned}$$

where the first stage determines the integer variables, $\mathbf{I}_t$, including the start-up, shut-down, and commitment decisions. The second stage finds the optimal dispatch $\mathbf{P}_t$ based on the commitment decisions from the first stage. The first constraint in (4-4) is the first-stage constraint, and the second constraint acts as a coupling constraint between two stages, in which (ω) represents the uncertain parameter with the scenario index ω. The parameters and constraints in this formulation are free to be assigned with other physical meanings, such as production costs, reserve regulations and minimum ON/OFF time constraints. This formulation befriends the operational hierarchy in the current wholesale market, and thus gains vast applications in a large amount of literature. For the real-time operation problem, (4-4) reduces to a single-stage SP model and thus is trivial to solve.

Another type of application on the stage-wise formulation is the temporal modeling of SP with scenario trees. Retaking this SUDAUC problem as an example, (4-5) presents another

form.

$$\min_{\mathbf{I}_{t,\omega},\mathbf{P}_{t,\omega}} \quad \sum_{t} \mathbb{E}_{\omega}\{\mathbf{c}^{\top}\mathbf{I}_{t,\omega} + \mathbf{g}^{\top}\mathbf{P}_{t,\omega}\} \tag{4-5}$$

$$\begin{aligned} \text{s.t.} \quad & \mathbf{A}\cdot\mathbf{I}_{t,\omega} \le \mathbf{J}, && \forall t, \forall \omega, \\ & \mathbf{B}\cdot\mathbf{I}_{t,\omega} + \mathbf{C}\cdot\mathbf{P}_{t,\omega} \le \mathbf{K}(\omega), && \forall t, \forall \omega, \\ & (\mathbf{I}_{t,\omega}, \mathbf{P}_{t,\omega}) = (\mathbf{I}_{t,n}, \mathbf{P}_{t,n}), && \forall t, \forall \omega, \end{aligned}$$

where n denotes the root node of the scenario tree. This formulation shows a typical multi-time-stage SP problem, which means the operation in each hour is solved individually with one column in the scenario tree and updated hour by hour. The system modeling of this temporal modeling is similar to the aforementioned hierarchical formulation, whereas the last constraint in (4-5) represents a non-anticipativity constraint. This constraint guarantees the same decisions obtained by scenarios from the same node in the tree and thus enforces the wait-and-see nature of the next time stage when solving the problem in the current stage.

For solving the multi-stage SP problem, strategies can be classified into two groups: stage-wise decomposition and scenario-wise decomposition. For the stage-wise decomposition, cutting-plane methods are the most typical techniques, which decompose the original problem into several small problems with hierarchical or distributed stages. Hyperplanes are used to relax the subproblems' solutions and then delivered to the master problem, which cut and thus shrink the optimality region of the original problem to accelerate the solution. The most representative technique among the cutting-plane methods is Benders decomposition (BD) or the L-shaped method, in which the hyperplanes are created via dual cuts. This algorithm requires the subproblems to be convex, while it is trivial to group all nonconvexities in the solar-integrated market operation such as the integer constraints to the master problem. Besides, other cutting planes like the primal cut generation via the Dantzig-Wolfe decomposition and recently updated stochastic decomposition also show their effectiveness towards the multi-stage SP problem. It is noteworthy that, for the multi-stage SP of temporal modeling, these stage-wise decomposition techniques are required to be nested [120],

while stochastic dynamic programming (SDP) is sometimes emphasized for its potency compared with the nested decomposition.

Scenario-wise decomposition, on the other hand, tends to enhance the computability by traversing scenarios instead of stages, which is related to augmented Lagrangian relaxation approaches. Lagrangian relaxation is originally designed to relax the complicating constraints that involve nonconvexity and transition the original problem to the unconstrained optimization. For its application in the multi-stage SP problem, the non-anticipativity constraint is therefore relaxed, by which the problem becomes single-scenario-based and solvable in a distributed manner for each scenario's realization. In most of the time when augmented Lagrangian relaxation solves SP problems, a regularization term, which could be proximal or entropic, is always required in the objective to penalize the optimality search, as shown in (4-6) that formulates the version using the proximal regularization, as known as L2 regularization in machine learning communities.

$$\begin{aligned} \min_{\mathbf{I}_{t,\omega},\mathbf{P}_{t,\omega}} \quad & \mathbf{c}^\top \mathbf{I}_{t,\omega} + \mathbf{g}^\top \mathbf{P}_{t,\omega} + \lambda_\omega^\top (\mathbf{I}_{t,\omega} - \hat{\mathbf{I}}_t) + \alpha \cdot \|\mathbf{I}_{t,\omega} - \hat{\mathbf{I}}_t\|_2 \\ \text{s.t.} \quad & (\mathbf{I}_{t,\omega}, \mathbf{P}_{t,\omega}) \in F, \qquad \forall t, \forall \omega, \end{aligned} \tag{4-6}$$

where λ_ω denotes the Lagrangian multiplier of the non-anticipativity constraint, α denotes the learning rate of the penalty, $\hat{\mathbf{I}}_t$ denotes the non-anticipative decision, and F is the constraint space. The most popular augmented Lagrangian method is the augmented direction method of multipliers (ADMM), which reduces to the method of progressive hedging (PH) if all of the Lagrangian multipliers are updated in one iteration. However, it is notable that, like other gradient-based methods, the convergence highly depends on the choice of the learning rate α and is not guaranteed to be obtained within finite iterations. Thus, the need for further investigating ADMM's convergence arises in the research field of distributed algorithms.

SP-based approaches benefit from exerting the exact historical data profiles to construct the scenarios and thus yielding preventative solutions for future uncertainties. However,

the industrial application of SP-based methods to date is still limited, mainly owing to the tremendous computational burden. As most of the research restrict themselves to small- or medium-scale standard test systems, SP can be hard to scale in real-world systems. Nonetheless, as SP fathers nearly all of the subsequent uncertainty-based models, it is still beneficial for both industry and academia to pay attention to the development of SP theory.

4.1.3.2. Robust Optimization

Though researchers have devoted considerable research efforts towards accelerating SP solutions, the curse of dimensionality of SP caused by a plethora of scenarios prevents it from practical implementations. In contrast, RO approaches leverage the boundary-based modeling of uncertainty to capture the extreme scenario and hence greatly relieve the computational burden. In this field, adaptive RO (ARO) and distributionally RO (DRO) have great potential in future applications.

4.1.3.2.1. Adaptive robust optimization

The name "adaptive" stems from the fact that the first stage needs to adapt to the worst-case scenario determined in the forward stages. Based on the polyhedral or ellipsoidal set constructed for the uncertainty, ARO considers a boundary-based operation problem to find the worst-case scenario, with which the robust and risk-averse solution is attained. Taking the SUDAUC as an example, (4-7) formulates the problem with the same constraints in (4-4):

$$\begin{aligned} \min_{\mathbf{I}_t,\mathbf{P}_t} \quad & \sum_t \mathbf{c}^\top \mathbf{I}_t + \max_{\mathbf{u}\in U} \min_{\mathbf{P}_t} \quad \sum_t \mathbf{g}^\top \mathbf{P}_t && && (4\text{-}7) \\ \text{s.t.} \quad & \mathbf{A}\cdot\mathbf{I}_t \le \mathbf{J}, && \forall t, \\ & \mathbf{B}\cdot\mathbf{I}_t + \mathbf{C}\cdot\mathbf{P}_t + \mathbf{D}\cdot\mathbf{u} \le \mathbf{K}(\omega), && \forall t, \end{aligned}$$

where $\mathbf{u}$ denotes the uncertain parameter constrained in the uncertainty set U. To determine the worst-case scenario, the subproblem needs to take a max-min form, and then the overall

problem finally yields a conservative solution averse to the worst case. This formulation (4-7) lays the foundation of numerous ARO applications in the uncertainty-based market operation.

For the solution strategy, decomposition techniques are also applied to accelerate. ARO problems are not as difficult as SP problems with redundant scenarios to solve, and hence the convex optimization techniques can efficiently tackle the problem. Among them, primal and dual decompositions still lead the mainstream, since they can conveniently solve the problem to global optimality with tractable accelerations. As BD becomes a typical representative of the dual decomposition, primal decompositions like column-and-constraint generation (C&CG) shows better convergence performance. In contrast to adding dual cuts in BD, the C&CG algorithm adds primal cuts and unifies the feasibility and optimality updates. However, C&CG imposes more variables and constraints to the master problem in each iteration than BD, which may lead to a longer solution time for each iteration. Thus, the choice of primal and dual decompositions is based on the tradeoff between the convergence speed and the computational time of one single iteration.

ARO-based models and strategies recently attract many industrial applications, as the problem structure and decision procedure well fit the practice. When ARO has strong model fidelity and ensures the system reliability, it has great potential to be generalized as a daily operation procedure in the future solar-integrated market operation.

4.1.3.2.2. Distributionally robust optimization

When ARO constructs the uncertainty set by explicitly modeling the boundaries of values as described in Section 4.1.2.2, DRO constructs the ambiguity set via the moment information of the uncertain parameters. By leveraging the ambiguity set created by either moment information or PDF's distance information, DRO yields a less conservative solution than ARO and better scalability than SP. As DRO has accumulated huge research interest in the field of operations research (OR), its application in the uncertainty-based electricity market operation recently dominates the research. The formulation of the DRO problem is identi-

cal with the ARO case, *i.e.*, (4-7), but the tractability is phenomenally damaged, which is mainly owing to the NP-hard nature from the dynamic moment ambiguity set. Even though the ambiguity set is well-defined and convex, the problem could remain computationally intractable.

To facilitate the solution, reformulation and decomposition techniques are proposed, many of which remain in the stage of theoretical optimization derivation. As the problem structure is similar to the ARO problem, ARO's solution strategies can also be applied to solve DRO problems, especially when the ambiguity set is defined to be convex. In the OR research field, on the other hand, literature focuses on using relaxation and reformulation to convexify intricate ambiguity sets, which is rarely an issue in the electricity market case, as the solar and other renewables possess trackable data patterns. However, the convexifying relaxation of the ambiguity set still has future potential when the uncertainty is considered to be multiplex.

Though DRO combines some of the advantages of SP and ARO, it is still hard to explain to system operators that how these uncertainties are realized in the daily operation and how it ensures the solution reliability, as they are modeled within a probability set. There also lacks a metric to evaluate the final solution quality. As the research on the application of DRO in the uncertainty-based market operation goes on, the real-world application of DRO will slowly spread until its interpretability and evaluation process are well addressed.

4.1.3.3. Intelligent Model-free Approaches

Despite the dominance of using model-based scheduling techniques in the local energy market, the dynamic game between prosumers, consumers and utilities is far from easy to be modeled precisely. Heretofore, there is no silver bullet towards solving such a dynamic and nonconvex problem to global optimality. Thus, intelligent model-free approaches with learning-based forecast and scenario generation try to find a feasible and good enough solution instead, which at least provides a practical reference and an evaluation metric for decision makers. The most typical method among them is RL, which is to find an opti-

mal strategy for single or multiple agents to maximize rewards in an either model-based or model-free environment. As the model-based RL techniques can be easily translated into variants of conventional or approximate dynamic programming, here we mainly discuss the model-free RL. Researchers have been looking into the application of this newly-revived intelligent method towards the complex and dynamic P2P game and other applications at various market scales.

It is widely known that model-free RL techniques can be divided into two groups, *i.e.*, value-based and policy-based methods. Value-based methods consider the problem as a Markov decision process (MDP), in which the decision of the current state only depends on the decision of the last state. The most common value-based approach is Q-learning together with its deep NN-based version, Deep Q Network, which lies in the category of asynchronous dynamic programming and heretofore is the most popular model-free approach adopted in the PV-integrated local energy trading. This method updates one state in each decision stage and eliminates the state-transition probabilities by assigning rewards and punishments according to necessary conditions like the Bellman equation, as presented in (4-8).

$$Q(s,a) = R(s,a) + \gamma \sum_{s' \epsilon S} p(s'|s,a)\pi(a'|s')Q(s',a'), \tag{4-8}$$

where (s,a) and (s',a') denote the current and the next state and action pair respectively, π denotes the agent behavior function, R denotes the reward value, p denotes the probability and Q is the so-called Q value evaluating the quality of performing this action. From this equation, it reflects a classical MDP where the current action quality is only associated with the reward and possible opportunity costs from the previous stage. It also acts as an update equation for the Q value as well as the revenue objective function.

The policy-based methods, on the other hand, evaluate the agents' behaviors with progressive policies continuously instead of explicit and discrete reward values. In this case, the value $\pi(a'|s')$ in (8) becomes a probability distribution $\pi_\theta(a'|s')$, where θ denotes the dynamic policy. As the action is continuous and policy changes dynamically, the gradient

of the policy part in (4-8), *i.e.*, Q minus R, needs to be computed to conduct state-space evaluations. Though current research on the solar-integrated market operations seldom investigates this method, its effectiveness has already been corroborated for the joint bidding and pricing design in the wholesale market and the strategic optimization in the domestic energy scheduling, where the uncertain patterns are similar to the solar and other renewables. As the value-based approaches consider discrete states that may not be applicable in the real-time market environment, a model-free continuous solar-integrated market setup cultivates considerable research potential from this standpoint.

4.1.4. Outlooks

As a salient participant in the current electricity market environment, solar energy poses significant technical challenges such as increased uncertainties and intermittencies for system operation and reliability. In this review, we mainly introduce the market operation with solar energy integration in the energy, ancillary service and transactive markets, and comment on the computational methodologies for enhancing the solar uncertainty modeling and operation efficiency proposed in both the academic research and industry projects. In summary of the discussions on the state-of-the-art solar-integrated market operations, future research directions are revealed in terms of market paradigm design, solar uncertainty modeling and solution strategies, which are specified as follows.

1. **Design of the Market Paradigm.** With the accelerating installation of renewable resources in the distribution systems that lie at the lower level in the current electricity market, the policy and paradigm of the market need to be updated. Most ISOs are currently using the estimated and forecasted information from the utilities to perform the deterministic market operation, whereas the increasing penetration of renewables now threatens their accuracy. Additionally, how to coordinate the ongoing distribution-level transactive energy market with the conventional market structure also calls for answers. From this perspective, the future outlooks for both the industry and academia are detailed in the following:

- Uncertainty-based policy-making and market applications. With the development of uncertainty models and stochastic optimization techniques, transitioning the current correction-based deterministic market operations to the risk-averse stochastic operations meets the increasing demand of tackling renewable intermittency and national development strategy.
- Development of unique renewable bidding strategies in energy and reserve markets. Renewable bidding and pricing rules are far from complete in the current market operation. Besides, though the role of renewable energy in the electricity market differs little from wind energy, it is requisite to design a more general and unique market rule for renewable participation.
- Coordination with lower-level markets. As the utility-scale renewable installation increases dramatically in distribution systems, market operators need to consider the coordination between upstream and downstream markets, particularly the transactive market.

2. **Uncertainty Modeling and Market Operations.** For the uncertainty modeling of renewable energy, albeit resourceful literature has been investigating the stochastic optimization throughout the years in the renewable-integrated market, the accuracy and tractability of the current strategies need to be further reinforced. Hence, the next research front converges to the improvement of the accuracy and interpretability of renewable forecast and scenario generation methods, plus the data-driven optimization for renewable-integrated market operations with fast and tractable solution strategies. In summary, the research potentials are detailed as follows.

    - Precise capture of the spatiotemporal correlation in the uncertainty modeling. Recent studies on the scenario generation start considering this issue with short-team correlations by using the learning-based uncertainty modeling, which is difficult to be covered by sampling-based and boundary-based models. Besides, the medium or long-term spatiotemporal correlation for renewable units in a large area and the model fidelity of the learning-based methods deserve further research before the real-world implementation.

- Data-driven models for the renewable-integrated market operation. The exploration on data-driven methods earns a promising future from the recent advancement of DRO on the distribution operation. However, the sophisticated interpretability of the data-driven models prevents them from the large-scale application and thereby needs to be investigated in future research.
- Algorithms with improved efficiency and accuracy. Current algorithms towards stochastic models need to be upgraded to follow the trend of highly distributed and decentralized market hierarchy. More accurate and more tractable solution strategies are of capital importance. Specifically, for stochastic models with nonlinearly correlated uncertainties, the performance of decomposition and distributed algorithms like Bender's Decomposition and Alternating Direction Method of Multipliers calls for further enhancement. Apart from the distributed algorithms, the advancement of the model-free intelligent algorithms such as policy-based reinforcement learning shows great potential for the data-driven market applications.

4.2. General Simulation Platform for Current and Future Short-term Electricity Market Operations

4.2.1. Nomenclature

We provide a detailed notation list for this section.

1) Indices:

$g\,/\,i$	Indices for generator / energy storage
t	Index for time interval

2) Parameters:

$RU_g \,/\, RD_g$	Ramp-up/down rate of unit g
$RU_i \,/\, RD_i$	Ramp-up/down rate of ESS i
$ResT^{PFR}$	PFR response time
$ResT^{AGC}$	AGC response time
$ResT^{SR}$	SR response time
$ResT^{NSR}$	NSR response time
$SUTime_g$	Startup time for unit g
$\Delta f^{\max}$	Maximum allowable frequency deviation
f_0	Nominal frequency
DB_g	Governor deadband for unit g
Ri_g	Equivalent droop curve for unit g
DCC_g	Droop curve coefficient of unit g
$P_g^{\min}$	Minimum power output of unit g
$P_g^{\max}$	Maximum power output of unit g
$CH_i^{\max}$	Charging power limit of ESS i
$DIS_i^{\max}$	Discharging power limit of ESS i
LR_i	Energy dissipation rate of ESS i
η_i	Energy efficiency of ESS i
$SOC_i^{\max}$	Maximum SOC limit of ESS i
$SOC_i^{\min}$	Lowest SOC allowable for ESS i

3) Variables:

$u_{g,t}$	Unit commitment variable for unit g at interval t (Binary)
$c_{i,t}$	Charging indicator for ESS i at interval t (Binary)
$d_{i,t}$	Discharging indicator for ESS i at interval t (Binary)
$p_{g(i),t}$	Active power of unit g (ESS i) at interval t
$pfr^{up}_{g(i),t}$	PFR provided by unit g (ESS i) at interval t
$agc^{up}_{g(i),t}$	AGC-up provided by unit g (ESS i) at interval t
$agc^{dn}_{g(i),t}$	AGC-dn provided by unit g (ESS i) at interval t
$sr^{up}_{g(i),t}$	SR provided by unit g (ESS i) at interval t
$nsr^{up}_{g,t}$	NSR provided by unit g at interval t
$dis_{i,t}$	Discharging power of ESS i at interval t
$ch_{i,t}$	Charging power of ESS i at interval t
$soc_{i,t}$	SOC of ESS i at interval t

4.2.2. Overview

Short-term electricity market operation has been summarized as a quintessential mathematical optimization with widely adopted yet evolving formulations. Typically, the independent system operator (ISO) carries out and monitors the market operation in both the day-ahead and real-time frames, including the unit commitment (UC) and economic dispatch (ED) [129]. The operation involves multi-timescale interactions between different modules, in which NP-hard models could be present, and thus it is not trivial to generalize in one single mathematical program. Considering the evolving structure of modern electricity markets, developing a general simulation platform concerning novel system elements with easily editable functions becomes an urgent task.

Though different ISOs might have different taxonomies and implementations on the mar-

ket operations, it is widely recognized that the day-ahead market and the real-time market consist of the short-term market operation's main body [130]. Particularly, day-ahead unit commitment (DAUC) optimally determines the units' commitment schedules on an hourly basis, often serving as the day-ahead market clearing. Real-time unit commitment (RTUC) re-commits fast-responsive units in a finer resolution with updated system information. Real-time economic dispatch (RTED) clears the real-time market yielding the unit dispatch and finalizes energy and reserve allocations. Under specific circumstances for market simulators, day-ahead economic dispatch (DAED) follows by DAUC to retrieve shadow prices in the day-ahead market. Hence, the coordination between these four multi-timescale operations highlights the essence of the short-term electricity market operation.

Currently, quite a few software platforms have looked into the market operation and built general tools to perform simulations. There is both open-source and commercial simulation software. The advantages of commercial software like PLEXOS [131] and ENERLYTIX [132] include that the operation is well-benchmarked by ISOs, and they are regulated and updated by professional teams for customer cares. However, the commercial tools are not friendly to academic researchers with limited accessibility, and they rarely consider state-of-the-art models for future market implementations. Thus, researchers developed open-source platforms such as FESTIV [133] and EGRET [134] trying to give a general solution for market simulations to the research community. Nonetheless, with the rapid growth of renewable technologies, current open-source tools are neither flexible for the multi-timescale operation nor with state-of-the-art market models. Thus, we release a new open-source Python library, MIDAS-S, abbreviated from Multi-timescale Integrated Dynamic And Scheduling - Scheduling, to fill the gap between the existing open-source tools and practical market operations.

Implementing a complete multi-timescale market operation needs to take a large variety of factors into accounts, such as the reserve product design and information exchange between different routines, which is the major feature that MIDAS-S nails down. For instance, the unit startup and shutdown processes in many ISOs are uncontrollable. Still, they contribute a moderate part of power during the transition state, which should be considered in

the power balance. Many existing academic works neglect this aspect, whereas G. Morales-Espana *et al.* [135] have experimentally shown that the neglect could result in commitment changes and a worse objective value. From the multi-timescale operation's perspective, the startup and shutdown processes become more difficult, which involve making real-time operations aware of the MW levels of generators during startup/shutdown after UC yields the commitment schedule. Similarly, another example would be that the energy storage system (ESS) needs to perform energy arbitrage in the day-ahead market, as regulated by typical ISOs [136]. In the real-time operations, ESSs should follow the day-ahead schedule or an optimized dispatch signal.

As renewable technologies proliferate in the current power system, the market framework should evolve with the optimized operation of sustainable resources and ESSs. Based on enhanced forecast techniques, state-of-the-art market models have already considered renewables in energy optimization. However, the ancillary service (AS) provision from renewables remains in the initial phase. Though smart inverters have been broadly deployed in many regions' renewable systems to support ASs [137], from the market operation's side, most ISOs in the US do not consider renewables providing ASs [138]. Nonetheless, the research community has delved into the design regarding renewable-supported AS markets for years. E. Ela. *et al.* [139] conducted pioneering works on integrating primary frequency response (PFR) with other ancillary service products. B. Olek *et al.* [140] studied the steady state and transient state of renewable providing ASs in a low-voltage network. More works focus on the ESS performance on ASs. N. Cobos *et al.* [141] presented a robust scheduling strategy for ESSs participating in the AS market. And N. Padmanabhan *et al.* [142] analyzed the ESS potential for providing spinning reserves via a production cost model. Above all, our proposed tool enhances the recent development of renewable and ESS strategies for AS provision, generalizes the choice of various models, and further validates the scheduling results via the system dynamic simulation.

Under most scenarios in the current industry practice, the market operation is decoupled with system dynamic analyses. With the integration of renewables and ESSs and their ca-

pability to provide reserves, executing dynamic simulation and posterior power flow analysis becomes necessary to verify the market decisions. Very few works consider using dynamic simulation to guide or correct the scheduling simulation. H. Yang *et al.* [143] proposed a fast Fourier transformation-based reserve requirement determination used in the UC problem with power flow check in PSS®E. In the proposed platform, PSS®E executes AC power flow check for the RTED and performs dynamic simulation for renewable units such as AGC modeling and inertia control simulation. The PSS®E results will guide the next-interval RTED by updating the generator parameters, real-time power loss values, and the ESS dispatch.

In summary, we release an open-source Python library as MIDAS-S, which gives a flexible solution towards state-of-the-art multi-timescale market operations with validations from dynamic simulations. We highlight the contributions of this work as follows.

- We propose a generalized flexible market operation consisting of day-ahead and real-time scheduling that considers multi-timescale information exchange.
- MIDAS-S is the first open-source electricity market simulation tool that considers multi-timescale operations with an interface for dynamic simulations.
- Multiple novel modeling features such as multi-timescale non-spinning reserve design and AS-enabled ESS scheduling are present in the platform.
- The library is easily editable with flexible function utilities for different user-defined modeling and executing alternatives.

We organize the remainder of this chapter as follows. Section 4.2.3 gives an overview of the four operating modes in the platform upon user preferences. Section 4.2.4 discusses highlights in the novel electricity market modeling, such as the multi-timescale AS model designs and ESS operations. Section 4.2.5 presents the flexible features of the library with user-friendly settings and the dynamic simulation interface. Section 4.2.6 provides simulation examples from an 18-bus system and the WECC system. Section 4.2.7 concludes the chapter.

4.2.3. Working Mode Design for the Multi-timescale Operation

As a standard simulation tool for short-term market operations, MIDAS-S has four operation modes that users can easily call and tune. We first give the following notes:

- For all modes, MIDAS-S could run for multiple days with adequate input data.
- According to user settings, all routines, *i.e.,* DAUC, DAED, RTUC, and RTED, could have adjustable look-ahead horizon and time resolution. For example, RTED can run as a 2-hour look ahead with a 5-minute resolution.
- To retrieve day-ahead market clearing prices for some solvers, DAED is optional to be executed right after any DAUC is executed.

Based on Figure 4.1, we detail the four modes as follows.

4.2.3.1. Mode 1: DAUC only

In some production cost modeling and commitment analysis scenarios, users would like to only run DAUC with multiple days, for which Mode 1 is called. In this case, based on the user-defined number of days, MIDAS-S will execute the DAUC routine with defined look-ahead hours. The current DAUC uses the last-interval data yielded from the previous DAUC as new inputs to update by default settings. In contrast, the very first DAUC will need the user-input initial statuses.

4.2.3.2. Mode 2: RTED only

For a brief analysis of real-time market operations, users may only want to run RTED. Mode 2 executes the RTED routine based on a virtual DAUC dataset provided by the user. That is, users need to import a complete set of commitment results and all other input parameters from the UC, such as the ESS arbitrage results. In real-time processes, this is an ISO's practice that the RTED considers all the UC results as input parameters [144]. Note that Mode 2 executes RTED only, which can be regarded as a single unit dispatch system with limited market functionalities. One should refer to Mode 3 or Mode 4 if real-time

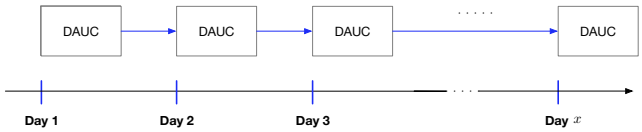

x is the specified day in the Input.xlsx.

(a). Mode 1: DAUC Only

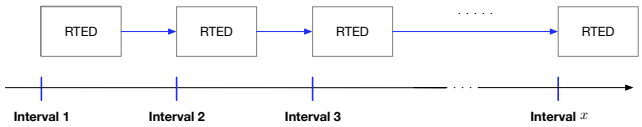

x is the specified interval in the Input.xlsx.
The first interval (current interval) results in the RTED will be sent to dynamic simulations.

(b). Mode 2: RTED Only

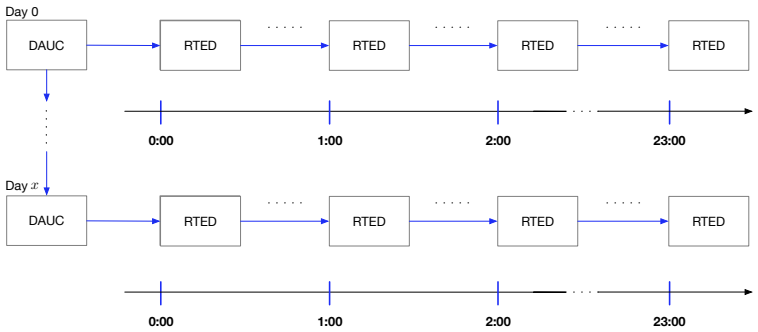

x is the specified interval in the Input.xlsx.
After the DAUC is executed, the whole-day RTED will be executed before the next-day DAUC.
Next-day DAUC uses current DAUC results as inputs.
The first interval (current interval) results of the RTED will be sent to dynamic simulations.

(c). Mode 3: DAUC + RTED

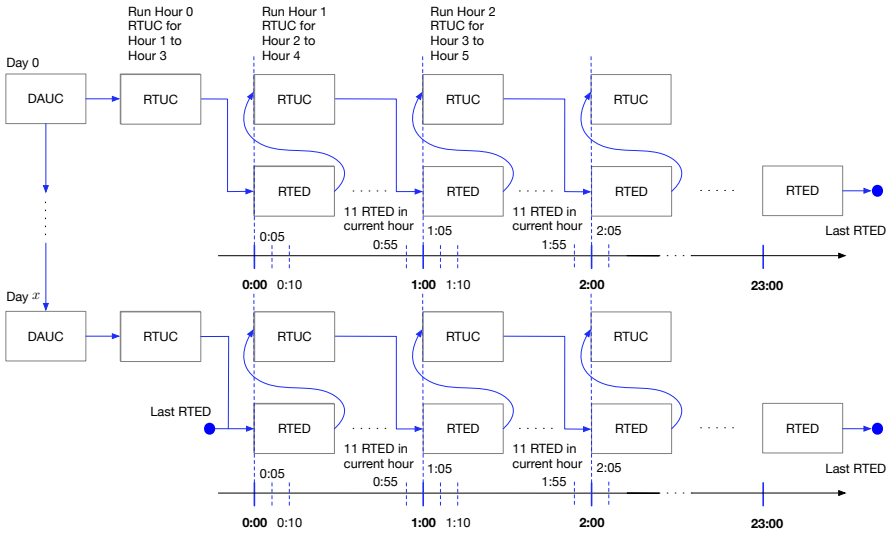

At the beginning of every hour, run a look-ahead RTED with 12 intervals (every 5 minutes).
After the DAUC is executed, the whole-day RTUC + RTED will be executed before the next-day DAUC.
The last interval results of the last interval RTED in one hour will be sent to the RTUC for the initial status of the hour-ahead RTUC.
The RTUC commitment results will be used for the next-hour RTED.
Next-day DAUC uses current DAUC results as inputs.
The first-interval RTED in the next day uses the last-interval RTED result in the current day as inputs.
The first interval (current interval) results of the RTED will be sent to dynamic simulations.

(d). Mode 4: DAUC + RTUC + RTED

Figure 4.1. Operation modes of MIDAS-S.

market operation details are required.

4.2.3.3. Mode 3: DAUC + RTED

Mode 3 serves as a simplified version of Mode 4, which runs DAUC first and then runs RTED accordingly. As shown in Fig. 1 (c), after the day's DAUC is executed, all RTEDs for this day will be executed based on the day's DAUC results. When it comes to the next day, the DAUC uses the previous day's DAUC results as initial inputs. This is because practically in many ISOs, one day's DAUC is executed on the last day, such as in ERCOT [145], when the previous day's RTEDs have not been finished yet. However, the day's first RTED will use not only the day's DAUC commitments but the last RTED dispatch results of the previous day as inputs. It makes the RTED instances consecutive.

4.2.3.4. Mode 4: DAUC + RTUC + RTED

Mode 4 is the complete execution of both the day-ahead and real-time market operation process, which is also the most complicated. RTUC serves as a recommitment process for fast-responsive units according to the varying real-time market environment. To better introduce, Fig. 1 (d) uses one time setting as an example. We set the time resolutions of DAUC, RTUC, and RTED as 1 hour, 1 hour, and 5 minutes, respectively, whereas their simulation horizons are 26 hours, 3 hours, and 2 hours. That is, in each hour, 12 RTEDs are executed.

The design philosophy is that the current hour's RTUC runs for intervals starting from the next hour. For example, the RTUC run at Hour 1 is for Hour 2-3-4 and is executed right after the first RTED instance at Hour 1 is executed. We detail the reasoning of this design as follows. For example, if the RTUC starting from 03:00 schedules a generator with a startup time of 20 minutes to start up at 03:00, its commitment effective time is 03:00. The generator will then need to start up from 02:40 in real-time due to its startup time. Hence, the RTED starting from 02:40 should be aware of the unit's startup, which means the RTUC starting from 03:00 should have been executed at least before 02:40. Since the purpose of

RTUC is to reschedule fast-responsive units in real-time, we deem 1 hour of the startup time by default for fast-responsive units. Hence, the RTUC executes one hour before the operating time as default in MIDAS-S. In the same example, Hour 1's RTUC's initial inputs should be the initial inputs of Hour 2, which comes from the results of Hour 1's RTED.

Based on the previous design, when the user sets each routine's time frames in this mode, the time coupling needs to be strict. For instance, since Hour 1's RTUC runs for Hour 2-3-4, it requires Hour 1's dispatch result as initial inputs, which should come from the first RTED at Hour 1. Hence, the first RTED at Hour 1 should have at least a 1-hour time horizon. Similarly, since the RTED horizon is 2 hours in this example, the last RTED runs for 01:55-03:55. Hence, the RTUC horizon at Hour 1 should have at least 3 hours time horizon to cover for Hour 2-3-4. It is recommended that first-time users adopt the default setting, as this example shows.

4.2.4. Novelties on Electricity Market Models

This section discusses MIDAS-S model novelties concerning evolving operations of renewables and ESS participations in both the energy and AS markets. We highlight our AS designs and ESS operations as follows.

4.2.4.1. Novel AS Designs

In MIDAS-S, we accommodate four kinds of AS products in the market, *i.e.,* PFR, regulation reserves (often refers to automatic generation control, AGC), spinning reserve (SR), and non-spinning reserve (NSR). Though different ISOs may have different taxonomies on the AS market, their general functionalities remain similar. Note that these reserves are related to the frequency response, and we do not consider voltage response procurement as there is no such relative product in the current U.S. market [146]. Note that in MIDAS-S, we only consider the reserve capacity procurement.

a). PFR models.

Though there are very few ISOs that procure PFR in the market, with the rapid growth of renewable technologies, PFR will become more and more important thanks to its fast-responsive feature. Hence, for the future market design, in MIDAS-S, we accommodate the PFR model considering thermal units' governor control and response time, which results in the following steady-state model.

$$0 \leq pfr_{g,t}^{up} \leq \frac{\Delta f^{\max} - DB_g}{Ri_g}, \tag{4-9}$$

$$Ri_g = \frac{DCC_g \cdot f_0}{P_g^{\max}}, \tag{4-10}$$

where (4-9) gives the physical limits of governor's PFR provision, (4-10) defines the governor droop curve. Ref. [139] provides more information regarding the modeling of generator governors. Note that for renewable units, by employing the virtual governor, we could still model their PFR provisions via this formulation, which we also conduct analyses in the system dynamic simulation. Other PFR formulations considering system inertia and power loss such as [147] are also available in MIDAS-S.

b). AGC and SR models.

Regulation reserves take a critical role in the ISOs' reserve categories. They are often expressed as how much power the unit can adjust due to frequency events, which means they relate to the units' ramping rate. It is similar for the SR, as another type of the upward reserves. Hence, we present the following steady-state model for regulation reserves and SR.

$$0 \leq agc_{g,t}^{up} \leq ResT^{AGC} \cdot RU_g, \tag{4-11}$$

$$0 \leq agc_{g,t}^{dn} \leq ResT^{AGC} \cdot RD_g, \tag{4-12}$$

$$0 \leq sr_{g,t}^{up} \leq ResT^{SR} \cdot RU_g, \tag{4-13}$$

where constraint (4-11), (4-12), and (4-13) regulate the AGC-up, AGC-down, and SR, respectively, by the response time and ramp rates.

c). NSR models.

NSR is also a vital reserve product in the current electricity market, but very few works have considered its complete modeling in the literature. It is non-trivial to include NSR in the multi-timescale scheduling framework since the response time of NSR is typically 15~30 minutes, which trespasses multiple intervals of the real-time operation. Though many ISOs perform the NSR scheduling in both day-ahead and real-time, real-time NSR scheduling typically occurs in the RTUC while RTEDs fix NSR values only to adjust units' headroom and ramp room [144]. Hence, we design the following model in DAUC and RTUC.

$$0 \leq nsr_{g,t}^{up} \leq (1 - u_{g,t}) \cdot \left[P_{g,t}^{\min} + RU_g \cdot (ResT^{NSR} - SUTime_g) \right] + u_{g,t} \cdot RU_g \cdot ResT^{NSR}, \quad (4\text{-}14)$$

where constraint (4-14) means that when the unit is offline, during the NSR response time, the maximum NSR it can provide is the minimum power output, using the startup time, plus the power level that it can ramp to using the rest of time. This implies that the unit is not eligible to provide NSR if its startup time is higher than the NSR response time. If the unit is online, it could also provide NSR restricted by the operation ramp rate.

The NSR scheduling is separately scheduled in both DAUC and RTUC, whereas for RTED, the NSR values are fixed to reflect the RTUC schedules in Mode 4 or DAUC schedules in Mode 3. Also, note that all renewables and ESSs are not eligible to provide NSR, which is also a common practice [144].

d). Unit headroom and ramp room.

The unit headroom and ramp room constraints for each generator are as follows.

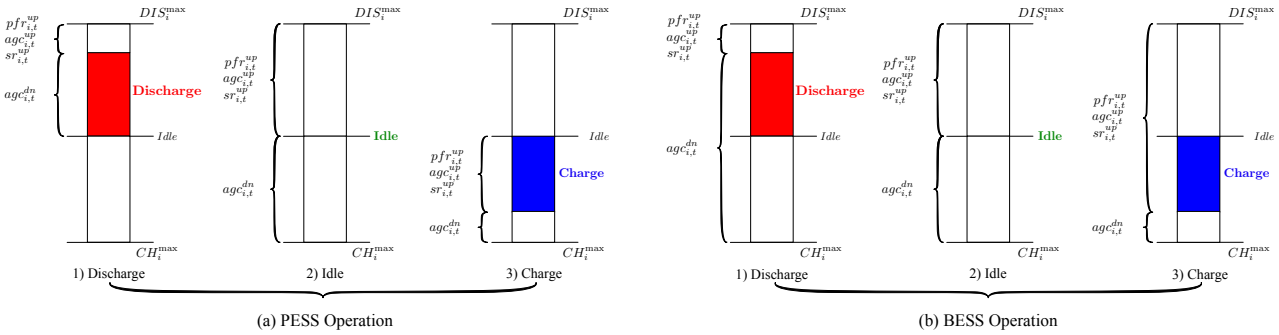

Figure 4.2. Two schemes for ESSs providing ASs.

$$P_g^{\min} \le p_{g,t} + pfr_{g,t}^{up} + agc_{g,t}^{up} + sr_{g,t}^{up} + nsr_{g,t}^{up} \le P_g^{\max}, \tag{4-15}$$

$$P_g^{\min} \le p_{g,t} - agc_{g,t}^{dn} \le P_g^{\max}, \tag{4-16}$$

$$p_{g,t} - p_{g,t-1} + pfr_{g,t}^{up} + agc_{g,t}^{up} + sr_{g,t}^{up} + nsr_{g,t}^{up} \le RU_g, \tag{4-17}$$

$$p_{g,t} - p_{g,t-1} - agc_{g,t}^{dn} \le -RD_g. \tag{4-18}$$

In MIDAS-S, we let all reserve products share the same headroom and ramp room. For some reserves, due to the response time difference, weighting factors might be applied to adjust their contributions of headroom, which can be user-defined in MIDAS-S. Also, note that some ISOs do not consider ASs in the ramping constraint, *e.g.*, MISO [144], but we still provide this flexibility to include (4c) and (4d) in the model.

4.2.4.2. MIDAS-S ESS Designs

In the MIDAS-S default setting, we model the ESS degradation cost as a linear cost function in the objective function, and use a three-status implementation of ESSs, *i.e.*,

charging, discharging, and idle. The operation constraints of ESSs are as follows.

$$p_{i,t} = dis_{i,t} - ch_{i,t}, \tag{4-19}$$

$$c_{i,t} + d_{i,t} \leq 1, \tag{4-20}$$

$$p_{i,t} - p_{i,t-1} + agc^{up}_{i,t} + pfr^{up}_{i,t} + sr^{up}_{i,t} \leq RU_i, \tag{4-21}$$

$$p_{i,t} - p_{i,t-1} - agc^{dn}_{i,t} \geq -RD_i, \tag{4-22}$$

$$ch_{i,t} \leq c_{i,t} \cdot CH_i^{\max}, \tag{4-23}$$

$$dis_{i,t} \leq d_{i,t} \cdot DIS_i^{\max}. \tag{4-24}$$

$$soc_{i,t} - soc_{i,t-1} \cdot (1 - LR_i) = ch_{i,t} \cdot \eta_i - dis_{i,t}/\eta_i, \tag{4-25}$$

$$soc_{i,t} + agc^{dn}_{i,t} \cdot ResT^{AGC} \leq SOC_i^{\max}, \tag{4-26}$$

$$soc_{i,t} - agc^{up}_{i,t} \cdot ResT^{AGC} - pfr^{up}_{i,t} \cdot ResT^{PFR} - sr^{up}_{i,t} \cdot ResT^{SR} \geq SOC_i^{\min}. \tag{4-27}$$

They are vanilla ESS operational constraints, where we enforce the idle status of ESSs in (4-20), and in (4-20)-(4-21) and (4-26)-(4-27), we enforce the similar ramp room constraints as in the generation part. The state-of-charge (SOC) limits consider AS capacities.

For the ESSs' headroom modeling, we consider a more refined formulation concerning various types of ESSs. Due to their power/energy ramping time, we treat the pumped energy storage system (PESS) and battery energy storage system (BESS) differently in MIDAS-S. Figure 4.2 depicts the operation logic of different flexibilities of ESS types. On the one hand, some ESS types, such as PESSs, require more time to change status in real-time. Hence, performing reserve scheduling for this type should only consider the reserve limit from the same direction. On the other hand, fast-responsive ESSs, such as BESSs, can quickly switch status, which allows it to allocate more reserves by using its opposite direction. Based on

Figure 4.2, we give an exact formulation for these two flexibility schemes of ESSs as follows.

$$PESS := \begin{cases} pfr_{i,t}^{up} + agc_{i,t}^{up} + sr_{i,t}^{up} \leq (1 - c_{i,t}) \cdot DIS_i^{\max} + ch_{i,t} - dis_{i,t}, \\ agc_{i,t}^{dn} \leq (1 - d_{i,t}) \cdot CH_i^{\max} + dis_{i,t} - ch_{i,t}. \end{cases} \tag{4-28}$$

$$BESS := \begin{cases} pfr_{i,t}^{up} + agc_{i,t}^{up} + sr_{i,t}^{up} \leq DIS_i^{\max} + ch_{i,t} - dis_{i,t}, \\ agc_{i,t}^{dn} \leq CH_i^{\max} + dis_{i,t} - ch_{i,t}. \end{cases} \tag{4-29}$$

It is straightforward to see that constraint (4-29) excludes all binary decision variables in (4-28) to achieve the logic. It is flexible in MIDAS-S to claim one ESS as PESS-type or BESS-type. Also, note that the ESS charging and discharging dispatch together with their binary indicators are termed as parameters in the RTED since the ESSs should participate in the energy arbitrage conducted in the day-ahead market operation. Only the reserve optimization and the SOC equations are included in RTED. To better reflect the real-time operation of ESSs, a linear interpolation of ESS dispatch based on DAUC results is performed in RTED. Note that all the formulations described in this section refer to [**?**], which is a prior work for the MIDAS framework. Then, we implement them in a generalized way in the MIDAS-S library.

4.2.4.3. Other Formulations

We omit other general formulations of UC and ED since they have been widely discussed and benchmarked in the literature, where we refer to [148] for interested readers. MIDAS-S provides a very flexible model library that can be modified and enhanced by users. Different modeling alternatives can be selected and tested in MIDAS-S.

4.2.5. Modularized Executables for User Flexibility

For different user preferences, modularized executables in each routine can be called and modified based upon various simulation goals. For high-level usages, users only need to modify the input data (by default in the form of MS Excel and CSV formats, as in

Listing 4.1. DAUC Model Example

```
UCmdl = pe.AbstractModel()
Params.DAUC_read_params(UCmdl)
Vars_base.load_base_vars(UCmdl)

# Define variables
getattr(Vars_gen_power, "DAUC_Piecewise_power")(UCmdl)
getattr(Vars_ess_power, "Idle_2var_power_soc")(UCmdl)

# Unit constraints
getattr(Constr_gen_ancillary_service, "DAUC_AS")(UCmdl)
getattr(Constr_ess_ancillary_service, "DAUC_AS")(UCmdl)

# System constraints
getattr(Constr_power_balance, "Nodal_power_balance")(UCmdl)
getattr(Constr_sys_reserve, "AS_Coupled")(UCmdl)

# Objective function
getattr(Objective_function, "DAUC_objective_basic")(UCmdl)
```

Listing 4.2. Generation AS Constraint Implementation

```
def _Define_PFRup(md):

    def pfr_pos_cap_rule(md, gi, hi):
        return md.gen_pfr_pos[gi,hi] <= (md.Df_Max - md.Gen_DB[gi]) /
            md.Gen_Ri[gi]

    md.gen_pfr_pos_cap = pe.Constraint(md.DPGEN_SET, md.INTER_SET, rule
        = pfr_pos_cap_rule)

@add_model_attr(component_name,
            requires = {'params_loader': None,
                        'base_var_loader': None,
                        'power_var_loader': None,
})
def DAUC_AS(md):

    _Define_PFRup(md)
```

FESTIV [133]) to change the problem setting and working mode, and the results will be automatically documented in both MS Excel and Python binary formats. However, users might want to modify the embedded optimization model internally. As MIDAS-S is built upon the Python optimization package Pyomo, descriptive implementation is allowable. The modularized executables that MIDAS-S offers could also help users easily customize their models and test operational variants. We discuss the scheduling part and dynamic part separately on this matter.

4.2.5.1. Scheduling Simulation Part

Taking the DAUC routine as an example, Listing 4.1 provides a simplified sketch of `DAUCModel.py`. Imports and function returns are omitted for brevity. After calling this function, the object `UCmdl` contains all the DAUC model information and is sent to the mode coordinator to execute. If the user would like to modify the model, taking the generator AS constraint for an example (Line 10), user could open its callback, *i.e.,* `Constr_gen_ancillary_service.py`, as shown in Listing 4.2, define a new function with a new name similar to `DAUC_AS`, and modify the object call `getattr` in `DAUCModel.py` accordingly. The `add_model_attr()` method is the utility protecting buffer for this flexible implementation.

The function `_Define_PFRup` in Listing 2 implements constraint (1a), which is very intuitive that all the parameters, variables, and constraints definitions are descriptive. Note that upon changing the model, users should follow the calling sequence as in Listing 1, *i.e.,* parameters → variables → constraints → objective function. This is a typical modeling sequence of any optimization model in Pyomo. If a prerequisite argument is missing, a warning will be raised.

Another advantage of the modularized executables is that users could call only a part of the MIDAS-S functions for utility usage. Flexible callable functions are stored in the utility library and are independent of each other. For example, suppose the user only wants to derive the power transfer distribution factors for the DC power flow. In that case, it can

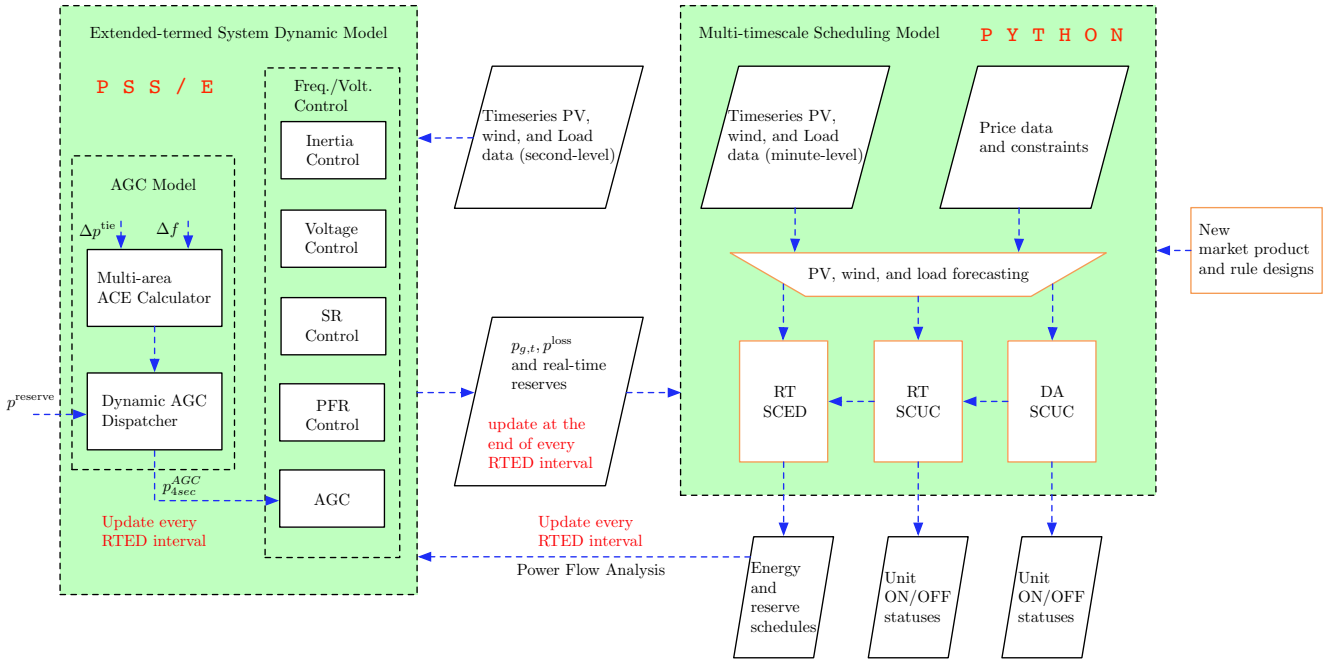

Figure 4.3. Scheduling-dynamic information exchange.

be achieved by just running `input.utils.cal_ptdf()`, where `input` is the object generated from the general input data sheet. These useful utility functions are all implemented in a vectorized fashion with fast and memory-saving features.

For DAUC and RTUC, we only generate the Pyomo abstract model one time since the mixed-integer programming problem is time-consuming to save when the system size grows. Then, for subsequent UC problems, we keep updating the model parameters in a rolling fashion. For DAED and RTED, We generate the model for DAED and RTED every time, as RTED does not impose a huge computational burden.

4.2.5.2. Dynamic Simulation Part

The dynamic simulation is by default executed in PSS®E, but other simulation platforms could also interface with MIDAS-S on this matter. After each RTED run, the scheduling part will save the RTED dispatch result in both CSV and Python binary formats. Afterward, the results will be sent to PSS®E for dynamic analyses, while the RTED routine will be halted,

waiting for the updated information is sent from the PSS®E, serving as new initial inputs for the next RTED. The information exchange process between the scheduling and dynamic simulation parts is detailed in Fig. 3. We omit the detailed discussion over the dynamic simulation part, which will be presented in another paper together with more comprehensive numerical experiments.

4.2.6. Simulation Examples

This section verifies the proposed platform by conducting market analyses on an 18-bus system with 5 generators and 1 ESS and a reduced WECC 243-bus system with 197 generators for scalability analyses. These two analyses are documented in the example gallery of MIDAS-S, where the network and unit data can also be found. Listing 3 shows the code executing four work modes for the 18-bus system with built-in summary and plotting functions. The dynamic simulation is embedded for both test systems (denoted as closed-loop simulation). All the subsequent simulations are performed in Intel Python 3.6.3 with MIDAS-S 0.6.6, NumPy 1.19.2, Pandas 1.1.2, and Pyomo 5.7 on a 2.9 GHz quad-core Intel Core i7 CPU with 16GB memory. We employ Gurobi 9.1 as the optimizer. Also, note that all figures in this section are generated from the built-in plotting functions.

4.2.6.1. 18-bus Test System

?? depicts the 18-bus system topology. Since DAUC and RTED are included in Mode 3 and 4, we focus on the economic assessment of them. Two consecutive days are considered in the simulation, while the second day's timeseries data is a copy of the first day adding Gaussian noise.

a). Mode 4 General Assessment.

In Mode 4, DAUC, RTUC, and RTED routines are executed in the multi-timescale coordinative fashion. Figure 4.5 depicts the dispatch share between generators in DAUC, RTUC, and RTED for the two days, and Table I tabulates the cost summary in Day 2. G1 and G3

Listing 4.3. Sample code for the 18-bus system run

```
import midass as ms

results_mode1 = ms.run_mode1(solver_name = "gurobi",
                             prefix_dir = r"midass/data/18_bus/",
                             verbose = True)
results_mode4 = ms.run_mode4(solver_name = "gurobi",
                             prefix_dir = r"midass/data/18_bus/",
                             psse_folder = r"PSSE/",
                             case_name = r"Case1",
                             run_name = r"Case1_24hr",
                             close_loop_flag = False,
                             ess_interpolate_method = True,
                             ess_dispatchable = False,
                             verbose = True)

Fig_Plot = ms.FigurePlot("DAUC",  results_mode4)
```

are inflexible units with a startup time longer than 1 hour, whereas G2 and G4 are flexible units with a startup time of less than 1 hour. Thus, G2 and G4 are re-committable in RTUC. We consider all four AS types in this test case, while the AS requirements are set as different portions of the load.

The overall dispatch pattern is intuitive. During the day when PV output is abundant, the ESS is charging using the excess PV power. When the time goes to the night, as the peak load occurs, the ESS is discharging to relieve the dispatch burden, during which the fast-start gas unit G2 is brought up for the demand increase. Since we assume RTUC uses the same timeseries profiles as in DAUC, there are not many differences between Figure 4.5 (a) and (b), while in Day 2, for Hour 7-10, RTUC shows a different dispatch profile with DAUC. When the load and renewable profiles are the same, this dispatch difference could be owing to the reserve relocation in RTUC when the simulation horizon for RTUC is only 3 hours. And RTED will strictly follow the RTUC commitments.

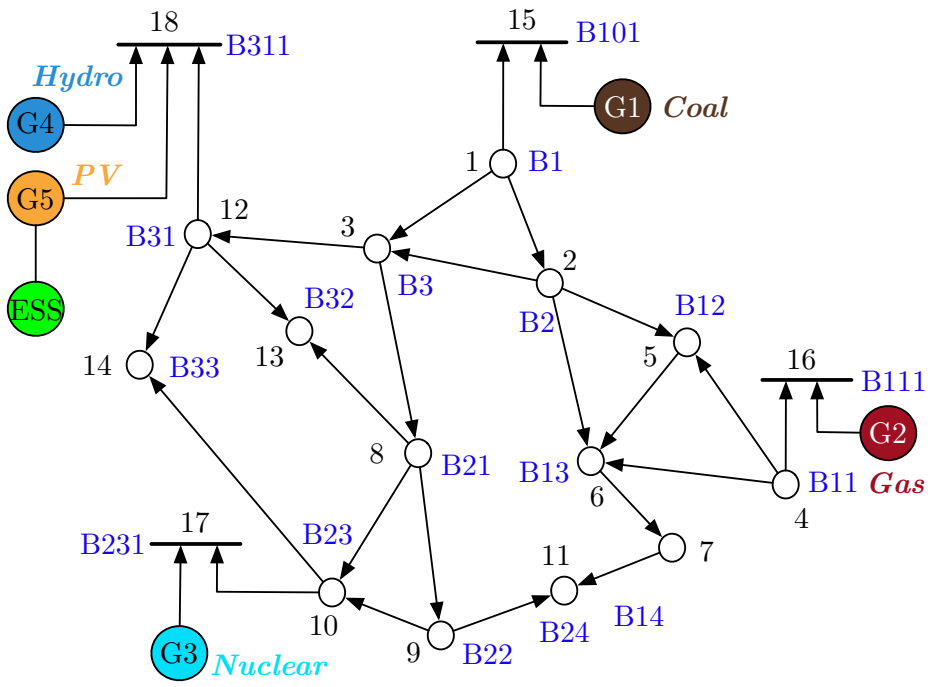

Figure 4.4. 18-bus diagram.

Table 4.2. Economic Assessment of Different Routines in Day 2

	DAUC	*RTUC*	*RTED*
Gen. Cost ($)	247,697	247,654	240,243
ESS Cost ($)	44	44	37
LS Penalty Cost ($)	0	0	22
Ramp Penalty Cost ($)	0	0	73,543
TX Penalty Cost ($)	0	0	0
SOC Penalty Cost ($)	0	0	0
PV Curtailment (MWh)	27	27	59

Gen.: Generator, LS: Load shedding.

For the unit startup/shutdown trajectory modeling, it is straightforward to observe that, in (c) and (f) during the startup and shutdown processes of G2, RTED models the linear trajectories explicitly. Especially in (f), as G2's startup time is 20 minutes, when the RTUC shown in (e) determines G2's startup at 18:00, RTED traverses four intervals in (f) for the

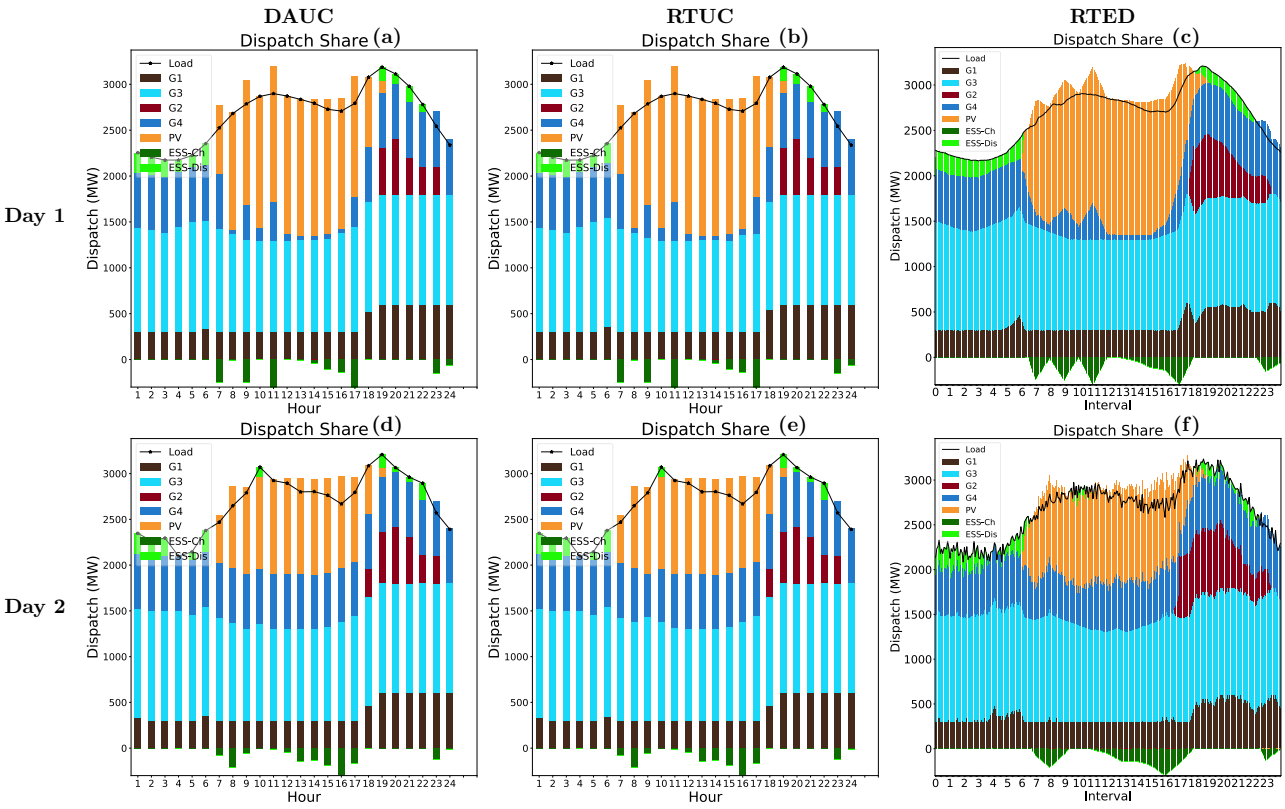

Figure 4.5. 18-bus system's Mode 4 dispatch results.

startup process. Then, once the startup process is completed at 18:00, thanks to the high operation ramp rate of G2, it ramps sharply to a high MW output for the peak load time. The shutdown process is also explicitly shown in this test case. It is noteworthy that the startup and shutdown process design discussed in subsection 4.2.3 contributes to the explicit modeling as shown in (c) and (f). Users could also choose other startup/shutdown modeling approaches as MIDAS-S can flexibly switch.

We could also observe the real-time ESS performance that strictly follows the DAUC and RTUC values. When the ESS performs the energy arbitrage in the day-ahead market coordinating with the PV power, real-time ESS dispatch values are interpolated but restricted to the SOC limits. However, the AS schedules for ESSs are still dispatchable in the real-time process in case any sudden event occurs.

In MIDAS-S, we generally put slack variables with customized penalty costs for most operational constraints, including the power balance, ramping constraints, power flow equations, SOC operations, and AS requirements, which is also an ISO's practice [144]. According to Table I, we could see that MIDAS-S conducts the market operation under moderate penalty values. We set very high penalty values, *e.g.,* \$100,000/MW for both load shedding and ramp violation. In practical operations, the penalty values are unavoidable in the optimization. Then, they will be removed after the market clearing is complete by a pricing rerun with violated constraint relaxation [149]. For PV curtailment, since we allow PV to provide ASs in MIDAS-S, the curtailment can be used to provide upward reserves. However, as we install an ESS in the system, the ESS takes the major responsibility to provide ASs due to its flexible feature, and PV is prone to use its full headroom to charge the ESS during the day. We could also see that the three modes' unit production costs are very close, which proves the consistency of the multi-timescale operation.

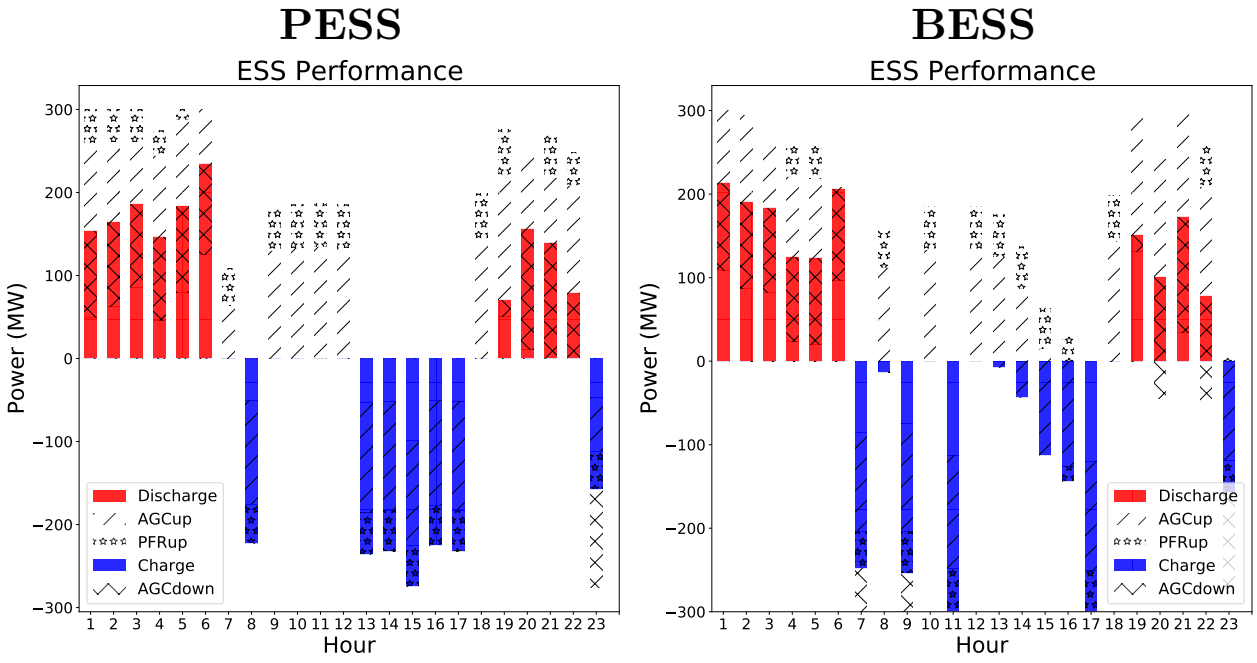

Figure 4.6. ESS Schedules in the 18-bus system.

b). Mode 4 ESS Performance with ASs.

We further validate the ESS implementation of the two operation schemes for different flexibilities on the AS provision. Figure 4.6 provides the comparison between setting the ESS as PESS-type and BESS-type. Note that we only show the DAUC results here since ESSs perform the energy arbitrage in the day-ahead market. It is clear the ESS in the BESS case covers a higher portion of ASs than the ESS in the PESS case as it can provide ASs by exceeding its opposite limits. As described in subsection 4.2.4 B, the BESS type has better flexibility of switching conditions and thus gains more capability to provide ASs. Figure 4.6 validates the exactness of the proposed ESS operating schemes. We also observe that the total cost of using the BESS type is lower than the case using the PESS type because when the AS burden is relieved by ESSs, generating units could leverage more power to perform the economic dispatch. Concerning the future dominance of ESS installations, system operators need to consider the ESS flexibilities in market operations.

c). Comparison between Four Modes.

To further validate the performance, we run Mode 1, 2, 3, and 4 on the 18-bus test system, and Table 4.3 gives the cost comparison. It is clear that for all modes, DAUC yields the same results. And Mode 2's RTEDs have the same outcomes as Mode 4's RTEDs since we feed in the previous results obtained by DAUC and RTUC in Mode 4. However, when comparing Mode 3 and Mode 4, we could find that Mode 4's RTEDs come to better results with lower production costs and penalty values. In Mode 3, the ramping penalty is high since

Table 4.3. Cost Comparison between Four Modes in Day 2

DAUC ($)	Mode 1	Mode 2	Mode 3	Mode 4
Prod. Cost	247,742	N/A	247,742	247,742
Penalty Cost	0	N/A	0	0
RTED ($)	Mode 1	Mode 2	Mode 3	Mode 4
Prod. Cost	N/A	240,298	242,893	240,298
Penalty Cost	N/A	0	528,327	73,602

Prod: Production.

Table 4.4. Computational Time for Test Systems

(Unit: sec)	Mode 1	Mode 2	Mode 3	Mode 4
18-bus W	1.32	493	496	542
18-bus S	0.84	127	128	151
WECC W	287	–	–	–
WECC S	193	–	–	–

W: Complete wall time; S: Solver time.

the ESS value inheritance is directly applied to the RTED and no generator is rescheduled in RTUC, which shrinks the ramp room of RTED's generators. This proves the importance of using RTUC in the short-term market operations.

4.2.6.2. Scalability Analysis

To test the scalability of MIDAS-S, we further run tests on the WECC 243-bus system and Table 4.4 tabulates the computational time for the two systems. For Mode 2, 3, and 4, the time is for one-day simulations. Note that we report both the solver execution time and the complete wall time including the time used for parsing models and information exchange. We could see that when the system size grows, the computational time also increases. But it is still within the acceptable range of execution time considering the workstation capability.

4.2.7. Summary

We propose and validate a Python-based open-source simulation library, MIDAS-S, for the short-term electricity market operations. The library is highly flexible for parameter tuning, result I/O, and model modifications based on different user preferences. We enhance the current electricity market operation model by new AS modeling and refined ESS operations, considering the recent advancement of renewable technologies. The MIDAS-S library also accommodates a unique and novel structure of DAUC-RTUC-RTED, validated via simulation-based economic assessment. The generalized implementation of complicated time-coupled market operations could help the open-source community understand com-

mercial electricity market frameworks. The ready-to-use interface between the scheduling and dynamic simulation paves a more accurate path for market analyses and provides new insights for future market operations.

Chapter 5

CONCLUDING REMARKS

Till now, we have conducted research on both the long-term and short-term market operations, considering the massive penetration of renewable energy. By leveraging the uncertainty-based optimization techniques, the decision-makings in electricity markets can be largely enhanced. The proposed stochastic optimization-based market framework provides a promising candidate solution towards the challenge that the proliferating renewables impose. We also investigate a combined simulation platform for future's potential electricity market designs, with emphasis on renewable impacts on the electricity market. Below is a detailed summary of what we have achieved in the finished works.

- **Long-term Operation:** We proposed a novel modeling framework and decompositionbased solution strategy combining SP and RO to deal with multiplex uncertainties in coordinated mid- and long-term power system planning. After solving a multi-year generation and transmission planning problem from an independent system operator (ISO)'s perspective, we analyzed the economic values of renewable energy comparing with other generation technologies in terms of the long-term investment payback. Considering the N-k contingencies and resource uncertainties, the hybrid stochastic and robust model was efficiently solved by a combined algorithm encoding the column-andconstraint generation and L-shaped method. We showed that the optimal investment portfolio in mid-term planning is the combined generation mix that includes both renewables and conventional units. In a longer-term planning study, the renewable companies show their growing cost-effectiveness due to the low operation cost. Note that the study we performed did not consider the energy storage and governmental and community incentives, strengthening the renewables' competitiveness. Hence, it is envisaged that a 100% renewable power system becomes feasible and economic in the future.

- **Short-term Operation:** We proposed a three-stage unit commitment model for the market operation of transmission and distribution coordination under the uncertainties of renewable generation and demand variations. Since the central operator will require more information about the increasingly active distribution networks, the T-D coordination becomes a promising solution. The novel T-D market paradigm we proposed quantitatively analyzed the typical market operation under a high distribution-level DER penetration. We showed that when considering the T-D coordination, the T and D boundary mismatches can be favorably reduced to zero, which saves hundreds of millions of dollars as operation costs. Besides, eliminating the active power mismatch could potentially help mitigate the frequency stability issue in both systems. To efficiently achieve this goal, our devised generalized decomposition technique greatly facilitates the solution of the coordinated market operation while considering complex system components such as the network reconfiguration.

- **Industry-level market simulation tool:** Heretofore, there lacks a general market operation simulation software that can integrate with the system dynamic simulation. Market operators keep a strong interest in capable software that can help simulate a realistic market environment considering both steady-state market products and transient-state system reliability. We design and implement such an open-source software based on Python programming language that could interface with commercial or free solvers and professional power system simulation software such as PSS®E. Within this open-source tool, various users from either industry or academia could easily get access to the core of the electricity market operations adopted in a general way for most scenarios in the world's electricity market. Novel research ideas and traditional engineering requirements synergize well within this platform to make a better future for the progress of the electricity market.

Appendix A

LINEAR RELAXATION TECHNIQUE

The product q of one binary variable z and one continuous variable x can be relaxed as follows. The relaxation is tight due to the convexity of the McCormick Envelope.

$$q \leq x + M(1 - z), \tag{A-1}$$

$$q \geq x - M(1 - z), \tag{A-2}$$

$$q \leq Mz, \tag{A-3}$$

$$q \geq -Mz. \tag{A-4}$$

Appendix B

FEASIBILITY GUARANTEE OF THE GND ALGORITHM

We provide two alternatives to guarantee the feasibility of the proposed GND algorithm. Upon infeasibility, a feasibility-check subproblem for the third-stage problem will need to be solved and return a feasibility cut to the second stage. Note that the second stage will not incur any infeasibility since the transmission ED problem has no integer and the load shedding variables enforce the feasibility of operational constraints. Hence, we only formulate the third-stage feasibility-check problem, as shown in (B-1).

$$\forall c: \min_{j_{mn,h,c}} \sum_{h}^{H} \sum_{mn} j^{+}_{mn,h,c} + j^{-}_{mn,h,c}, \tag{B-1}$$

subject to

$$\text{Constraint (3-3a)-(3-3f), (3-3l)-(3-3r),} \tag{B-1a}$$

$$x^{D}_{mn,h,c} \geq 0, \qquad \forall h, \tag{B-1b}$$

$$x^{D}_{mn,h,c} = 0, \qquad \forall n \in A^{D}_{T}, \forall h, \tag{B-1c}$$

$$x^{D}_{mn,h,c} + x^{D}_{nm,h,c} = 1 + j^{+}_{mn,h,c} - j^{-}_{mn,h,c}, \quad \forall n \in F^{D} \backslash F^{D}_{Q}, \forall h, \tag{B-1d}$$

$$x^{D}_{mn,h,c} + x^{D}_{nm,h,c} = z^{*}_{q,h,c} + j^{+}_{mn,h,c} - j^{-}_{mn,h,c}, \quad \forall n \in F^{D}_{Q}, \forall h, \tag{B-1e}$$

$$\sum_{n:(m,n)\in F^{D}} x_{mn,h,c} = 1, \qquad \forall m \in A^{D} \backslash A^{D}_{T}, \forall h, \tag{B-1f}$$

$$j^{+}_{mn,h,c}, j^{-}_{mn,h,c} \geq 0, \qquad \forall (m,n) \in F^{D}, \forall h, \tag{B-1g}$$

If we write in a compact form and for each scenario, we attain (B-2).

$$\forall c, \forall \omega^{D}_{c}: \quad S_{d}(w_{c}, \omega^{D}_{c}) = \min_{\mathbf{j}} \ \mathbf{j}, \tag{B-2}$$

subject to

$$\|\mathbf{H}_2\mathbf{y}^* + \mathbf{K}_2\mathbf{z} + \mathbf{e}\|_2 \leq \mathbf{q}^\top\mathbf{y}^* + \mathbf{p}^\top\mathbf{z} + \mathbf{k}^\top\mathbf{j} + \mathbf{H}_3\mathbf{x}_2^* + \mathbf{r_2}(\omega_c^D), \tag{B-2a}$$

where $j^+_{mn,h,c}$ and $j^-_{mn,h,c}$ are positive slack variables imposed on the distribution reconfiguration constraints, $\mathbf{j}$ is their vector form. After we solve (B-2), the feasibility cut can be formulated as in (B-3).

$$\mathbf{u}^\top(\mathbf{H}_2\mathbf{y}^* + \mathbf{e}) - \mathbf{v}(\mathbf{q}^\top\mathbf{y}^* + \mathbf{k}^\top\mathbf{j} + \mathbf{H}_3\mathbf{x}_2^* + \mathbf{r}_2(\omega_c^D)) \leq 0, \tag{B-3}$$

Note that any infeasible set of distribution reconfigurations will incur infeasibility in all scenarios of this distribution network. Hence, upon encountering an infeasible subproblem instance, a feasibility cut will be generated and all other scenarios will be terminated because (B-3) contains enough feasibility information. The feasibility cut will be added into the second-stage problem. Afterwards, the second-stage problem will be solved and add a cut containing both feasibility and optimality information to the first stage. Then the iteration continues from the first stage. This procedure is called Fast Forward and Fast Back [72], which also coincides with (B-3). One of this method's benefits is that distribution networks can return their feasibility cut individually without compromising other distribution systems' optimality.

Adding feasibility cuts, however, naturally increases the computational burden as the algorithm would require more iterations to converge. As discussed in [150], we can simply replace the constraints in problem (3-3) with the ones in problem (B-1) and add a huge penalty for these slack variables in the objective function, which makes the third-stage problem always feasible. This manuever could avoid adding any feasibility cut while maintaining feasibility. Again, as shown in (B-1), not all operational constraints should be relaxed but only the ones with integer variables as they are the potential sources of infeasibility.

Note that, though without a concrete proof, evidence has been found that enforcing a feasible subproblem appears to be more computationally efficient than adding feasibility

cuts [150] and corresponds to the ISO's practice [151]. However, adding cuts is an exact and canonical way. Nevertheless, both methods are able to eliminate the infeasibility issue to different extents.

BIBLIOGRAPHY

[1] S. Tam, "Real-time Security-Constrained Economic Dispatch and Commitment in the PJM : Experiences and Challenges," tech. rep., PJM, June 2011.

[2] S. Richard, *Design of Electricity Markets for Efficient Balancing of Wind Power Generation*. Doctoral Thesis, KTH Royal Institute of Technology, Stockholm, Sweden, 2015.

[3] "Global Wind & Solar Installations in Gigawatts (GW)."

[4] "Renewables – Global Energy Review 2020 – Analysis."

[5] J. Hu, R. Harmsen, W. Crijns-Graus, E. Worrell, and M. van den Broek, "Identifying barriers to large-scale integration of variable renewable electricity into the electricity market: A literature review of market design," *Renewable and Sustainable Energy Reviews*, vol. 81, pp. 2181–2195, Jan. 2018.

[6] A. Moreira, D. Pozo, A. Street, and E. Sauma, "Reliable Renewable Generation and Transmission Expansion Planning: Co-Optimizing System's Resources for Meeting Renewable Targets," *IEEE Transactions on Power Systems*, vol. 32, pp. 3246–3257, July 2017.

[7] "Distribution System Operator (DSO) Models for Utility Stakeholders," tech. rep., Black & Veatch Management Consulting, Jan. 2020.

[8] "Examination of Federal Financial Assistance in the Renewable Energy Market: Implications and Opportunities for Commercial Deployment of Small Modular Reactors," tech. rep., Scully Capital, 2018.

[9] S. Hong, H. Cheng, and P. Zeng, "N-k Constrained Composite Generation and Transmission Expansion Planning With Interval Load," *IEEE Access*, vol. 5, pp. 2779–2789, 2017.

[10] L. Baringo and A. Baringo, "A Stochastic Adaptive Robust Optimization Approach for the Generation and Transmission Expansion Planning," *IEEE Transactions on Power Systems*, vol. 33, pp. 792–802, Jan 2018.

[11] A. Baharvandi, J. Aghaei, T. Niknam, M. Shafie-Khah, R. Godina, and J. P. S. Catalao, "Bundled Generation and Transmission Planning Under Demand and Wind Generation Uncertainty Based on a Combination of Robust and Stochastic Optimization," *IEEE Transactions on Sustainable Energy*, vol. 9, pp. 1477–1486, July 2018.

[12] Q. Wang, J. Watson, and Y. Guan, "Two-Stage Robust Optimization for N-k Contingency-constrained Unit Commitment," *IEEE Transactions on Power Systems*, vol. 28, pp. 2366–2375, Aug 2013.

[13] A. Moreira, A. Street, and J. M. Arroyo, "An Adjustable Robust Optimization Approach for Contingency-Constrained Transmission Expansion Planning," *IEEE Transactions on Power Systems*, vol. 30, pp. 2013–2022, July 2015.

[14] B. Chen, J. Wang, L. Wang, Y. He, and Z. Wang, "Robust Optimization for Transmission Expansion Planning: Minimax Cost vs. Minimax Regret," *IEEE Transactions on Power Systems*, vol. 29, pp. 3069–3077, Nov 2014.

[15] R. A. Jabr, "Robust Transmission Network Expansion Planning with Uncertain Renewable Generation and Loads," *IEEE Transactions on Power Systems*, vol. 28, pp. 4558–4567, Nov 2013.

[16] F. Beltrán, W. de Oliveira, and E. C. Finardi, "Application of Scenario Tree Reduction via Quadratic Process to Medium-term Hydrothermal Scheduling Problem," *IEEE Transactions on Power Systems*, vol. 32, pp. 4351–4361, Nov 2017.

[17] X. Zhang and A. J. Conejo, "Robust Transmission Expansion Planning Representing Long- and Short-Term Uncertainty," *IEEE Transactions on Power Systems*, vol. 33, pp. 1329–1338, March 2018.

[18] L. A. Gallego, L. P. Garces, M. Rahmani, and R. A. Romero, "High-performance Hybrid Genetic Algorithm to Solve Transmission Network Expansion Planning," *IET Generation, Transmission Distribution*, vol. 11, no. 5, pp. 1111–1118, 2017.

[19] C. Roldán, R. Mínguez, R. García-Bertrand, and J. M. Arroyo, "Robust Transmission Network Expansion Planning under Correlated Uncertainty," *IEEE Transactions on Power Systems*, vol. 34, pp. 2071–2082, May 2019.

[20] E. Du, N. Zhang, B. Hodge, Q. Wang, C. Kang, B. Kroposki, and Q. Xia, "The Role of Concentrating Solar Power toward High Renewable Energy Penetrated Power Systems," *IEEE Transactions on Power Systems*, vol. 33, pp. 6630–6641, Nov 2018.

[21] Z. Zhuo, N. Zhang, J. Yang, C. Kang, C. Smith, M. Omalley, and B. Kroposki, "Transmission Expansion Planning Test System for AC/DC Hybrid Grid with High Variable Renewable Energy Penetration," *IEEE Transactions on Power Systems*, pp. 1–1, 2019.

[22] B. Zeng and L. Zhao, "Solving Two-stage Robust Optimization Problems Using a Column-and-Constraint Generation Method," *Oper. Res. Lett.*, vol. 41, pp. 457–461, 2013.

[23] R. M. Van Slyke and R. Wets, "L-shaped linear programs with applications to optimal control and stochastic programming," *SIAM Journal on Applied Mathematics*, vol. 17, no. 4, pp. 638–663, 1969.

[24] Q. Wang, J. Watson, and Y. Guan, "Two-stage Robust Optimization for N-k Contingency-Constrained Unit Commitment," *IEEE Transactions on Power Systems*, vol. 28, pp. 2366–2375, Aug 2013.

[25] C. Zhao and R. Jiang, "Distributionally Robust Contingency-Constrained Unit Commitment," *IEEE Transactions on Power Systems*, vol. 33, pp. 94–102, Jan 2018.

[26] "2013 Assessment of Reliability Performance," tech. rep., Texas Reliability Entity, April 2014.

[27] IIT Power Group, Available: http://motor.ece.iit.edu/data/, *Index of Data*, 2018.

[28] GAMS Development Corporation, Washington, DC, USA, *GAMS - A User's Guide, GAMS Release 25.3.0*, 2018.

[29] M. R. Bussieck, M. C. Ferris, and T. Lohmann, *GUSS: Solving Collections of Data Related Models Within GAMS*, pp. 35–56. Berlin, Heidelberg: Springer Berlin Heidelberg, 2012.

[30] "Capital Cost Estimates for Utility Scale Electricity Generating Plants," tech. rep., U.S. Energy Information Administrative, 2016.

[31] "Cost and Performance Characteristics of New Generating Technologies, Annual Energy Outlook 2020," tech. rep., U.S. Energy Information Administrative, 2020.

[32] F. Deng, X. Zeng, and L. Pan, "Research on Multi-terminal Traveling Wave Fault Location Method in Complicated Networks Based on Cloud Computing Platform," *Protection and Control of Modern Power Systems*, vol. 2, May 2017.

[33] ERCOT, Available: http://www.ercot.com/gridinfo, *Generation & Load - Grid Information*.

[34] J. Dupačová, N. Gröwe-Kuska, and W. Römisch, "Scenario Reduction in Stochastic Programming," *Mathematical Programming*, vol. 95, pp. 493–511, Mar 2003.

[35] H. Heitsch and W. Römisch, "Scenario Tree Reduction for Multistage Stochastic Programs," *Computational Management Science*, vol. 6, pp. 117–133, May 2009.

[36] A. Vafamehr, M. E. Khodayar, S. D. Manshadi, I. Ahmad, and J. Lin, "A Framework for Expansion Planning of Data Centers in Electricity and Data Networks Under Uncertainty," *IEEE Transactions on Smart Grid*, vol. 10, pp. 305–316, Jan 2019.

[37] M. Farhoumandi, F. Aminifar, and M. Shahidehpour, "Generation Expansion Planning Considering the Rehabilitation of Aging Generating Units," *IEEE Transactions on Smart Grid*, pp. 1–1, 2020.

[38] "HOMER Pro User Manual 3.13 - Glossary," tech. rep., HOMER Energy, 2019.

[39] J. Koornneef, T. van Keulen, A. Faaij, and W. Turkenburg, "Life Cycle Assessment of a Pulverized Coal Power Plant with Post-Combustion Capture, Transport and Storage of CO2," *International Journal of Greenhouse Gas Control*, vol. 2, no. 4, pp. 448 – 467, 2008. TCCS-4: The 4th Trondheim Conference on CO2 Capture, Transport and Storage.

[40] C. L. Lara, D. S. Mallapragada, D. J. Papageorgiou, A. Venkatesh, and I. E. Grossmann, "Deterministic Electric Power Infrastructure Planning: Mixed-Integer Programming Model and Nested Decomposition algorithm," *European Journal of Operational Research*, vol. 271, no. 3, pp. 1037 – 1054, 2018.

[41] J. E. Price, "Benchmarking a Reduced Test-bed Model of WECC Region for Unit Commitment and Flexible Dispatch," in *2013 IEEE Power Energy Society General Meeting*, pp. 1–5, July 2013.

[42] N. Helistö, J. Kiviluoma, H. Holttinen, J. D. Lara, and B.-M. Hodge, "Including operational aspects in the planning of power systems with large amounts of variable generation: A review of modeling approaches," *WIREs Energy and Environment*, vol. 8, no. 5, p. e341, 2019.

[43] S. Yin, J. Wang, and F. Qiu, "Decentralized electricity market with transactive energy – A path forward," *The Electricity Journal*, vol. 32, no. 4, pp. 7 – 13, 2019.

[44] "Coordination of Transmission and Distribution Operations in High Distributed Energy Resource Electric Grid," Tech. Rep. 17-IEPR-12, CAISO, June 2017.

[45] A. Zegers and H. Brunner, "TSO-DSO interaction: An Overview of current interaction between transmission and distribution system operators and an assessment of their cooperation in Smart Grids," tech. rep., ISGAN, Sept. 2014.

[46] Z. Li, Q. Guo, H. Sun, and J. Wang, "Coordinated Economic Dispatch of Coupled Transmission and Dstribution Systems Using Heterogeneous Decomposition," *IEEE Trans. on Power Systems*, vol. 31, pp. 4817–4830, Nov 2016.

[47] Z. Li, Q. Guo, H. Sun, and J. Wang, "A New LMP-Sensitivity-Based Heterogeneous Decomposition for Transmission and Distribution Coordinated Economic Dispatch," *IEEE Trans. on Smart Grid*, vol. 9, pp. 931–941, March 2018.

[48] P. Li, Q. Wu, M. Yang, Z. Li, and N. Hatziargyriou, "Distributed distributionally robust dispatch for integrated transmission-distribution systems," *IEEE Transactions on Power Systems*, pp. 1–1, 2020.

[49] R. Roofegari nejad, W. Sun, and A. Golshani, "Distributed restoration for integrated transmission and distribution systems with ders," *IEEE Transactions on Power Systems*, vol. 34, no. 6, pp. 4964–4973, 2019.

[50] J. Zhao, H. Wang, Y. Liu, Q. Wu, Z. Wang, and Y. Liu, "Coordinated restoration of transmission and distribution system using decentralized scheme," *IEEE Transactions on Power Systems*, vol. 34, no. 5, pp. 3428–3442, 2019.

[51] M. K. Arpanahi, M. E. H. Golshan, and P. Siano, "A comprehensive and efficient decentralized framework for coordinated multiperiod economic dispatch of transmission and distribution systems," *IEEE Systems Journal*, pp. 1–12, 2020.

[52] A. Nawaz and H. Wang, "Stochastically coordinated transmission and distribution system operation with large-scale wind farms," *CSEE Journal of Power and Energy Systems*, pp. 1–10, 2020.

[53] "ERCOT Nodal Protocols Section 4: Day-Ahead Operations," tech. rep., ERCOT, 2020.

[54] S. Yin, J. Wang, Z. Li, and X. Fang, "State-of-the-art short-term electricity market operation with solar generation: A review," *Renewable and Sustainable Energy Reviews*, vol. 138, p. 110647, 2021.

[55] M. R. Dorostkar-Ghamsari, M. Fotuhi-Firuzabad, M. Lehtonen, A. Safdarian, and A. S. Hoshyarzade, "Stochastic operation framework for distribution networks hosting high wind penetrations," *IEEE Transactions on Sustainable Energy*, vol. 10, pp. 344–354, Jan 2019.

[56] Y. Zhang, J. Wang, and Z. Li, "Uncertainty modeling of distributed energy resources: Techniques and challenges," *Current Sustainable/Renewable Energy Reports*, Apr 2019.

[57] J. Wang, M. Shahidehpour, and Z. Li, "Security-constrained unit commitment with volatile wind power generation," *IEEE Transactions on Power Systems*, vol. 23, pp. 1319–1327, Aug 2008.

[58] A. Papavasiliou, Y. Mou, L. Cambier, and D. Scieur, "Application of Stochastic Dual Dynamic Programming to the Real-Time Dispatch of Storage Under Renewable Supply Uncertainty," *IEEE Trans. on Sustainable Energy*, vol. 9, pp. 547–558, April 2018.

[59] R. T. Rockafellar and R. J.-B. Wets, "Scenarios and policy aggregation in optimization under uncertainty," *Mathematics of Operations Research*, vol. 16, no. 1, pp. 119–147, 1991.

[60] H. Shuai, J. Fang, X. Ai, Y. Tang, J. Wen, and H. He, "Stochastic Optimization of Economic Dispatch for Microgrid Based on Approximate Dynamic Programming," *IEEE Trans. on Smart Grid*, pp. 1–1, 2018.

[61] A. Shapiro, "Analysis of stochastic dual dynamic programming method," *European Journal of Operational Research*, vol. 209, no. 1, pp. 63 – 72, 2011.

[62] J. Zou, S. Ahmed, and X. A. Sun, "Multistage stochastic unit commitment using stochastic dual dynamic integer programming," *IEEE Transactions on Power Systems*, vol. 34, no. 3, pp. 1814–1823, 2019.

[63] M. N. Hjelmeland, J. Zou, A. Helseth, and S. Ahmed, "Nonconvex medium-term hydropower scheduling by stochastic dual dynamic integer programming," *IEEE Transactions on Sustainable Energy*, vol. 10, no. 1, pp. 481–490, 2019.

[64] M. Shahidehpour, T. Ding, Q. Ming, C. Huang, Z. Wang, and P. Du, "Multi-period active distribution network planning using multi-stage stochastic programming and nested decomposition by sddip," *IEEE Transactions on Power Systems*, pp. 1–1, 2020.

[65] M. Bragin, Y. Dvorkin, and A. Darvishi, "Toward coordinated transmission and distribution operations," in *2018 IEEE Power Energy Society General Meeting (PESGM)*, pp. 1–5, 2018.

[66] M. Farivar and S. H. Low, "Branch Flow Model: Relaxations and Convexification: Part i," *IEEE Trans. on Power Systems*, vol. 28, pp. 2554–2564, Aug 2013.

[67] B. Kocuk, S. S. Dey, and X. A. Sun, "Strong SOCP Relaxations for the Optimal Power Flow Problem," *Operations Research*, vol. 64, no. 6, pp. 1177–1196, 2016.

[68] J. A. Taylor and F. S. Hover, "Convex models of distribution system reconfiguration," *IEEE Transactions on Power Systems*, vol. 27, no. 3, pp. 1407–1413, 2012.

[69] M. R. Dorostkar-Ghamsari, M. Fotuhi-Firuzabad, M. Lehtonen, and A. Safdarian, "Value of Distribution Network Reconfiguration in Presence of Renewable Energy Resources," *IEEE Transactions on Power Systems*, vol. 31, pp. 1879–1888, May 2016.

[70] M. Nick, R. Cherkaoui, and M. Paolone, "Optimal Planning of Distributed Energy Storage Systems in Active Distribution Networks Embedding Grid Reconfiguration," *IEEE Trans. on Power Systems*, vol. 33, pp. 1577–1590, March 2018.

[71] H. Zhang, S. J. Moura, Z. Hu, W. Qi, and Y. Song, "Joint PEV Charging Network and Distributed PV Generation Planning Based on Accelerated Generalized Benders Decomposition," *IEEE Transactions on Transportation Electrification*, vol. 4, pp. 789–803, Sep. 2018.

[72] J. Murphy, "Benders, nested benders and stochastic programming: An intuitive introduction," 2013.

[73] G. Infanger and D. Morton, "Cut sharing for multistage stochastic linear programs with interstage dependency," *Mathematical Programming*, vol. 75, pp. 241–256, 11 1996.

[74] Y. Zhang, X. Wang, J. Wang, and Y. Zhang, "Deep reinforcement learning based volt-var optimization in smart distribution systems," *IEEE Transactions on Smart Grid*, vol. 12, no. 1, pp. 361–371, 2021.

[75] A. Kargarian and Y. Fu, "System of Systems Based Security-Constrained Unit Commitment Incorporating Active Distribution Grids," *IEEE Trans. on Power Systems*, vol. 29, pp. 2489–2498, Sept 2014.

[76] NREL, "https://www.nrel.gov/analysis/data-products.html."

[77] Q. Li, R. Ayyanar, and V. Vittal, "Convex optimization for des planning and operation in radial distribution systems with high penetration of photovoltaic resources," *IEEE Transactions on Sustainable Energy*, vol. 7, no. 3, pp. 985–995, 2016.

[78] M. Shahidehpour, H. Yamin, and Z. Li, *Market Operations in Electric Power Systems: Forecasting, Scheduling, and Risk Management*. Wiley Press, 2002.

[79] Q. P. Zheng, J. Wang, and A. L. Liu, "Stochastic optimization for unit commitment—a review," *IEEE Transactions on Power Systems*, vol. 30, no. 4, pp. 1913–1924, 2015.

[80] NREL and CAISO, "Maintaining bulk power system reliability while integrating variable energy resources – caiso approach," tech. rep., 2013.

[81] FERC, "Participation of distributed energy resource aggregations in markets operated by regional transmission organizations and independent system operators," tech. rep., 2020.

[82] R. C. Energy, "Proactively managing risks to accomplish your longterm renewable energy goals," tech. rep., 2018.

[83] A. Campoccia, L. Dusonchet, E. Telaretti, and G. Zizzo, "An analysis of feed'in tariffs for solar pv in six representative countries of the european union," *Solar Energy*, vol. 107, pp. 530–542, 2014.

[84] P. Cramton, "Electricity market design," *Oxford Review of Economic Policy*, vol. 33, pp. 589–612, 11 2017.

[85] J. Bushnell, "Building Blocks: Investment in Renewable and Nonrenewable Technologies," RSCAS Working Papers 2011/53, European University Institute, Oct. 2011.

[86] L. Marshall, A. Bruce, and I. MacGill, "Zero operating cost renewables and shadow bidding in wholesale electricity markets," in *2019 IEEE Power Energy Society General Meeting (PESGM)*, pp. 1–5, 2019.

[87] P. Li, S. Sekar, and B. Zhang, "A capacity-price game for uncertain renewables resources," *IEEE Transactions on Sustainable Computing*, pp. 1–1, 2019.

[88] J. Yang, J. Zhao, J. Qiu, and F. Wen, "A distribution market clearing mechanism for renewable generation units with zero marginal costs," *IEEE Transactions on Industrial Informatics*, vol. 15, no. 8, pp. 4775–4787, 2019.

[89] Z. Li, J. Wang, H. Sun, F. Qiu, and Q. Guo, "Robust estimation of reactive power for an active distribution system," *IEEE Transactions on Power Systems*, pp. 1–1, 2019.

[90] A. Ademola-Idowu and B. Zhang, "Frequency stability using mpc-based inverter power control in low-inertia power systems," *IEEE Transactions on Power Systems*, vol. 36, no. 2, pp. 1628–1637, 2021.

[91] A. Hirsch, Y. Parag, and J. Guerrero, "Microgrids: A review of technologies, key drivers, and outstanding issues," *Renewable and Sustainable Energy Reviews*, vol. 90, pp. 402–411, 2018.

[92] A. Jafari, H. Ganjeh Ganjehlou, T. Khalili, and A. Bidram, "A fair electricity market strategy for energy management and reliability enhancement of islanded multi-microgrids," *Applied Energy*, vol. 270, p. 115170, 2020.

[93] T. Khalili, S. Nojavan, and K. Zare, "Optimal performance of microgrid in the presence of demand response exchange: A stochastic multi-objective model," *Computers Electrical Engineering*, vol. 74, pp. 429–450, 2019.

[94] P. Du, N. V. Mago, W. Li, S. Sharma, Q. Hu, and T. Ding, "New ancillary service market for ercot," *IEEE Access*, vol. 8, pp. 178391–178401, 2020.

[95] G. De Zotti, S. A. Pourmousavi, H. Madsen, and N. Kjølstad Poulsen, "Ancillary services 4.0: A top-to-bottom control-based approach for solving ancillary services problems in smart grids," *IEEE Access*, vol. 6, pp. 11694–11706, 2018.

[96] D. Jay and K. S. Swarup, "Game theoretical approach to novel reactive power ancillary service market mechanism," *IEEE Transactions on Power Systems*, vol. 36, no. 2, pp. 1298–1308, 2021.

[97] I. Celik, A. B. Philips, Z. Song, Y. Yan, R. J. Ellingson, M. J. Heben, and D. Apul, "Energy payback time (epbt) and energy return on energy invested (eroi) of perovskite tandem photovoltaic solar cells," *IEEE Journal of Photovoltaics*, vol. 8, no. 1, pp. 305–309, 2018.

[98] C. Messmer, A. Fell, F. Feldmann, N. Wöhrle, J. Schön, and M. Hermle, "Efficiency roadmap for evolutionary upgrades of perc solar cells by topcon: Impact of parasitic absorption," *IEEE Journal of Photovoltaics*, vol. 10, no. 2, pp. 335–342, 2020.

[99] S. Wang, Q. Liu, S. Yuksel, and H. Dincer, "Hesitant linguistic term sets-based hybrid analysis for renewable energy investments," *IEEE Access*, vol. 7, pp. 114223–114235, 2019.

[100] E. Du, N. Zhang, B.-M. Hodge, Q. Wang, C. Kang, B. Kroposki, and Q. Xia, "The role of concentrating solar power toward high renewable energy penetrated power systems," *IEEE Transactions on Power Systems*, vol. 33, no. 6, pp. 6630–6641, 2018.

[101] L. Marí and N. Nabona, "Renewable energies in medium-term power planning," *IEEE Transactions on Power Systems*, vol. 30, no. 1, pp. 88–97, 2015.

[102] R. Henrion, C. Küchler, and W. Römisch, "Scenario reduction in stochastic programming with respect to discrepancy distances," *Computational Optimization and Applications*, vol. 43, pp. 67–93, May 2009.

[103] L. Baringo and A. Conejo, "Correlated wind-power production and electric load scenarios for investment decisions," *Applied Energy*, vol. 101, pp. 475–482, 2013. Sustainable Development of Energy, Water and Environment Systems.

[104] W. Römisch, "Scenario reduction techniques in stochastic programming," in *Stochastic Algorithms: Foundations and Applications* (O. Watanabe and T. Zeugmann, eds.), (Berlin, Heidelberg), pp. 1–14, Springer Berlin Heidelberg, 2009.

[105] S. Talari, M. Yazdaninejad, and M.-R. Haghifam, "Stochastic-based scheduling of the microgrid operation including wind turbines, photovoltaic cells, energy storages and responsive loads," *IET Generation, Transmission & Distribution*, vol. 9, no. 12, pp. 1498–1509, 2015.

[106] G. E. Constante-Flores and M. Illindala, "Data-driven probabilistic power flow analysis for a distribution system with renewable energy sources using monte carlo simulation," in *2017 IEEE/IAS 53rd Industrial and Commercial Power Systems Technical Conference (I CPS)*, pp. 1–8, 2017.

[107] H. Ye and Z. Li, "Robust security-constrained unit commitment and dispatch with recourse cost requirement," *IEEE Transactions on Power Systems*, vol. 31, no. 5, pp. 3527–3536, 2016.

[108] P. Li, X. Guan, J. Wu, and X. Zhou, "Modeling dynamic spatial correlations of geographically distributed wind farms and constructing ellipsoidal uncertainty sets for optimization-based generation scheduling," *IEEE Transactions on Sustainable Energy*, vol. 6, no. 4, pp. 1594–1605, 2015.

[109] Z. Zhang, Y. Chen, J. Ma, X. Liu, and W. Wang, "Two-stage robust security constrained unit commitment considering the spatiotemporal correlation of uncertainty prediction error," *IEEE Access*, vol. 7, pp. 22891–22901, 2019.

[110] A. Street, F. Oliveira, and J. M. Arroyo, "Contingency-constrained unit commitment with $n-k$ security criterion: A robust optimization approach," *IEEE Transactions on Power Systems*, vol. 26, no. 3, pp. 1581–1590, 2011.

[111] R. Wang, P. Wang, and G. Xiao, "A robust optimization approach for energy generation scheduling in microgrids," *Energy Conversion and Management*, vol. 106, pp. 597–607, 2015.

[112] A. Zare, C. Y. Chung, J. Zhan, and S. O. Faried, "A distributionally robust chance-constrained milp model for multistage distribution system planning with uncertain renewables and loads," *IEEE Transactions on Power Systems*, vol. 33, no. 5, pp. 5248–5262, 2018.

[113] Y. Chen, Q. Guo, H. Sun, Z. Li, W. Wu, and Z. Li, "A distributionally robust optimization model for unit commitment based on kullback–leibler divergence," *IEEE Transactions on Power Systems*, vol. 33, no. 5, pp. 5147–5160, 2018.

[114] C. Duan, W. Fang, L. Jiang, L. Yao, and J. Liu, "Distributionally robust chance-constrained approximate ac-opf with wasserstein metric," *IEEE Transactions on Power Systems*, vol. 33, no. 5, pp. 4924–4936, 2018.

[115] M. Kakimoto, Y. Endoh, H. Shin, R. Ikeda, and H. Kusaka, "Probabilistic solar irradiance forecasting by conditioning joint probability method and its application to electric power trading," *IEEE Transactions on Sustainable Energy*, vol. 10, no. 2, pp. 983–993, 2019.

[116] Y.-Y. Hong, J. J. F. Martinez, and A. C. Fajardo, "Day-ahead solar irradiation forecasting utilizing gramian angular field and convolutional long short-term memory," *IEEE Access*, vol. 8, pp. 18741–18753, 2020.

[117] F. M. Lopes, R. Conceição, H. G. Silva, R. Salgado, and M. Collares-Pereira, "Improved ecmwf forecasts of direct normal irradiance: A tool for better operational strategies in concentrating solar power plants," *Renewable Energy*, vol. 163, pp. 755–771, 2021.

[118] Y. Chen, Y. Wang, D. Kirschen, and B. Zhang, "Model-free renewable scenario generation using generative adversarial networks," *IEEE Transactions on Power Systems*, vol. 33, pp. 3265–3275, May 2018.

[119] A. Bracale, G. Carpinelli, and P. De Falco, "A probabilistic competitive ensemble method for short-term photovoltaic power forecasting," *IEEE Transactions on Sustainable Energy*, vol. 8, no. 2, pp. 551–560, 2017.

[120] R. Ben Ammar, M. Ben Ammar, and A. Oualha, "Photovoltaic power forecast using empirical models and artificial intelligence approaches for water pumping systems," *Renewable Energy*, vol. 153, pp. 1016–1028, 2020.

[121] J. Faraji, A. Ketabi, H. Hashemi-Dezaki, M. Shafie-Khah, and J. P. S. Catalão, "Optimal day-ahead self-scheduling and operation of prosumer microgrids using hybrid machine learning-based weather and load forecasting," *IEEE Access*, vol. 8, pp. 157284–157305, 2020.

[122] I. Genc, R. Diao, V. Vittal, S. Kolluri, and S. Mandal, "Decision tree-based preventive and corrective control applications for dynamic security enhancement in power systems," *IEEE Transactions on Power Systems*, vol. 25, no. 3, pp. 1611–1619, 2010.

[123] Q. Li, Y. Xu, and C. Ren, "A hierarchical data-driven method for event-based load shedding against fault-induced delayed voltage recovery in power systems," *IEEE Transactions on Industrial Informatics*, vol. 17, no. 1, pp. 699–709, 2021.

[124] L. Zhu, D. J. Hill, and C. Lu, "Hierarchical deep learning machine for power system online transient stability prediction," *IEEE Transactions on Power Systems*, vol. 35, no. 3, pp. 2399–2411, 2020.

[125] W. M. Villa-Acevedo, J. M. López-Lezama, and D. G. Colomé, "Voltage stability margin index estimation using a hybrid kernel extreme learning machine approach," *Energies*, vol. 13, no. 4, 2020.

[126] Y. Zhang, Y. Xu, Z. Y. Dong, and R. Zhang, "A hierarchical self-adaptive data-analytics method for real-time power system short-term voltage stability assessment," *IEEE Transactions on Industrial Informatics*, vol. 15, no. 1, pp. 74–84, 2019.

[127] H. Liu, F. Hussain, Y. Shen, S. Arif, A. Nazir, and M. Abubakar, "Complex power quality disturbances classification via curvelet transform and deep learning," *Electric Power Systems Research*, vol. 163, pp. 1–9, 2018.

[128] R. Ahmed, V. Sreeram, Y. Mishra, and M. Arif, "A review and evaluation of the state-of-the-art in pv solar power forecasting: Techniques and optimization," *Renewable and Sustainable Energy Reviews*, vol. 124, p. 109792, 2020.

[129] M. Shahidehpour, Z. Li, and H. Yamin, "Market Operations in Electric Power Systems : Forecasting, Scheduling, and Risk Management," 2002.

[130] T. Brijs, C. De Jonghe, B. F. Hobbs, and R. Belmans, "Interactions between the Design of Short-term Electricity Markets in the CWE Region and Power System Flexibility," *Applied Energy*, vol. 195, pp. 36–51, 2017.

[131] "PLEXOS Electricity Brochure." https://energyexemplar.com/wp-content/uploads/PLEXOS_Electricity_Brochure.pdf. Accessed on 02.21.2021.

[132] Enerlytix, "Enerlytix Solutions." http://www.enelytix.com/. Accessed on 02.21.2021.

[133] E. Ela, M. Milligan, and M. O'Malley, "A Flexible Power System Operations Simulation Model for Assessing Wind Integration." https://www.nrel.gov/grid/festiv-model.html. Accessed on 02.21.2021.

[134] B. Knueven, J. Ostrowski, and J.-P. Watson, "On Mixed-Integer Programming Formulations for the Unit Commitment Problem," *INFORMS Journal on Computing*, vol. 32, pp. 857–876, June 2020. Publisher: INFORMS.

[135] D. A. Tejada-Arango, S. Lumbreras, P. Sánchez-Martín, and A. Ramos, "Which Unit-Commitment Formulation is Best? A Comparison Framework," *IEEE Transactions on Power Systems*, vol. 35, no. 4, pp. 2926–2936, 2020.

[136] PJM, "Electric Storage Resource Participation Model." https://www.pjm.com/-/media/committees-groups/committees/mic/20190206/20190206-item-07c-faq-for-order-841-and-hybrids.ashx. Accessed on 02.21.2021.

[137] T. T. Ku, C. H. Lin, C. T. Hsu, C. S. Chen, Z. Y. Liao, S. D. Wang, and F. F. Chen, "Enhancement of Power System Operation by Renewable Ancillary Service," *IEEE Transactions on Industry Applications*, vol. 56, no. 6, pp. 6150–6157, 2020.

[138] S. Yin, J. Wang, Z. Li, and X. Fang, "State-of-the-art Short-term Electricity Market Operation with Solar Generation: A Review," *Renewable and Sustainable Energy Reviews*, vol. 138, p. 110647, 2021.

[139] E. Ela, V. Gevorgian, A. Tuohy, B. Kirby, M. Milligan, and M. O'Malley, "Market Designs for the Primary Frequency Response Ancillary Service—Part I: Motivation and Design," *IEEE Transactions on Power Systems*, vol. 29, no. 1, pp. 421–431, 2014.

[140] B. Olek and M. Wierzbowski, "Ancillary Services Provided by Renewable Energy Sources," in *IET Conference on Power in Unity: a Whole System Approach*, pp. 1–7, 2013.

[141] N. G. Cobos, J. M. Arroyo, N. Alguacil, and J. Wang, "Robust Energy and Reserve Scheduling Considering Bulk Energy Storage Units and Wind Uncertainty," *IEEE Transactions on Power Systems*, vol. 33, no. 5, pp. 5206–5216, 2018.

[142] N. Padmanabhan, M. Ahmed, and K. Bhattacharya, "Battery Energy Storage Systems in Energy and Reserve Markets," *IEEE Transactions on Power Systems*, vol. 35, no. 1, pp. 215–226, 2020.

[143] H. Yang, Y. Wu, and J. Liao, "Economic Dispatch and Frequency-regulation Reserve Capacity Integrated Optimization for High-penetration Renewable Smart Grids," in *2019 IEEE Innovative Smart Grid Technologies - Asia (ISGT Asia)*, pp. 2980–2985, 2019.

[144] MISO, "Business Practices Manual: Energy and Operating Reserve Markets - Attachment D: Real-Time Energy and Operating Reserve Market Software Formulations and Business Logic," 2021.

[145] ERCOT, "Module 6: Day-Ahead Through Real-Time Operations." http://www.ercot.com/content/wcm/training_courses/109600/TRN101_M6_DAM_RT_2017.pdf. Accessed on 02.21.2021.

[146] Y. G. Rebours, D. S. Kirschen, M. Trotignon, and S. Rossignol, "A Survey of Frequency and Voltage Control Ancillary Services—Part I: Technical Features," *IEEE Transactions on Power Systems*, vol. 22, no. 1, pp. 350–357, 2007.

[147] H. Chávez, R. Baldick, and S. Sharma, "Governor Rate-Constrained OPF for Primary Frequency Control Adequacys," *IEEE Transactions on Power Systems*, vol. 29, no. 3, pp. 1473–1480, 2014.

[148] J. Wang, M. Shahidehpour, and Z. Li, "Security-Constrained Unit Commitment With Volatile Wind Power Generation," *IEEE Transactions on Power Systems*, vol. 23, no. 3, pp. 1319–1327, 2008.

[149] E. Ela, M. Milligan, A. Bloom, A. Botterud, A. Townsend, and T. Levin, "Evolution of Wholesale Electricity Market Design with Increasing Levels of Renewable Generation." http://www.nrel.gov/docs/fy14osti/61765.pdf. Accessed on 02.21.2021.

[150] A. Nasri, S. J. Kazempour, A. J. Conejo, and M. Ghandhari, "Network-constrained ac unit commitment under uncertainty: A benders' decomposition approach," *IEEE Transactions on Power Systems*, vol. 31, no. 1, pp. 412–422, 2016.

[151] "Business Practices Manual: Energy and Operating Reserve Markets - Attachment B: Day-Ahead Energy and Operating Reserve Market Software Formulations and Business Logic," Tech. Rep. BPM-002-r19, MISO, 2019.

[152] I. Schneider and M. Roozbehani, "Energy market design for renewable resources: Imbalance settlements and efficiency–robustness tradeoffs," *IEEE Transactions on Power Systems*, vol. 33, no. 4, pp. 3757–3767, 2018.

[153] J. Yang, J. Zhao, J. Qiu, and F. Wen, "A distribution market clearing mechanism for renewable generation units with zero marginal costs," *IEEE Transactions on Industrial Informatics*, vol. 15, no. 8, pp. 4775–4787, 2019.

[154] *IBM ILOG CPLEX V12.8: User's manual for CPLEX*. Oct. 2017.

[155] A. Bagheri, J. Wang, and C. Zhao, "Data-driven stochastic transmission expansion planning," *IEEE Transactions on Power Systems*, vol. 32, pp. 3461–3470, Sept 2017.

[156] R. M. Van Slyke and R. Wets, "L-shaped Linear Programs with Applications to Optimal Control and Stochastic Programming," *SIAM Journal on Applied Mathematics*, vol. 17, no. 4, pp. 638–663, 1969.

[157] S. Ahmed, "Two-stage stochastic integer programming: A brief introduction," in *Wiley Encyclopedia of Operations Research and Management Science*, (NJ, USA), 2011.

[158] L. L. Garver, "Transmission network estimation using linear programming," *IEEE Transactions on Power Apparatus and Systems*, vol. PAS-89, pp. 1688–1697, Sept 1970.

[159] L. P. Garces, A. J. Conejo, R. Garcia-Bertrand, and R. Romero, "A bilevel approach to transmission expansion planning within a market environment," *IEEE Transactions on Power Systems*, vol. 24, pp. 1513–1522, Aug 2009.

[160] L. K. et al., "A Tale of Two Visions: Designing a Decentralized Transactive Electric System," *IEEE Power and Energy Magazine*, vol. 14, pp. 63–69, May 2016.

[161] M. E. Baran and F. F. Wu, "Network reconfiguration in distribution systems for loss reduction and load balancing," *IEEE Transactions on Power Delivery*, vol. 4, pp. 1401–1407, April 1989.

[162] S. Yin, J. Wang, and Z. Li, "Decomposable solution paradigm for uncertainty-based transmission and distribution coordinated economic dispatch," in *2019 IEEE Power Energy Society General Meeting (PESGM)*, pp. 1–5, Aug 2019.

[163] J. R. Birge, "Decomposition and partitioning methods for multistage stochastic linear programs," *Operations Research*, vol. 33, no. 5, pp. 989–1007, 1985.

[164] Z. Chen and M. S. L. Wu, "Effective Load Carrying Capability Evaluation of Renewable Energy via Stochastic Long-Term Hourly Based SCUC," *IEEE Trans. on Sustainable Energy*, vol. 6, pp. 188–197, Jan 2015.

[165] R. A. Jabr, R. Singh, and B. C. Pal, "Minimum Loss Network Reconfiguration Using Mixed-Integer Convex Programming," *IEEE Transactions on Power Systems*, vol. 27, pp. 1106–1115, May 2012.

[166] J. R. Birge and F. Louveaux, *Introduction to Stochastic Programming*. Springer Publishing Company, Incorporated, 2nd ed., 2011.

[167] Y. Yang and W. Wu, "A Distributionally Robust Optimization Model for Real-time Power Dispatch in Distribution Networks," *IEEE Trans. on Smart Grid*, pp. 1–1, 2018.

[168] L. M. Lopez-Ramos, V. Kekatos, A. Marques, and G. Giannakis, "Two-timescale stochastic dispatch of smart distribution grids," *IEEE Trans. on Smart Grid*, vol. 9, pp. 4282–4292, Sept 2018.

[169] W. Wei, F. Liu, S. Mei, and Y. Hou, "Robust energy and reserve dispatch under variable renewable generation," *IEEE Trans. on Smart Grid*, vol. 6, pp. 369–380, Jan 2015.

[170] Z. Chen, L. Wu, and M. Shahidehpour, "Effective Load Carrying Capability Evaluation of Renewable Energy via Stochastic Long-Term Hourly Based SCUC," *IEEE Trans. on Sustainable Energy*, vol. 6, pp. 188–197, Jan 2015.

[171] R. Li, Q. Wu, and S. Oren, "Distribution Locational Marginal Pricing for Optimal Electric Vehicle Charging Management," *IEEE Trans. on Power Systems*, vol. 29, pp. 203–211, Jan 2014.

[172] J. Carr and L. V. McCall, "Divergent evolution and resulting characteristics among the world's distribution systems," *IEEE Transactions on Power Delivery*, vol. 7, pp. 1601–1609, July 1992.

[173] A. Papavasiliou, Y. Mou, L. Cambier, and D. Scieur, "Application of stochastic dual dynamic programming to the real-time dispatch of storage under renewable supply uncertainty," *IEEE Trans. on Sustainable Energy*, vol. 9, pp. 547–558, April 2018.

[174] Z. Li, Q. Guo, H. Sun, and J. Wang, "Coordinated Transmission and Distribution AC Optimal Power Flow," *IEEE Trans. on Smart Grid*, vol. 9, pp. 1228–1240, March 2018.

[175] H. Yeh, D. F. Gayme, and S. H. Low, "Adaptive VAR Control for Distribution Circuits with Photovoltaic Generators," *IEEE Trans. on Power Systems*, vol. 27, pp. 1656–1663, Aug 2012.

[176] M. Farivar and S. H. Low, "Branch flow model: Relaxations and convexification—part i," *IEEE Transactions on Power Systems*, vol. 28, pp. 2554–2564, Aug 2013.

[177] S. M. M. Khodayar, "A Hierarchical Electricity Market Structure for the Smart Grid Paradigm," *IEEE Trans. on Smart Grid*, vol. 7, July 2016.

[178] IUST, "IEEE Modified 30-bus Data: [available online] http://een.iust.ac.ir/profs/jadid/scpm.pdf."

[179]